# PALEOBIOLOGY OF MAMMALS USING FUNCTIONAL TRAIT-ENVIRONMENT RELATIONSHIPS ACROSS SPACE AND THROUGH TIME FOR CONSERVATION AND PUBLIC UNDERSTANDING OF SCIENCE

A Dissertation

by

RACHEL ANN SHORT

Submitted to the Office of Graduate and Professional Studies of
Texas A&M University
in partial fulfillment of the requirements for the degree of

DOCTOR OF PHILOSOPHY

| | |
|---|---|
| Chair of Committee, | A. Michelle Lawing |
| Committee Members, | Perry S. Barboza |
| | Jim I. Mead |
| | X. Ben Wu |
| Head of Department, | Kirk O. Winemiller |

August 2020

Major Subject: Ecosystem Science and Management

# ABSTRACT

Large mammal communities are impacted by environmental changes that challenge conservation efforts. We can better predict responses to these ongoing changes if we understand responses that have been preserved in the information-rich fossil record. Interdisciplinary work presented here investigates trait-environment relationships to provide a common currency for integrating paleontological data, modern data, and future projections. Additionally, this work highlights informal learning institutions as locations for scientists to engage the public with their studies. To improve the rigor of the trait-environment approach, I use a well-known dataset of tooth crown height and precipitation to explore the implications of various analytical methods. When tested with Pleistocene fossil sites, paleoprecipitation predictions closely match global climate models from the last glacial period. Next, I build a modern trait-environment model for the Order Artiodactyla with measures of calcaneal gear ratio to determine if the trait can be used as an environmental indicator as it has been for carnivorans. I demonstrate that, for artiodactyls, community-level gear ratio is related to ecoregion division, vegetation cover, and precipitation. I apply the model to historical and modern data in Kenya to illustrate that calcaneal gear ratio has potential to serve as an environmental predictor in the fossil record. Then, I describe a community of large mammals from a late Pleistocene site (~40,000 years old) in northern Mexico. This is a prolific site that fills a geographic gap in an area with an otherwise poorly understood paleontological record. The complex mammalian fauna includes the region's first Rancholabrean occurrences of

Palaeolama, Procyon, and Smilodon. To facilitate the communication of environmental knowledge, I conduct a comprehensive analysis of the geographic capacity of informal STEM learning institutions to reach underserved populations. Three groups of counties have considerably fewer informal learning opportunities than expected, and higher than expected populations of groups who are underrepresented in STEM careers. Dissemination of this research will contribute to understanding how mammals are functionally related to their environment and will help us prepare for alternative environmental futures.

# DEDICATION

To Adam, Kolten, Sofia, and all other children —

you deserve to grow up in a world full of wildlife.

# ACKNOWLEDGEMENTS

I would like to thank my committee chair, Michelle Lawing, for her guidance, support, and friendship throughout this research. Her mentoring has made me a better researcher. I would also like to thank my committee, Ben Wu, Perry Barboza, and Jim Mead, for their willingness to provide advice and assistance. Jim Mead accepted me into the master's program in the Department of Geosciences at East Tennessee State University nine years ago, and he and Sandy Swift remain constant sources of support.

This dissertation would not have been possible without my family. I am especially indebted to Jeff Martin for his encouragement, strength, and patience over the last 10 years. He is always ready to talk about a crazy research idea, help with data collection (even when it means dragging boxes of giraffe bones around an attic in Berlin), or just sit in the yard with our dog, Koda, who is a calming force in my life. I am forever thankful to Linda Cox, for taking me to every museum and zoo within a day's drive of central Illinois (and many beyond) and buying me every book on history, science, and geography when I was growing up. Bill Cox and Kimberly Gould were along for many of those experiences and waited (mostly) patiently while I saw "just one more thing." These experiences are the reason I am a scientist. Though it has been difficult to be away for so long, it has been made easier by the love and support of family, and their endless willingness to dog sit during research trips.

I could not have asked for better friends and colleagues through this process, and I will inevitably and unintentionally miss recognizing some people. Laura Emmert,

Sharon Holte, and Marina Van der Eb are my closest friends and cheerleaders. Paul Klockow and Sascha Lodge have been great friends that helped me adjust to Texas and co-founders of The Write Stuff – our writing group that provided immeasurable support. I am thankful to consider Jill Zarestky, Rhonda Struminger, and Lauren Vilen my friends and collaborators. I especially appreciate Jill Zarestky's help getting over hurdles during the late stages of dissertation writing. I appreciate the insights provided by my labmates: Leila Siciliano-Martina, John Jacisin, Louis Addae-Wireko, James West, Wesley Vermillion, and Chase Brooke. The Brooke family has become my Texas family, and I value the time spent on their ranch and in their houses.

I appreciate everyone who discussed my research with me and reviewed manuscripts in this dissertation. This is more people than I can list here but include: Evan Doughty, Laura Emmert, Jason Head, Sharon Holte, Christine Janis, Jenny McGuire, Jeff Martin, David Polly, and Josh Samuels. Anthony Barnosky reviewed chapter 5, and his thoughtful comments improved the research. Ingrid Luffman also reviewed chapter 5 and provided insight on working with spatial autocorrelation. This research would be incomplete without the contributions of undergraduate students who have worked alongside me. Katherine Pinson, James Pippin, and Minna Wong participated in research and are co-authors on chapters included here. Kyle Brown completed an internship that included hours spent with spreadsheets and taxonomy books to make museum visits easier.

I am fortunate that my research took me to Washington DC, 11 states, and 9 countries outside of Texas and the United States. My extensive travel would not have

been possible without a number of people opening their homes to me: Betsy Brooke, Ed and Keri Brooke, Steve Cox, Laura Emmert, Anne-Claire Fabre, Sharon Holte, and Jill Zarestky. I am thankful that Jeff Martin and Sharon Holte were willing to travel to many of these places with me, share hotel rooms, and listen to me strategize data collection at museums or practice talks before conferences.

I am enormously grateful to the museums and collections managers who supported my data collection: Paolo Agnelli - Museo di Storia Naturale; Brian Compton - East Tennessee Museum of Natural History; John Demboski - Denver Museum of Nature and Science; Christiane Funk - Museum für Naturkunde; Richard Hulbert – Florida Museum of Natural History; Jessica Light - Texas A&M Biological Research and Teaching Collections; Darren Lunde and John Ososky - Smithsonian National Museum of Natural History; Meredith Mahoney - Illinois State Museum, USA; Ogeto Mwebi - National Museums of Kenya; Roberto Portela-Miguez - Natural History Museum; and Chris Sagebiel - Texas Vertebrate Paleontology Collections. Brian Compton, Jessica Light, and Meredith Mahoney frequently and graciously opened their collections to me in the early stages of research exploration.

Finally, I am grateful to the professors who have invested their effort to prepare me for this endeavor: Loni Walker and William Jaeckle at Illinois Wesleyan University; Jim Mead, Blaine Schubert, and Steven Wallace at East Tennessee State University; Susan McKay at the University of Maine; and Michelle Lawing, Ben Wu, and Perry Barboza at Texas A&M. These people have trained me in scientific writing, critical thinking, and always asking “so what?” to make my research mean something.

## CONTRIBUTORS AND FUNDING SOURCES

This work was supervised by a dissertation committee consisting of Dr. A. Michelle Lawing (chair) and Dr. X. Ben Wu of the Department of Ecology and Conservation Biology, Dr. Perry S. Barboza of the Departments of Ecology and Conservation Biology and Rangeland, Wildlife, and Fisheries Management, and Dr. Jim I. Mead of The Mammoth Site.

My co-authors for Chapter 2 are Katherine Pinson, Department of Geology and Geophysics, Texas A&M University; and A. Michelle Lawing, Department of Ecology and Conservation Biology, Texas A&M University. Laura G. Emmert, Center of Excellence in Paleontology, East Tennessee State University, provided Figure 2.1.

My co-author for Chapter 3 is A. Michelle Lawing, Department of Ecology and Conservation Biology, Texas A&M University. Kyle Brown, Department of Ecology and Conservation Biology, Texas A&M University, completed an internship under my direction and contributed to data collection and curation for this chapter.

My co-authors for Chapter 4 are Laura G. Emmert, Center of Excellence in Paleontology, East Tennessee State University; Nicholas A. Famoso, John Day Fossil Beds National Monument, U.S. National Park Service; Jeff M. Martin, Department of Rangeland, Wildlife, and Fisheries Management, Texas A&M University; Jim I. Mead and Sandy L. Swift, The Mammoth Site, Hot Springs, SD; and Arturo Baez, College of Agriculture and Life Sciences, University of Arizona. Eric Scott, Cogstone Resource Management, and Brianna McHorse, Department of Organismic and Evolutionary Biology, Harvard University, provided data for this research.

My co-authors for Chapter 5 are Rhonda Struminger, James Pippin, Minna Wong, and A. Michelle Lawing, Department of Ecology and Conservation Biology, Texas A&M University; and Jill Zarestky and Lauren Vilen, School of Education, Colorado State University.

All other work conducted for the dissertation was completed independently.

This work was made possible by funding from Texas A&M University: Merit Fellowship and Tom Slick Graduate Research Fellowship from the College of Agriculture and Life Sciences, Dishman-Lucas Graduate Assistantship and four Graduate Student Travel and Research Grants from the Department of Ecosystem Science and Management, and Travel Awards from the Graduate and Professional Student Council, Office of Graduate and Professional Studies, and Institute of Data Science. This research was supported in part by the National Science Foundation under grants numbers NSF-DRL 1713359 and NSF-DRL 1713351. This work was partly supported by the USDA NIFA Hatch projects 1003462, 1020451, and 1021915, and Integrative Climate Change Biology (a scientific program of the International Union of Biological Sciences). Additional travel funding came from the Society of Vertebrate Paleontology and the North American Paleontological Conference. The contents of the dissertation are solely the responsibility of the authors and do not necessarily represent the official views of the funding sources.

TABLE OF CONTENTS

Page

LIST OF FIGURES

Page

LIST OF TABLES

Page

# 1. INTRODUCTION

It has long been observed that functional traits and specific environmental factors are highly correlated. For example, previous studies demonstrated a shift in herbivore communities from predominately low-crowned teeth to high-crowned teeth with increasing aridity during the late Cenozoic (Janis et al. 2000, 2002, Fortelius et al. 2002, Eronen et al. 2010b). Increased hypsodonty provides the adaptive advantage of being able to better ingest abrasive foods (Strömberg 2002, 2006, Merceron et al. 2016) and environmental grit (Janis et al. 2002, Fortelius et al. 2006, Semprebon et al. 2019). However, until recently, it has been challenging to study trait-environment relationships over broad scales because of the focus on taxon-based methods (Barnosky et al. 2017). With the advent of spatial analyses using major trait-based databases, readily available museum specimens for identifying new traits, and climate surfaces, we can now explore these relationships in novel ways.

Ecometrics is the study of community-level functional trait-environment relationships (Eronen et al. 2010a). Because traits have a functional relationship with environment, the morphology of a community will change through time as environment changes (Violle et al. 2007, Enquist et al. 2015). Thus, trait-environment relationships can be used to capture biological processes, such as adaptation, speciation, geographic distribution shifts, and extinction, that drive functional diversity and community assembly (Polly et al. 2011, 2016, Cadotte et al. 2013, Polly and Head 2015, Barnosky et al. 2017, Start and Gilbert 2019). Community-level morphology can be a better indicator

of environment than any single species (Polly and Head 2015). With the focus on functional trait change rather than species change, this method more easily enables faunal studies through time (Polly and Head 2015).

When measured in the fossil record, morphological traits can be used for a thorough understanding of biotic responses to corresponding environmental changes, which can contribute to improved predictions for future faunal communities (Ceballos et al. 2005, 2015, Barnosky et al. 2011). Conservation paleobiology aims to use knowledge of the past to make informed predictions about the future of Earth's threatened biodiversity (Dietl and Flessa 2011, Dietl et al. 2015, Barnosky et al. 2017). Detection of ecological and evolutionary processes in the fossil record facilitates a better understanding of biological responses to environmental changes and provides critical information about biodiversity to researchers, conservationists, and managers that can be used to anticipate responses to projected changes.

### 1.1. Research objectives and hypotheses

This interdisciplinary dissertation contributes to scientific efforts by enabling a more complete understanding of ecosystems through time and across space to facilitate more informed decision-making to conserve biodiversity and the ecosystem services it provides (Figure 1.1). I do this through four research projects: 1) investigating implications of analytical methods selected for use in studies of trait-environment relationships; 2) demonstrating the value of a new trait-environment relationship model; 3) describing a faunal community from the Pleistocene of Sonora, Mexico; and 4)

highlighting institutions of informal learning as resources for increasing public understanding of science.

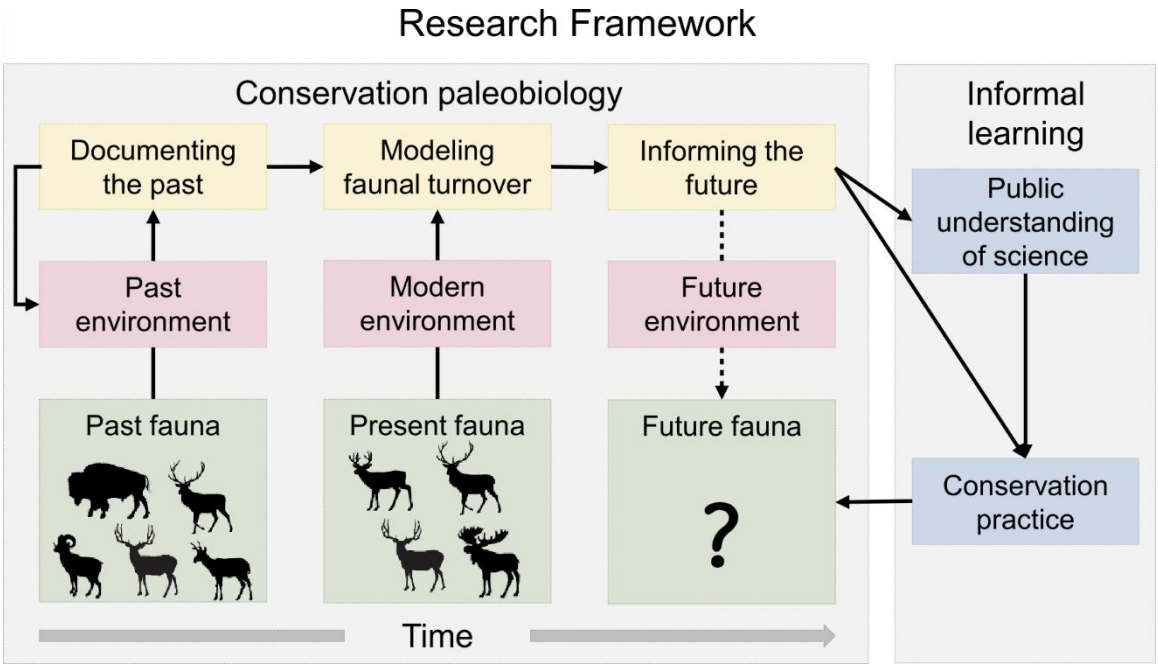


**Figure 1.1. Research framework for this interdisciplinary dissertation. Conservation paleobiology integrates research on documenting the past (systematic paleontology and paleoenvironmental reconstructions), modeling faunal turnover (ecological modeling and environmental change), informing the future (faunal predictions and conservation practice). Informal learning research aims to increase public understanding of science in support of conservation practice.**

First, I investigate four analytical methods used in ecometric studies that have been used or have the potential to be used in ecometric analyses for predicting paleoenvironment. A clear understanding of the implications of the different methods will increase the potential for more meaningful interpretations. I evaluate four methods to determine whether there have been systematic differences in paleoenvironmental

interpretation due to method choice. Specifically, I use linear regression, polynomial regression, nearest neighbor, and maximum likelihood methods with a well-known ecometric dataset of mammalian herbivore hypsodonty metrics (i.e., molar tooth crown to root height ratio; Figure 1.2A) and annual precipitation (Eronen et al. 2010c, Lawing et al. 2017). Differences in observed and predicted modern precipitation are compared to explore the predictive ability of the relationship, and each method is applied to 43 Pleistocene fossil sites. Sites were categorized as glacial or interglacial, and paleoprecipitation predictions were compared to the appropriate global climate model. I expect maximum likelihood to produce the most accurate precipitation predictions because the method fits a model to a localized subset of communities that have similar trait values. For that reason, I also expect maximum likelihood to predict paleoprecipitation that most closely align with global climate models.

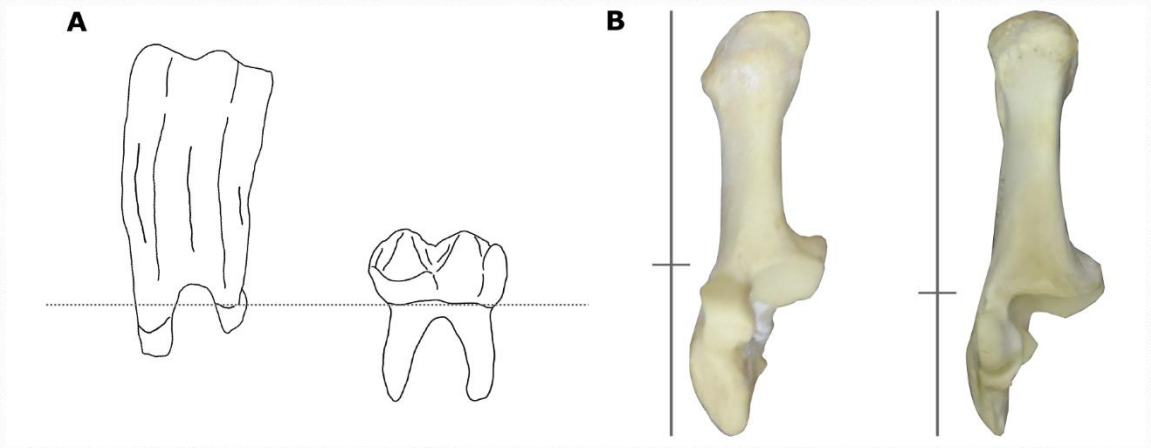


**Figure 1.2. Ecometric traits used in this dissertation. A, Herbivore hypsodonty (i.e., molar tooth crown to root height ratio) ranging from high (left; *Equus caballus*) to low (right; *Tapirus terrestris*); B, Calcaneal gear ratio (i.e., the ratio of the overall length of the calcaneum to the length of the calcaneal tuber at the sustentacular facet) ranging from high (left, *Pecari tajacu*) to low (right; *Odocoileus virginianus*).**

Second, I developed an ecometric model using the calcaneal gear ratio of Artiodactyla across the globe. The gear ratio is a measurement of the overall length of the calcaneum divided by the length of the in-lever, i.e. calcaneal tuber; a low gear ratio indicates a long in-lever and a more plantigrade stance, whereas a high gear ratio indicates a short in-lever and a more unguligrade stance (Figure 1.2B; Polly 2010). In communities of carnivorans, this measure is related to ecoregion province, vegetation cover, and temperature (Polly 2010). Artiodactyls are the primary large herbivores in most communities, they have a nearly global distribution in almost all ecosystems, and species frequently overlap geographically creating a myriad of unique communities (Wilson and Reeder 2005, Foss and Prothero 2007).

I collect gear ratio measurements from six museum collections, sample species composition of artiodactyl communities using distribution maps from IUCN, and calculate the mean and standard deviation of community-level gear ratio at 50 km equidistant points across the globe. For the same communities, I also sample temperature, precipitation, elevation, Matthews' vegetation type, and Bailey's ecoregion divisions to determine which environmental variables are most strongly related to the geographic distribution of artiodactyl gear ratio. I expect ecoregion division, vegetation cover, and precipitation to be strongly related to community gear ratio measures because this faunal group is herbivorous, and ranges will be constricted by vegetation patterns. To demonstrate the application of ecometric models, I apply this new model to six sites

in Kenya with historical and modern fauna records (Tóth et al. 2019). Using the trait-environment relationship, I can relate faunal changes to environmental changes.

Third, I describe the large mammals from the paleontological deposit near San Clemente de Térapa (hereafter referred to as Térapa). Térapa represents one of the very few Rancholabrean North American Land Mammal Age sites within northeastern Sonora, Mexico (Mead et al. 2006). At that time, pinyon-juniper-oak woodlands were common in the area while riparian corridors most likely followed local rivers to the Gulf of Mexico (Mead et al. 2006, Van Devender 2007). Summers were cooler and drier and winters were wetter than currently experienced in northern Mexico (Nunez et al. 2010, Bright et al. 2016). This new review of specimens provides a more thorough description of the material as well as amends incorrect initial identifications. I expect the fauna at Térapa to fill geographic gaps in the distributions of Pleistocene taxa because of its location in northwest Mexico, which has a poorly documented Ice Age fauna (Ferrusquía-Villafranca et al. 2010). This location is positioned between temperate and tropical faunas and may have served as a point of exchange during faunal range shifts.

Finally, conservation and other science-based practices benefit from increased public understanding of science and greater inclusion of underrepresented groups. Moreover, interacting with a scientist or STEM professional can result in positive learning outcomes for participants, such as increased interest in science, learning, and awareness of STEM careers (Wiehe 2014, Boyette and Ramsey 2019). Informal learning institutions (ILIs), such as botanical gardens and arboretums, zoos and aquariums, public libraries, National Park Service lands, and biological field stations and marine

laboratories, create opportunities to increase scientific literacy and promote better representation of underrepresented groups in STEM careers (NASEM 2016); however, they are not equally distributed across the US.

Using kernel density surfaces, I explore which types of ILIs occur in areas with higher or lower densities of other ILIs. I identify geographic gaps in the ILI landscape and, using simple densities at the county-level, identify three groups of underserved counties based on the interaction between population density and poverty percentage. Within those underserved counties, I consider racial and ethnic populations to connect the density of ILIs to populations of groups underrepresented in STEM careers. I expect areas of low population density and high poverty to have the lowest density of ILIs because the communities may have few resources. I expect groups already underrepresented in STEM to have higher than expected populations in the areas that are considered underserved by ILIs.

### 1.2. Science and society

I relate modern and past mammal morphology, climate, and environmental data to advance our understanding of Earth's biodiversity and inform on mammalian responses to habitat loss and climate change. In the 20th century, many species, including many plants, mammals, birds, and butterflies, shifted their geographical ranges more than 10km north per decade (Parmesan and Yohe 2003, Hickling et al. 2006, Loarie et al. 2009). With three research chapters focused on faunal responses to environmental change, I advance our study of biodiversity response to environmental change though time. My fourth research chapter facilitates the transfer of knowledge

from scientists to the public by highlighting informal learning opportunities that can be leveraged to increase public understanding of science and environmental stewardship.

**References**


Barnosky AD, Hadly EA, Gonzalez P, Head J, Polly PD, Lawing AM, Eronen JT, Ackerly DD, Alex K, Biber E, Blois J, Brashares J, Ceballos G, Davis E, Dietl GP, Dirzo R, Doremus H, Fortelius M, Greene HW, Hellmann J, Hickler T, Jackson ST, Kemp M, Koch PL, Kremen C, Lindsey EL, Looy C, Marshall CR, Mendenhall C, Mulch A, Mychajliw AM, Nowak C, Ramakrishnan U, Schnitzler J, Das Shrestha K, Solari K, Stegner L, Stegner MA, Stenseth NC, Wake MH, Zhang Z. 2017. Merging paleobiology with conservation biology to guide the future of terrestrial ecosystems. Science 355: eaah4787.

Barnosky AD, Matzke N, Tomiya S, Wogan GOU, Swartz B, Quental TB, Marshall C, McGuire JL, Lindsey EL, Maguire KC, Mersey B, Ferrer EA. 2011. Has the Earth's sixth mass extinction already arrived? Nature 471: 51–57.

Boyette T, Ramsey JR. 2019. Does the messenger matter? Studying the impacts of scientists and engineers interacting with public audiences at science festival events. Journal of Science Communication 18: 1–16.

Bright J, Orem CA, Mead JI, Baez A. 2016. Late Pleistocene (OIS 3) paleoenvironmental reconstruction for the Térapa vertebrate site, northcentral Sonora, Mexico, based on stable isotopes and autecology of ostracodes. Revista Mexicana de Ciencias Geologicas 33: 239–253.

Cadotte M, Albert CH, Walker SC. 2013. The ecology of differences: Assessing community assembly with trait and evolutionary distances. Ecology Letters 16: 1234–1244.

Ceballos G, Ehrlich PR, Barnosky AD, García A, Pringle RM, Palmer TM. 2015. Accelerated modern human-induced species losses: Entering the sixth mass extinction. Science Advances 1: 1–5.

Ceballos G, Ehrlich PR, Soberón J, Salazar I, Fay JP. 2005. Global mammal conservation: What must we manage? Science 309: 603–607.

Van Devender TR. 2007. Ice ages in the Sonoran Desert: Pinyon pines and Joshua trees in the Dry Borders Region. Pages 58–68 in Felger RS and Broyles B, eds. Dry Borders: Great Natural Reserves of the Sonoran Desert. University of Utah Press.

Dietl GP, Flessa KW. 2011. Conservation paleobiology: Putting the dead to work. Trends in Ecology and Evolution 26: 30–37.

Dietl GP, Kidwell SM, Brenner M, Burney DA, Flessa KW, Jackson ST, Koch PL. 2015. Conservation paleobiology: Leveraging knowledge of the past to inform conservation and restoration. Annual Review of Earth and Planetary Sciences 43: 79–103.

Enquist BJ, Norberg J, Bonser SP, Violle C, Webb CT, Henderson A, Sloat LL, Savage VM. 2015. Scaling from traits to ecosystems: Developing a general trait driver theory via integrating trait-based and metabolic scaling theories. Advances in Ecological Research 52: 249–318.

Eronen JT, Polly PD, Fred M, Damuth J, Frank DC, Mosbrugger V, Scheidegger C, Stenseth NC, Fortelius M. 2010a. Ecometrics: The traits that bind the past and present together. Integrative Zoology 5: 88–101.

Eronen JT, Puolamäki K, Liu L, Lintulaakso K, Damuth J, Janis C, Fortelius M. 2010b. Precipitation and large herbivorous mammals II: Application to fossil data. Evolutionary Ecology Research 12: 235–248.

Eronen JT, Puolamäki K, Liu L, Lintulaakso K, Damuth J, Janis C, Fortelius M. 2010c. Precipitation and large herbivorous mammals I: Estimates from present-day communities. Evolutionary Ecology Research 12: 217–233.

Ferrusquía-Villafranca I, Arroyo-Cabrales J, Martínez-Hernández E, Gama-Castro J, Ruiz-González J, Polaco OJ, Johnson E. 2010. Pleistocene mammals of Mexico: A critical review of regional chronofaunas, climate change response and biogeographic provinciality. Quaternary International 217: 53–104.

Foley JA, DeFries R, Asner GP, Barford C, Bonan G, Carpenter SR, Chapin FS, Coe MT, Daily GC, Gibbs HK, Helkowski JH, Holloway T, Howard EA, Kucharik CJ, Monfreda C, Patz JA, Prentice IC, Ramankutty N, Snyder PK. 2005. Global consequences of land use. Science 309: 570–574.

Fortelius M, Eronen J, Jernvall J, Liu L, Pushkina D, Rinne J, Tesakov A, Vislobokova I, Zhang Z, Zhou L. 2002. Fossil mammals resolve regional patterns of Eurasian climate change over 20 million years. Evolutionary Ecology Research 4: 1005–1016.

Fortelius M, Eronen J, Liu L, Pushkina D, Tesakov A, Vislobokova I, Zhang Z. 2006. Late Miocene and Pliocene large land mammals and climatic changes in Eurasia. Palaeogeography, Palaeoclimatology, Palaeoecology 238: 219–227.

Foss S, Prothero D. 2007. Introduction. Pages 1–3 in Prothero D and Foss S, eds. The Evolution of Artiodactyls. Johns Hopkins University Press.

Hickling R, Roy DB, Hill JK, Fox R, Thomas CD. 2006. The distributions of a wide

range of taxonomic groups are expanding polewards. Global Change Biology 12: 450–455.

Janis CM, Damuth J, Theodor JM. 2000. Miocene ungulates and terrestrial primary productivity: Where have all the browsers gone? Proceedings of the National Academy of Sciences 97: 7899–7904.

Janis CM, Damuth J, Theodor JM. 2002. The origins and evolution of the North American grassland biome: The story from the hoofed mammals. Palaeogeography, Palaeoclimatology, Palaeoecology 177: 183–198.

Lawing AM, Eronen JT, Blois JL, Graham CH, Polly PD. 2017. Community functional trait composition at the continental scale: The effects of non-ecological processes. Ecography 40: 651–663.

Loarie SR, Duffy PB, Hamilton H, Asner GP, Field CB, Ackerly DD. 2009. The velocity of climate change. Nature 462: 1052–1055.

McGill BJ, Enquist BJ, Weiher E, Westoby M. 2006. Rebuilding community ecology from functional traits. Trends in Ecology and Evolution 21: 178–185.

Mead JI, Baez A, Swift SL, Carpenter MC, Hollenshead M, Czaplewski NJ, Steadman DW, Bright J, Arroyo-Cabrales J. 2006. Tropical marsh and savanna of the Late Pleistocene in northeastern Sonora, Mexico. The Southwestern Naturalist 51: 226–239.

Merceron G, Ramdarshan A, Blondel C, Boisserie JR, Brunetiere N, Francisco A, Gautier D, Milhet X, Novello A, Pret D. 2016. Untangling the environmental from the dietary: Dust does not matter. Proceedings of the Royal Society B: Biological Sciences 283: 20161032.

[NASEM] National Academies of Sciences Engineering and Medicine. 2016. Science Literacy: Concepts, Contexts, and Consequences. The National Academies Press.

Nunez EE, Macfadden BJ, Mead JI, Baez A. 2010. Ancient forests and grasslands in the desert: Diet and habitat of Late Pleistocene mammals from northcentral Sonora, Mexico. Palaeogeography, Palaeoclimatology, Palaeoecology 297: 391–400.

Parmesan C, Yohe G. 2003. A globally coherent fingerprint of climate change impacts across natural systems. Nature 421: 37–42.

Polly PD. 2010. Tiptoeing through the trophics: Geographic variation in carnivoran locomotor ecomorphology in relation to environment. Pages 374–410 in Goswami A and Friscia A, eds. Carnivoran Evolution: New Views on Phylogeny, Form, and Function. Cambridge University Press.

Polly PD, Eronen JT, Fred M, Dietl GP, Mosbrugger V, Scheidegger C, Frank DC, Damuth J, Stenseth NC, Fortelius M. 2011. History matters: Ecometrics and integrative climate change biology. Proceedings of the Royal Society B: Biological Sciences 278: 1131–1140.

Polly PD, Head JJ. 2015. Measuring Earth-life transitions: Ecometric analysis of functional traits from late Cenozoic vertebrates. Pages 21–46 in Polly PD, Head JJ, and Fox DL, eds. Earth-Life Transitions: Paleobiology in the Context of Earth System Evolution, vol. 21. The Paleontological Society.

Polly PD, Lawing AM, Eronen JT, Schnitzler J. 2016. Processes of ecometric patterning: Modelling functional traits, environments, and clade dynamics in deep time. Biological Journal of the Linnean Society 118: 39–63.

Semprebon G, Rivals F, Janis CM. 2019. The role of grass vs. exogenous abrasives in the paleodietary patterns of North American ungulates. Frontiers in Ecology and Evolution 7: 1–23.

Start D, Gilbert B. 2019. Trait variation across biological scales shapes community structure and ecosystem function. Ecology 100: e02769.

Strömberg CAE. 2002. The origin and spread of grass-dominated ecosystems in the late Tertiary of North America: Preliminary results concerning the evolution of hypsodonty. Palaeogeography, Palaeoclimatology, Palaeoecology 177: 59–75.

Strömberg CAE. 2006. Evolution of hypsodonty in equids: Testing a hypothesis of adaptation. Paleobiology 32: 236–258.

Tóth AB, Lyons SK, Barr WA, Behrensmeyer AK, Blois JL, Bobe R, Davis M, Du A, Eronen JT, Faith JT, Fraser D, Gotelli NJ, Graves GR, Jukar AM, Miller JH, Pineda-Munoz S, Soul LC, Villaseñor A, Alroy J. 2019. Reorganization of surviving mammal communities after the end-Pleistocene megafaunal extinction. Science 365: 1305–1308.

Violle C, Navas ML, Vile D, Kazakou E, Fortunel C, Hummel I, Garnier E. 2007. Let the concept of trait be functional! Oikos 116: 882–892.

Wiehe B. 2014. When science makes us who we are: Known and speculative impacts of science festivals. Journal of Science Communication 13: C02.

Wilson D, Reeder D. 2005. Mammal Species of the World: A Taxonomic and Geographic Reference. 3rd ed. Johns Hopkins University Press.

# 2. COMPARISON OF ENVIRONMENTAL INFERENCE APPROACHES FOR ECOMETRIC ANALYSES: USING HYPSODONTY TO PREDICT PRECIPITATION

## 2.1. Introduction

Functional traits are measurable features that influence an organism's interaction with its environment (McGill et al. 2006, Violle et al. 2007). When measured in the fossil record, functional traits can be used for a thorough understanding of biotic responses to corresponding environmental changes (Eronen et al. 2010a), which can contribute to improved predictions of future faunal communities as they face severe impacts from environmental change (Ceballos et al. 2005, 2015, Barnosky et al. 2011). With climate expected to continue changing at unprecedented rates (IPCC 2014, Wuebbles et al. 2017), it is important to better understand the past so that we can anticipate future faunal responses.

Ecometric analyses were developed to predict paleoclimatic conditions from fossil assemblages by providing a linkage between paleontological data, modern data, and projections of functional responses to impending climate change (Polly et al. 2011, Polly and Head 2015). These studies use the trait-environment relationship to study assemblage-level responses over spatial and temporal scales (Eronen et al. 2010a, Polly et al. 2011, Polly and Head 2015). When there is a strong trait-environment relationship, the traits can act as predictors of environment (McGill et al. 2006, Eronen et al. 2010a), and paleontology can inform conservation efforts by providing a long-term record of change (Dietl and Flessa 2011, Dietl et al. 2015, Barnosky et al. 2017).

Previous research has demonstrated relationships between community-level trait composition and environmental variables, including for plant leaf margins (Wolfe 1979, Nicotra et al. 2011, Peppe et al. 2011, Royer et al. 2012), herbivore teeth (Eronen et al. 2010b, Evans 2013, Fortelius et al. 2016), and locomotor skeletal elements of bovids (Barr 2017), carnivorans (Polly 2010), and snakes (Lawing et al. 2012), but the estimation methods have varied. Wolfe (1979) used linear regression to demonstrate that areas with high mean annual temperatures are dominated by leaves with entire margins while areas with low temperatures are dominated by leaves with non-entire margins. Eronen, Puolamäki, Liu, Lintulaakso, Damuth et al. (2010c) used linear regression and regression tree analysis to predict Eurasian paleoprecipitation from large mammal hypsodonty values. Barr (2017) used general linear models to study the relationship between bovid postcranial elements and vegetation cover and precipitation. Fortelius et al. (2016) used regression and k-nearest neighbor (kNN) on dental characters to investigate paleoenvironment in the Turkana Basin between 7 and 1 million years ago. Polly (2010) and Lawing et al. (2012) used maximum likelihood estimation to explore the ecometric value of carnivoran calcaneal morphology and relative snake tail length, respectively. The community of scientists using ecometrics for conservation paleontology will benefit from a discussion of when to use which methods because less accurate methods will cause misinterpretations when ecometric relationships are applied to the paleontological record.

Although the use of ecometrics has increased in recent years, only Fortelius et al. (2016) compares multiple methods—regression and k-nearest neighbor (kNN)—by also

using hypsodonty as the ecometric trait. In this case, the authors discuss merits of regression, which is easier to interpret because it produces an equation, and kNN, which is more sensitive to variation because it is non-linear. An analysis of additional estimation methods will enable better comparisons and address potential weaknesses of paleoenvironmental interpretations.

### 2.1.1. Herbivore hypsodonty

Hypsodonty is the ratio of the tooth crown height to root height of the molars, and the relationship between hypsodonty and annual precipitation and is highly correlated in large and small mammals (Eronen et al. 2010b, Lawing et al. 2017). Hypsodonty is functionally related to the durability of teeth in herbivores and provides biomechanical advantages, including more restricted areas of stress and increased occlusal pressure, to support more efficient mastication of grass and other tough, poor quality vegetation (Demiguel et al. 2016, Solounias et al. 2019). Increased hypsodonty has been linked to more roughage in the diet (Strömberg 2002, 2006, Erickson 2014, Merceron et al. 2016) and increased environmental grit consumed during feeding (Damuth and Janis 2011, Jardine et al. 2012, Semprebon et al. 2019). It is possible that both diet and habitat play a role in the development of hypsodont dentition (Williams and Kay 2001, Toljagić et al. 2018), so that hypsodonty at the community level has changed with environments over time.

North American habitats became more open and grass-dominated in the Miocene (Edwards et al. 2010, Strömberg 2011). There were approximately 4 million years between the establishment of $C_3$ grasslands and the origination of equid hypsodonty in

the Great Plains of North America (Strömberg 2006); it was approximately another 10 million years until specialized grazers appeared (Janis 2008). Eventually, there was a turnover from predominately low-crowned to high-crowned taxa, so that communities with higher hypsodonty indices are generally found in more open and arid grasslands (Janis et al. 2000, 2002, Fortelius et al. 2002, Eronen et al. 2010c, Strömberg 2011). Annual precipitation predictions based on tooth morphology closely match predictions from climate modeling and paleovegetation records in Eurasia over the past 23 million years (Eronen et al. 2010c), and the same trait-environment relationship has been used to indicate changes in precipitation in Eurasia (Fortelius et al. 2002, Eronen et al. 2012), Italy (Meloro and Kovarovic 2013), and Kenya (Žliobaitė et al. 2016).

Here, we use the trait-environment relationship between hypsodonty and annual precipitation to compare four methods of ecometric estimation – linear regression, polynomial regression, nearest neighbor, and maximum likelihood. We aim to 1) explore differences in the predictive ability of each method and 2) apply each method to Late Pleistocene fossil localities to demonstrate the potential impact of method selection on paleoenvironmental interpretations. We expect maximum likelihood to produce the most accurate predictions of precipitation from community hypsodonty values because the method predicts precipitation by fitting a model to a localized subset of communities that have similar trait values. For that reason, we also expect maximum likelihood to predict paleoprecipitation that most closely align with global climate models.

## 2.2. Materials and methods

We used modern communities of herbivores and annual precipitation data to evaluate four prediction methods for ecometric analyses and investigate the capacity of each method to predict paleoprecipitation for paleontological sites.

### 2.2.1. Study area and taxa

We used the extant species of Artiodactyla, Perissodactyla, Rodentia, and Lagomorpha (n = 404) in North America, because they represent the primary herbivores in North American mammalian communities. Jardine et al. (2012) suggested not including fossorial rodents and lagomorphs in studies of precipitation because these taxa are under selective pressures that do not co-vary with aridity. However, hypsodonty, as well as fossorial behavior, of small mammals increased as habitats became more dry and open (Samuels and Hopkins 2017), and the relationship between hypsodonty and precipitation occurs in Dipodidae, which includes fossorial species (Ma et al. 2017). Thus, we have included all Glires here to encompass the majority of the herbivorous mammal community.

We recognize that the North American fauna is biased following the Pleistocene mass extinction (Carrasco et al. 2009, Barnosky et al. 2011) and, therefore, the predictive abilities of the methods will be lower. However, because the relationship between hypsodonty and precipitation is well-established, it provides a good dataset for relative comparisons of paleoenvironmental reconstruction methods.

### 2.2.2. Traits and communities

Hypsodonty data for this paper came from an existing dataset, which has been used to investigate trait composition at the community level in North America (Lawing et al. 2017). Crown height for each species was assigned a value of 3 (hypsodont, high crown height), 2 (mesodont, moderate crown height), or 1 (brachydont, low crown height) (Fortelius et al., 2002; Figure 2.1). An additional 72 species were assigned hypsodonty values based on literature for a total of 446 species. Some members of Rodentia and Lagomorpha have evolved hypselodont dentition in which the teeth continue to emerge throughout the lifespan; these taxa are classified as hypsodont for the purposes of this study following Fortelius et al. (2003).

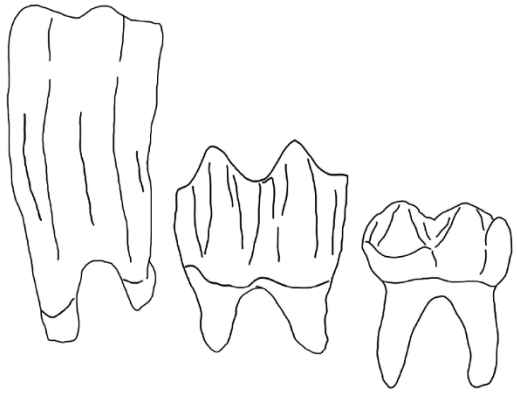

**Figure 2.1. Three levels of hypsodonty. Left, Hypsodont, or high tooth crown-root ratio, as represented by *Equus caballus*; Middle, Mesodont, or moderate tooth crown-root ratio, as represented by *Cervus canadensis*; Right, Brachydont, or low tooth crown-root ratio, as represented by *Tapirus terrestris*.**

Community composition was sampled using an equidistant 50-km point system (9,699 sampling points) in North America (Polly 2010, Lawing et al. 2012, 2017) from overlapping expert drawn polygon maps from NatureServe to produce community lists of North American Artiodactyla, Perissodactyla, Rodentia, and Lagomorpha with extant presence and native or reintroduced origin (those data were produced in collaboration with Bruce Patterson, Wes Sechrest, Marcelo Tognelli, Gerardo Ceballos, The Nature Conservancy – Migratory Bird Program, Conservation International – CABS, World Wildlife Fund – US, and Environment Canada – WILDSPACE; Patterson, Ceballos, Sechrest, Tognelli, Brooks, et al., 2007). Taxonomy associated with hypsodonty data and range maps were reviewed to ensure consistency following Wilson and Reeder (2005). Only sampling points with a species richness of five or more were kept. We calculated the mean (Figure 2.2A) and standard deviation of hypsodonty for every sample point.

Our dataset on communities included the presumed presence or absence of species at each sampling location across North America because the ranges are not based only on direct observations. Another measure of community composition could include recording the presumed abundance of species within communities. That would allow us to weigh the traits by the most commonly occurring taxa (sensu Faith, Du, & Rowan, 2019). Faith et al. (2019) show that using abundance instead of occurrence allows for weighted ecometric means that can produce more robust paleoclimate predictions. Despite these benefits, we chose to use occurrences rather than abundance to 1) use range maps in place of observational data for the modern communities, ensuring larger coverage, 2) mirror available data at fossil sites that lack abundance descriptions, 3)

overcome potential sampling bias that occurs in a dataset that includes both small and large mammals, and 4) replicate methods most commonly used in ecometric studies. In addition, gathering abundance data from the fossil record is highly susceptible to taphonomy and collection practices (Hernández Fernández and Vrba 2006, Crees et al. 2019).

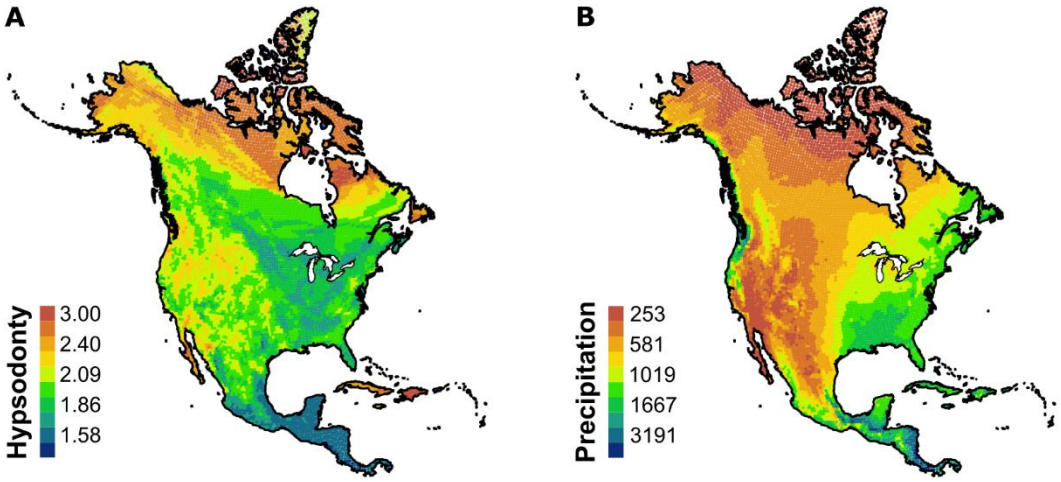


**Figure 2.2. Data used in this study. Legend values are the maximum values for the bin. A, Mean community hypsodonty values; B, Mean annual precipitation in log mm.**

### 2.2.3. Environmental data

Annual precipitation data were downloaded from the WorldClim database at the 2.5-degree grid scale (Hijmans et al. 2005) and extracted at each sampling point across North America (Figure 2.2B). The natural log of annual precipitation was used to transform the data for normality.

### 2.2.4. Ecometric analyses

Four inference methods were selected for comparison: linear regression, polynomial regression, nearest neighbor, and maximum likelihood. Linear regression and polynomial regression produced predictions using the formula of a line of best fit that is either linear or nonlinear, respectively. Nearest neighbor predicted precipitation by using training data and the *k* closest communities of hypsodonty values. We used 20% of the data as training data and $k = 15$ to include the 15 nearest neighbors in the analysis following Fortelius et al. (2016) who used $k = 15$ using a cross-validation analysis of hypsodonty and precipitation. For the maximum likelihood, communities were binned into 25 x 25 cells based on the mean and standard deviation their hypsodonty values following Lawing et al. (2012) and Vermillion et al. (2018). Each bin was analyzed to estimate the most likely precipitation value for communities with the same trait mean and standard deviation.

Maps of predicted annual precipitation were produced using the community hypsodonty data and each of the inference methods. This step allowed for precipitation predictions to be evaluated through comparisons with the observed precipitation dataset. Predicted values were subtracted from the observed values, and differences were mapped to generate anomaly maps (Polly and Sarwar 2014); smaller differences between predicted and observed values indicated a less biased prediction. Predictions were used to test the Pearson correlation of each method with observed precipitation and the other three methods. An ANOVA test was used to compare the group means across the methods.

### 2.2.5. Fossil sites application

Inference methods were applied to Late Pleistocene North American fossil sites to demonstrate differences in paleoprecipitation predictions. Case study sites were downloaded from the Paleobiology Database on 12 March 2019, using the following parameters: longitude = -230.449 – 36.5625, latitude = -5.0909 – 64.3969, time interval = Pleistocene, Orders = Artiodactyla, Perissodactyla, Rodentia, and Lagomorpha. Sites were further restricted to the Late Pleistocene (0.126 ma – 0.0117 ma) time bin and were limited to communities with at least five species (n = 43; Table A-1). Fossil taxa were assigned a hypsodonty index value based on literature and the New and Old World (NOW) Database of Fossil Mammals (The NOW Community 2019). Fossil sites were categorized as interglacial or glacial using literature sources that primarily reported relative dates with many of the site descriptions including either Sangamonian (i.e., interglacial) or Wisconsinan (i.e., glacial) terminology.

Global climate models (GCM) were downloaded for the last glacial maximum at 2.5 minutes resolution (Fick and Hijmans 2017) and for the last interglacial at 30 arc-seconds resolution (Otto-Bliesner et al. 2006, Fick and Hijmans 2017). Precipitation values were extracted from the GCM models at each site, and an average value was used for the two glacial GCMs – CCSM4 and MIROC-ESM. These models provided additional precipitation predictions to evaluate the accuracy of the ecometric predictions. For each fossil community, hypsodonty mean and standard deviation were calculated using only one occurrence of each species to prevent duplicating the trait value of any repeated taxa.

Four precipitation predictions were made for each community using the hypsodonty metrics and each inference method. Predictions were compared to the GCM values and to predictions from the other methods using Pearson's correlation tests. Anomalies were calculated by subtracting the predicted values from the GCM values at each site. All analyses were performed in R Statistical Package (R Core Team 2016).

**2.3. Results**

Linear regression predicts precipitation with anomalies that range between -4.90 log mm and 4.26 log mm (mean = 0.00 log mm, $R^2 = 0.408$, $p < 0.001$; Figure 2.3A), and polynomial regression produces anomalies that range between -4.86 log mm and 4.42 log mm (mean = 0.00 log mm, $R^2 = 0.436$, $p < 0.001$; Figure 2.3B). These methods overpredict precipitation in dry areas and underpredict precipitation in wet areas. Both regression methods overpredict precipitation in the North American deserts, the northern Great Plains, and the tundra, and underpredict precipitation along the Pacific Northwest coastline, throughout most of the eastern portion of the continent, and somewhat in Central America.

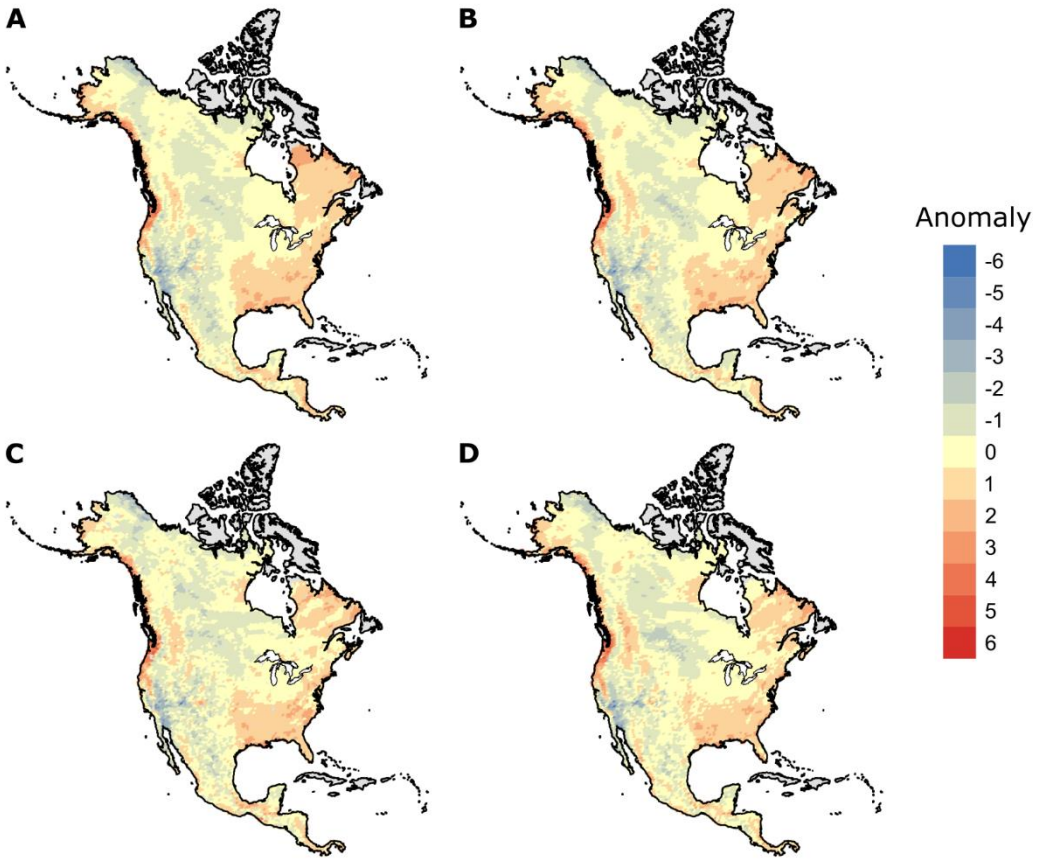


**Figure 2.3. Anomaly maps of differences between observed and predicted precipitation from four inference methods. A, linear regression; B, polynomial regression; C, nearest neighbor; and D, maximum likelihood. Scale is log mm and values are the mean of each color bin.**

Nearest neighbor predicts precipitation anomalies that range between -4.33 log mm and 4.28 log mm (mean = -0.020 log mm; Figure 2.3C), and maximum likelihood produces anomalies that range between -5.19 log mm and 4.23 log mm (mean = -0.003 log mm; Figure 2.3D). Nearest neighbor and maximum likelihood overpredict precipitation in dry areas, such as the arid southwest and in the tundra, and underpredict precipitation in wet areas, such as the Pacific Northwest coast and in the eastern part of

the continent. Nearest neighbor also overpredicts precipitation in the Rocky Mountains, and maximum likelihood also underpredicts precipitation in Central America. There is not a significant difference in anomalies between the four methods ($F(3, 30071) = 0.694$, $p = 0.556$), but maximum likelihood produces the most neutral (i.e., equal to zero) or nearly neutral anomalies suggesting more accurate predictions overall (Figure 2.4).

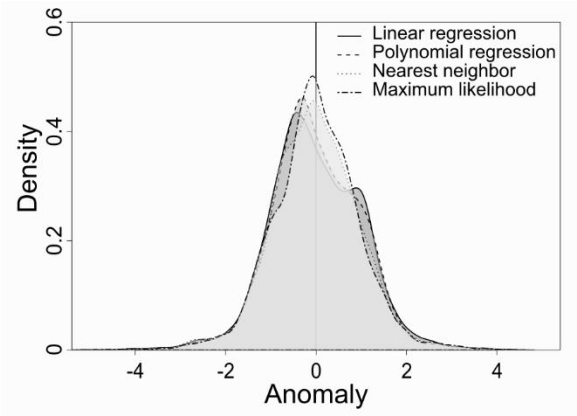


**Figure 2.4. Density of anomalies between observed and predicted precipitation using four inference methods.**

The four inference methods are all highly correlated with log precipitation and with the other methods, and all correlations are significant at $p < 0.001$ (Table 2.1). Precipitation is consistently correlated with each of the four methods ($r = 0.640 – 0.690$). Linear regression and polynomial regression are the most highly correlated methods ($r = 0.966$), whereas linear regression and maximum likelihood are the least correlated methods ($r = 0.897$).

**Table 2.1. Correlation matrix of observed and predicted precipitation values. All correlations are significant at $p < 0.001$.**

| | Precipitation (log mm) | Linear regression | Polynomial regression | Nearest neighbor |
|---|---|---|---|---|
| Linear regression | 0.640 | | | |
| Polynomial regression | 0.663 | 0.966 | | |
| Nearest neighbor | 0.673 | 0.901 | 0.911 | |
| Maximum likelihood | 0.690 | 0.897 | 0.930 | 0.904 |

### 2.3.1. Paleoenvironment of fossil sites

Most of the paleontological case study sites are glacial (72%; Figure 2.5). Glacial and interglacial fossil communities are primarily hypsodont with some mesodont communities in the southeast; there are no brachydont communities. Interglacial predictions are higher than the GCMs across all sites (Figure 2.6A). Interglacial anomalies are centered at approximately -1.5 log mm and have a smaller range than glacial predictions (Figure 2.6B). At the interglacial sites, maximum likelihood is more closely aligned with the GCM mean. Glacial predictions are higher than the GCMs at high latitudes and converge at approximately 38°N (Strait Canyon, Virginia; Figure 2.6C). Differences in glacial precipitation predictions and GCMs are centered just below 0 log mm with a small increase at approximately 3 log mm (Figure 2.6D). Maximum likelihood produces bimodal anomalies at 0 log mm and -2 log mm, but other methods do not display this pattern. Predictions of precipitation at glacial sites more closely match the GCMs than do the predictions at interglacial sites (Figure 2.6).

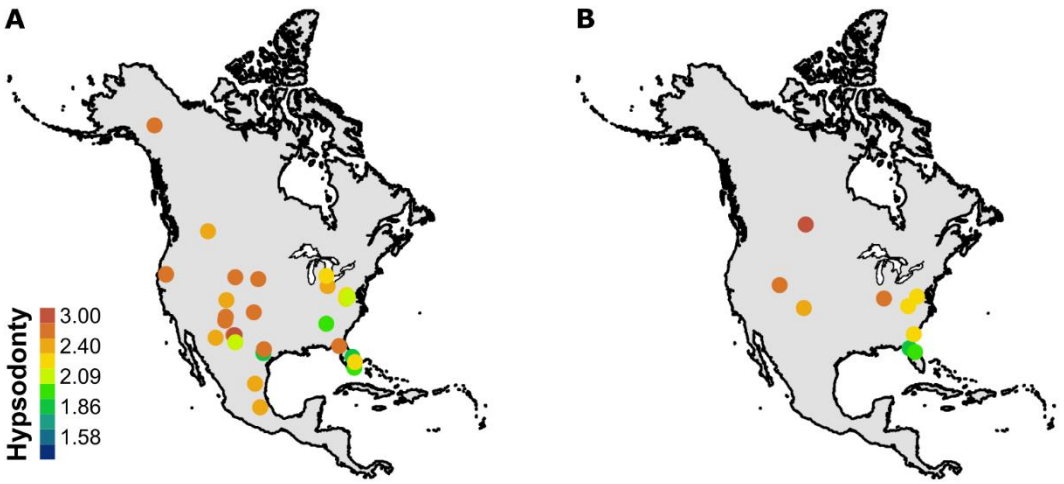


**Figure 2.5. Hypsodonty measures of fossil communities. Hypsodonty values are the maximum values for the bin. A, Glacial sites; B, Interglacial sites.**

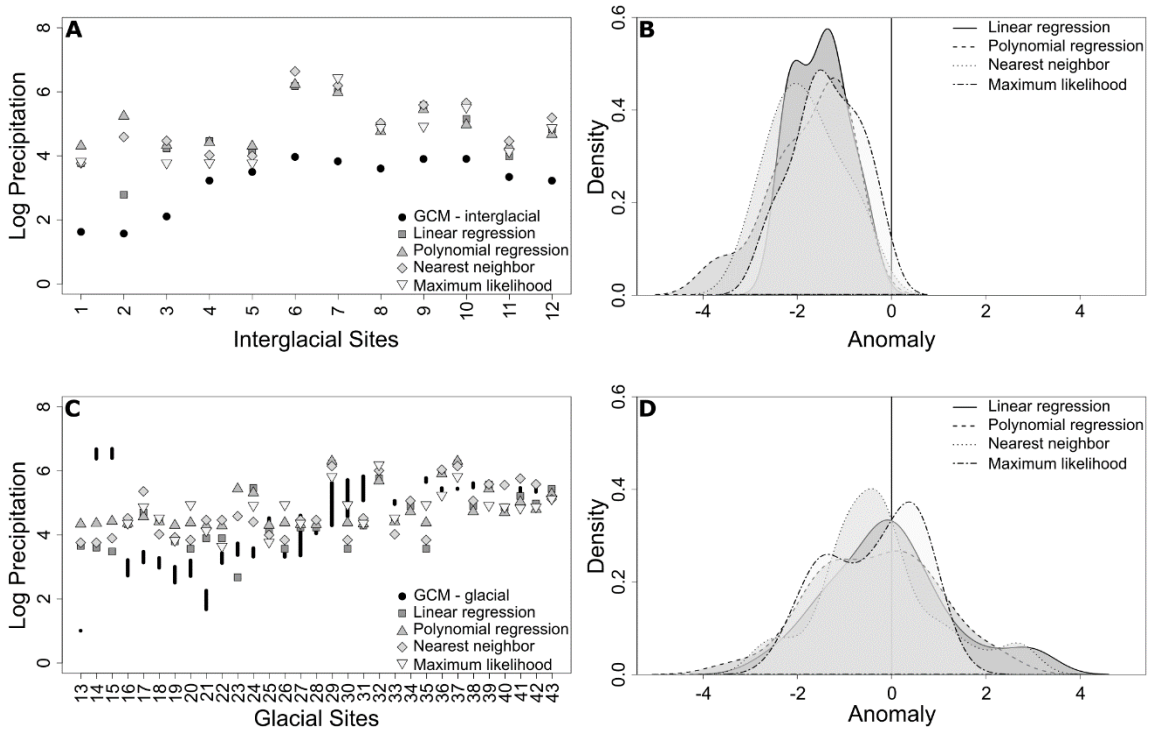


**Figure 2.6. Four predictions of precipitation for glacial and interglacial fossil sites. Glacial and interglacial global climate model predictions are for comparison. A, Predictions for interglacial sites; B, Predictions for glacial sites; C, Density plot of anomalies for interglacial sites; and D, Density plot of anomalies for glacial sites.**

## 2.4. Discussion

Trait-environment relationships can be used for understanding past environmental changes and corresponding biotic responses (Eronen et al. 2010a, Polly et al. 2011). Because there are minimal differences between inference methods (Figures 2.3, 2.4), we expect that, when a strong ecometric relationship exists, any of the investigated methods will capture the relationship between hypsodonty and precipitation. Therefore, any of the methods can be used to predict the environment from the distribution of trait values within a community. Hypsodonty and annual precipitation have a well-established relationship, but these methods may show more differences with a weaker trait-environment relationship.

Each method has constraints that should be considered when selecting a method for ecometric analyses. Linear regression is the least sensitive to variation in the trait-environment relationship because the inference model is derived from a fitted regression line. When the model is applied to new trait data to predict precipitation, each prediction comes from the equation of that regression line. Because precipitation predictions are forced to fit the regression line, there is a reasonable chance of over- and underprediction. Therefore, the precipitation predictions from the linear regression model have the weakest correlation with the observed precipitation (Table 2.1).

Similarly, polynomial regression uses a fitted regression curve of best fit for the inference model. Predictions of precipitation using polynomial regression places a known hypsodonty value along that curve. In this study, precipitation predictions from polynomial regression are more highly correlated with observed precipitation values

than those from linear regression or nearest neighbor (Table 2.1). However, polynomial regression is unable to predict precipitation values under 4.45 log mm because of the sinusoidal shape of the regression curve. Because of this lower limit of the curve, polynomial regression analyses will overpredict precipitation for communities dominated by taxa with hypsodont dentition because the model cannot predict low precipitation values.

Nearest neighbor uses a subset of data, i.e., training data, to construct a model. A training dataset should be large enough to provide a robust sample for model fit, thus it is more advantageous to use *k*-nearest neighbor with a large dataset (Bhatia 2010). In this study, the training data was 20% of the whole data set. The *k* value can also be changed to include more or fewer surrounding data points to determine the precipitation value associated with a known reference value. Here, the spatial pattern of overprediction in the arid southwest, tundra, and Rocky Mountains and underprediction in the Pacific Northwest and eastern North America is generally consistent with the other methods (Figure 2.3C), but precipitation predictions from nearest neighbor have the lowest correlations with the predictions from the other three methods (Table 2.1).

Maximum likelihood cannot predict precipitation for communities with a trait composition outside of the ecometric trait space used to calibrate the likelihood space. The ecometric trait space is constructed from the trait composition of modern communities. Therefore, in the paleontological case studies, two interglacial sites and seven glacial sites (21% of total sites) did not receive a maximum likelihood prediction of precipitation because the hypsodonty values fall outside of the occupied bins

designated based on the modern communities (Figure 2.6). Despite this limitation, precipitation predictions from maximum likelihood are the most highly correlated with observed precipitation (Table 2.1) and produce the most neutral or nearly neutral anomalies between predicted and observed precipitation values (Figure 2.4).

With evolutionary trends of increasing hypsodonty (Jernvall and Fortelius 2002, Jardine et al. 2012, Tapaltsyan et al. 2015), we might expect predictions built on extant taxa to generally underpredict paleoprecipitation. Because of the relationship between high hypsodonty and low precipitation, as hypsodonty increases through time, precipitation predictions would likely decrease. Here, the analyses are on a geologically small temporal scale of approximately 125,000 years, so it is unlikely this evolutionary pattern affected the trait-environment relationship, and the four methods mostly overpredicted or accurately predicted precipitation for the fossil sites when compared to the global climate models (Figure 2.6).

It might also be expected that today's interglacial fauna should more accurately predict paleoprecipitation at interglacial sites rather than glacial sites. However, the interglacial predictions are consistently offset from the interglacial global climate models, but more closely align with the glacial global climate models (Figure 2.7). In this case, today's interglacial faunal communities are, perhaps, more similar to the glacial communities. It is possible that the extant fauna is lagging behind the climate, so that the fauna has not fully responded to interglacial conditions. On the timescale of interglacial and glacial cycles, community reassembly, rather than evolutionary adaptation, may drive changes in trait composition (Polly et al. 2017). In the Holocene,

community assembly is largely affected by anthropogenic effects that have changed community structure patterns to include more segregated species pairs and restricted the interglacial reassembly that would have occurred, if not for the anthropogenic influence, following the last glacial maximum (Lyons et al. 2016).

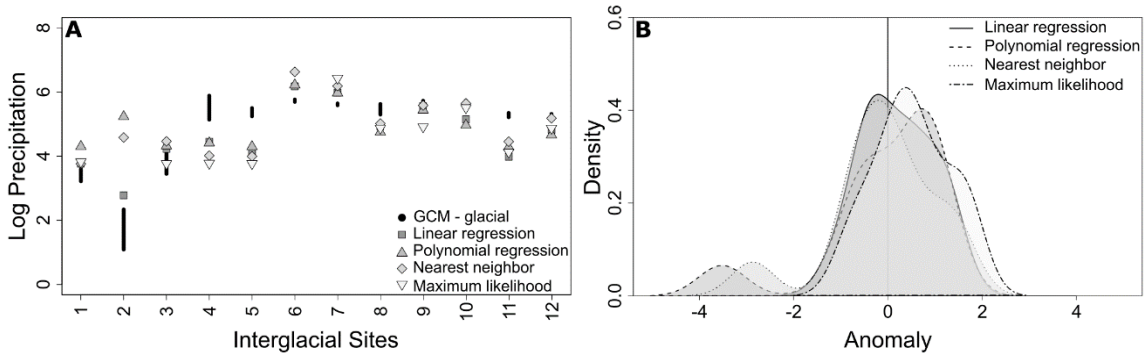


**Figure 2.7. Four predictions of precipitation for interglacial fossil sites compared to glacial global climate model predictions. A, Predictions for interglacial sites; and B, Density plot of anomalies for interglacial estimates of precipitation and glacial global climate models.**

### 2.4.1. Limitations

In this paper, we used community species lists extracted from expert drawn polygons of species geographic ranges, which typically overpredict species' presence within communities (Jetz et al. 2008, Cantú-Salazar and Gaston 2013). This could affect the trait values of communities that occur along distribution margins and weaken the predictive ability of the inference methods. Furthermore, although species occurrence data are from distribution estimates updated in 2007 (Patterson et al. 2007), precipitation is an average of data from 1970 – 2000 (Fick and Hijmans 2017). This temporal

mismatch may introduce a bias as faunal assemblages are increasingly affected by anthropogenic pressures, such as land use and habitat loss (Lyons et al. 2016, Hobbs et al. 2018). For example, a current species range map may no longer capture precipitation regime from 1970 – 2000, but may be a reflection of distribution constraints, such as habitat loss and competition from invasive or introduced species.

We have limited our modern community species lists to only native and reintroduced taxa. Extirpation or extinction of native species and the presence of invasives and non-native species can potentially change the trait values of a community, but, with a strong trait-environment relationship, it is unlikely that these taxa would change the trait values enough to notably change the environmental interpretation (Polly and Sarwar 2014). For instance, it was expected that the Pleistocene megafaunal extinction would create a bias and make the functions unable to predict precipitation of glacial sites. However, the glacial predictions more closely aligned with the global climate models (Figure 2.6).

Fossil sites were designated as interglacial and glacial using relative dating. Literature often described the fossil sites as having a Sangamonian (interglacial) or Wisconsinan (glacial) fauna, which made it difficult to use finer temporal resolution. Because of the consistent predictions within interglacial sites and glacial sites (Figure 2.6), it is unlikely that this caused a misinterpretation of results. It would be beneficial to further evaluate the pattern of overpredicting interglacial precipitation across sites using only fossil sites with absolute dating.

### 2.4.2. Implications

Evaluating ecological and evolutionary processes from data archived in the fossil record provides critical information about biodiversity to researchers, conservationists, and managers by facilitating a better understanding of anticipated biological responses to expected environmental changes (Dietl and Flessa 2011, Dietl et al. 2015, Barnosky et al. 2017). Paleobiological records provide a broader and deeper perspective that allow us to forecast how impending climate change will affect species and communities (Burney and Burney 2007, Lawing et al. 2016). Therefore, researchers are increasingly considering conservation implications in their paleontological work and, as such, it is important that we consider the methods used to define the trait-environment relationship. We show that the hypsodonty-precipitation relationship is identifiable with four different inference methods (Figure 2.3); although, maximum likelihood produces a better fit to observed data and more neutral anomalies than the other methods (Figure 2.4).

In this study, paleoprecipitation predictions of interglacial fossil communities were more closely aligned with glacial global climate models (Figures 2.6, 2.7). This pattern may be due to anthropogenic constraints on community reassembly in the Holocene (Lyons et al. 2016). For instance, today, only 41% of natural areas in the U.S. demonstrate climate connectivity, so that species can shift their ranges as climate change continues (McGuire et al. 2016). Thus, today's interglacial fauna may not be wholly representative of the fauna from the last interglacial period, but rather is more representative of the last glacial period. Future studies should consider this when working with glacial and interglacial faunal communities.

For a more complete understanding of community responses to environmental change through time, it is imperative that we further explore trait-environment relationships in the paleontological record that can be used in conjunction with other proxies and models, such as global climate models. By using multiple proxies either in parallel or in merged multi-proxy models, we can provide a more complete interpretation of past communities, which will be needed to anticipate faunal responses to ongoing environmental changes.

**References**


Barnosky AD, Hadly EA, Gonzalez P, Head J, Polly PD, Lawing AM, Eronen JT, Ackerly DD, Alex K, Biber E, Blois J, Brashares J, Ceballos G, Davis E, Dietl GP, Dirzo R, Doremus H, Fortelius M, Greene HW, Hellmann J, Hickler T, Jackson ST, Kemp M, Koch PL, Kremen C, Lindsey EL, Looy C, Marshall CR, Mendenhall C, Mulch A, Mychajliw AM, Nowak C, Ramakrishnan U, Schnitzler J, Das Shrestha K, Solari K, Stegner L, Stegner MA, Stenseth NC, Wake MH, Zhang Z. 2017. Merging paleobiology with conservation biology to guide the future of terrestrial ecosystems. Science 355: eaah4787.

Barnosky AD, Matzke N, Tomiya S, Wogan GOU, Swartz B, Quental TB, Marshall C, McGuire JL, Lindsey EL, Maguire KC, Mersey B, Ferrer EA. 2011. Has the Earth's sixth mass extinction already arrived? Nature 471: 51–57.

Barr WA. 2017. Bovid locomotor functional trait distributions reflect land cover and annual precipitation in sub-Saharan Africa. Evolutionary Ecology Research 18: 253–269.

Bhatia N. 2010. Survey of nearest neighbor techniques. International Journal of Computer Science and Information Security 8: 302–305.

Burney DA, Burney LP. 2007. Paleoecology and 'inter-situ' restoration on Kaua'i, Hawai'i. Frontiers in Ecology and the Environment 5: 483–490.

Cantú-Salazar L, Gaston KJ. 2013. Species richness and representation in protected areas of the Western hemisphere: Discrepancies between checklists and range maps. Diversity and Distributions 19: 782–793.

Carrasco MA, Barnosky AD, Graham RW. 2009. Quantifying the extent of North American mammal extinction relative to the pre-anthropogenic baseline. PLoS

ONE 4: 8331.

Ceballos G, Ehrlich PR, Barnosky AD, García A, Pringle RM, Palmer TM. 2015. Accelerated modern human-induced species losses: Entering the sixth mass extinction. Science Advances 1: 1–5.

Ceballos G, Ehrlich PR, Soberón J, Salazar I, Fay JP. 2005. Global mammal conservation: What must we manage? Science 309: 603–607.

Crees JJ, Collen B, Turvey ST. 2019. Bias, incompleteness and the 'known unknowns' in the Holocene faunal record. Philosophical Transactions of the Royal Society B: Biological Sciences 374: 20190216.

Damuth J, Janis CM. 2011. On the relationship between hypsodonty and feeding ecology in ungulate mammals, and its utility in palaeoecology. Biological Reviews 86: 733–758.

Demiguel D, Azanza B, Cegoñino J, Ruiz I, Morales J. 2016. The interplay between increased tooth crown-height and chewing efficiency, and implications for Cervidae evolution. Lethaia 49: 117–129.

Dietl GP, Flessa KW. 2011. Conservation paleobiology: Putting the dead to work. Trends in Ecology and Evolution 26: 30–37.

Dietl GP, Kidwell SM, Brenner M, Burney DA, Flessa KW, Jackson ST, Koch PL. 2015. Conservation paleobiology: Leveraging knowledge of the past to inform conservation and restoration. Annual Review of Earth and Planetary Sciences 43: 79–103.

Edwards EJ, Osborne CP, Strömberg CAE, Smith SA, C4 Grasses Consortium. 2010. The origins of C4 grasslands: Integrating evolutionary and ecosystem science. Science 328: 587–591.

Erickson KL. 2014. Prairie grass phytolith hardness and the evolution of ungulate hypsodonty. Historical Biology 26: 737–744.

Eronen JT, Fortelius M, Micheels A, Portmann FT, Puolamäki K, Janis CM. 2012. Neogene aridification of the northern hemisphere. Geology 40: 823–826.

Eronen JT, Polly PD, Fred M, Damuth J, Frank DC, Mosbrugger V, Scheidegger C, Stenseth NC, Fortelius M. 2010a. Ecometrics: The traits that bind the past and present together. Integrative Zoology 5: 88–101.

Eronen JT, Puolamäki K, Liu L, Lintulaakso K, Damuth J, Janis C, Fortelius M. 2010b. Precipitation and large herbivorous mammals I: Estimates from present-day

communities. Evolutionary Ecology Research 12: 217–233.

Eronen JT, Puolamäki K, Liu L, Lintulaakso K, Damuth J, Janis C, Fortelius M. 2010c. Precipitation and large herbivorous mammals II: Application to fossil data. Evolutionary Ecology Research 12: 235–248.

Evans AR. 2013. Shape descriptors as ecometrics in dental ecology. Hystrix 24: .

Faith JT, Du A, Rowan J. 2019. Addressing the effects of sampling on ecometric-based paleoenvironmental reconstructions. Palaeogeography, Palaeoclimatology, Palaeoecology 528: 175–185.

Fick SE, Hijmans RJ. 2017. WorldClim 2: New 1-km spatial resolution climate surfaces for global land areas. International Journal of Climatology 37: 4302–4315.

Fortelius M, Eronen J, Jernvall J, Liu L, Pushkina D, Rinne J, Tesakov A, Vislobokova I, Zhang Z, Zhou L. 2002. Fossil mammals resolve regional patterns of Eurasian climate change over 20 million years. Evolutionary Ecology Research 4: 1005–1016.

Fortelius M, Eronen J, Liu L, Pushkina D, Tesakov A, Vislobokova I, Zhang Z. 2003. Continental-scale hypsodonty patterns, climatic paleobiogeography and dispersal of Eurasian Neogene large mammal herbivores. Deinsea 10: 1–11.

Fortelius M, Žliobaitė I, Kaya F, Bibi F, Bobe R, Leakey L, Leakey M, Patterson D, Rannikko J, Werdelin L. 2016. An ecometric analysis of the fossil mammal record of the Turkana Basin. Philosophical Transactions of the Royal Society B: Biological Sciences 371: 20150232.

Hernández Fernández M, Vrba ES. 2006. Plio-Pleistocene climatic change in the Turkana Basin (East Africa): Evidence from large mammal faunas. Journal of Human Evolution 50: 595–626.

Hijmans RJ, Cameron SE, Parra JL, Jones PG, Jarvis A. 2005. Very high resolution interpolated climate surfaces for global land areas. International Journal of Climatology 25: 1965–1978.

Hobbs RJ, Valentine LE, Standish RJ, Jackson ST. 2018. Movers and stayers: Novel assemblages in changing environments. Trends in Ecology and Evolution 33: 116–128.

[IPCC] Intergovernmental Panel on Climate Change. 2014. Climate Change 2014: Synthesis Report. Contribution of Working Groups I, II, and III to the 5th Assessment Report of the Intergovernmental Panel on Climate Change.

Janis CM. 2008. An Evolutionary History of Browsing and Grazing Ungulates. Pages 21–45 in Gordon IJ and Prins HHT, eds. The Ecology of Browsing and Grazing. Springer-Verlag.

Janis CM, Damuth J, Theodor JM. 2000. Miocene ungulates and terrestrial primary productivity: Where have all the browsers gone? Proceedings of the National Academy of Sciences 97: 7899–7904.

Janis CM, Damuth J, Theodor JM. 2002. The origins and evolution of the North American grassland biome: The story from the hoofed mammals. Palaeogeography, Palaeoclimatology, Palaeoecology 177: 183–198.

Jardine PE, Janis CM, Sahney S, Benton MJ. 2012. Grit not grass: Concordant patterns of early origin of hypsodonty in Great Plains ungulates and Glires. Palaeogeography, Palaeoclimatology, Palaeoecology 365–366: 1–10.

Jernvall J, Fortelius M. 2002. Common mammals drive the evolutionary increase of hypsodonty in the Neogene. Nature 417: 538–540.

Jetz W, Sekercioglu CH, Watson JEM. 2008. Ecological correlates and conservation implications of overestimating species geographic ranges. Conservation Biology 22: 110–119.

Lawing AM, Eronen JT, Blois JL, Graham CH, Polly PD. 2017. Community functional trait composition at the continental scale: The effects of non-ecological processes. Ecography 40: 651–663.

Lawing AM, Head JJ, Polly PD. 2012. The ecology of morphology: The ecometrics of locomotion and macroenvironment in North American snakes. Pages 117–146 in Louys J, ed. Paleontology in Ecology and Conservation. Springer-Verlag Berlin Heidelberg.

Lawing AM, Polly PD, Hews DK, Martins EP. 2016. Including fossils in phylogenetic climate reconstructions: A deep time perspective on the climatic niche evolution and diversification of spiny lizards (*Sceloporus*). American Naturalist 188: 133–148.

Lyons SK, Amatangelo KL, Behrensmeyer AK, Bercovici A, Blois JL, Davis M, Dimichele WA, Du A, Eronen JT, Tyler Faith J, Graves GR, Jud N, Labandeira C, Looy C V., McGill B, Miller JH, Patterson D, Pineda-Munoz S, Potts R, Riddle B, Terry R, Tóth A, Ulrich W, Villaseñor A, Wing S, Anderson H, Anderson J, Waller D, Gotelli NJ. 2016. Holocene shifts in the assembly of plant and animal communities implicate human impacts. Nature 529: 80–83.

Ma H, Ge D, Shenbrot G, Pisano J, Yang Q, Zhang Z. 2017. Hypsodonty of Dipodidae

(Rodentia) in correlation with diet preferences and habitats. Journal of Mammalian Evolution 24: 485–494.

McGill BJ, Enquist BJ, Weiher E, Westoby M. 2006. Rebuilding community ecology from functional traits. Trends in Ecology and Evolution 21: 178–185.

McGuire JL, Lawler JJ, Mcrae BH, Nuñez TA, Theobald DM. 2016. Achieving climate connectivity in a fragmented landscape. PNAS 113: 7195–7200.

Meloro C, Kovarovic K. 2013. Spatial and ecometric analyses of the Plio-Pleistocene large mammal communities of the Italian peninsula. Journal of Biogeography 40: 1451–1462.

Merceron G, Ramdarshan A, Blondel C, Boisserie JR, Brunetiere N, Francisco A, Gautier D, Milhet X, Novello A, Pret D. 2016. Untangling the environmental from the dietary: Dust does not matter. Proceedings of the Royal Society B: Biological Sciences 283: .

Nicotra AB, Leigh A, Boyce CK, Jones CS, Niklas KJ, Royer DL, Tsukaya H. 2011. The evolution and functional significance of leaf shape in the angiosperms. Functional Plant Biology 38: 535–552.

Otto-Bliesner BL, Marshall SJ, Overpeck JT, Miller GH, Hu A. 2006. Simulating arctic climate warmth and icefield retreat in the last interglaciation. Science 311: 1751–1753.

Patterson B, Ceballos G, Sechrest W, Tognelli M, Brooks T, Luna L, Ortega P, Salazar I, Young B. 2007. Digital Distribution Maps of the Mammals of the Western Hemisphere, version 3.0. NatureServe.

Peppe DJ, Royer DL, Cariglino B, Oliver SY, Newman S, Leight E, Enikolopov G, Fernandez-Burgos M, Herrera F, Adams JM, Correa E, Currano ED, Erickson JM, Hinojosa LF, Hoganson JW, Iglesias A, Jaramillo CA, Johnson KR, Jordan GJ, Kraft NJB, Lovelock EC, Lusk CH, Niinemets Ü, Peñuelas J, Rapson G, Wing SL, Wright IJ. 2011. Sensitivity of leaf size and shape to climate: Global patterns and paleoclimatic applications. New Phytologist 190: 724–739.

Polly PD. 2010. Tiptoeing through the trophics: Geographic variation in carnivoran locomotor ecomorphology in relation to environment. Pages 374–410 in Goswami A and Friscia A, eds. Carnivoran Evolution: New Views on Phylogeny, Form, and Function. Cambridge University Press.

Polly PD, Eronen JT, Fred M, Dietl GP, Mosbrugger V, Scheidegger C, Frank DC, Damuth J, Stenseth NC, Fortelius M. 2011. History matters: Ecometrics and integrative climate change biology. Proceedings of the Royal Society B: Biological

Sciences 278: 1131–1140.

Polly PD, Fuentes-Gonzalez J, Lawing AM, Bormet AK, Dundas RG. 2017. Clade sorting has a greater effect than local adaptation on ecometric patterns in Carnivora. Evolutionary Ecology Research 18: .

Polly PD, Head JJ. 2015. Measuring Earth-life transitions: Ecometric analysis of functional traits from late Cenozoic vertebrates. Pages 21–46 in Polly PD, Head JJ, and Fox DL, eds. Earth-Life Transitions: Paleobiology in the Context of Earth System Evolution, vol. 21. The Paleontological Society.

Polly PD, Sarwar S. 2014. Extinction, extirpation, and exotics: Effects on the correlation between traits and environment at the continental level. Annales Zoologici Fennici 51: 209–226.

R Core Team. 2016. R: A language and environment for statistical computing. .

Royer DL, Peppe DJ, Wheeler EA, Niinemets Ü. 2012. Roles of climate and functional traits in controlling toothed vs. untoothed leaf margins. American Journal of Botany 99: 915–922.

Samuels JX, Hopkins SSB. 2017. The impacts of Cenozoic climate and habitat changes on small mammal diversity of North America. Global and Planetary Change 149: 36–52.

Semprebon G, Rivals F, Janis CM. 2019. The role of grass vs. exogenous abrasives in the paleodietary patterns of North American ungulates. Frontiers in Ecology and Evolution 7: 1–23.

Solounias N, Danowitz M, Buttar I, Coopee Z. 2019. Hypsodont crowns as additional roots: A new explanation for hypsodonty. Frontiers in Ecology and Evolution 7: 1–10.

Strömberg CAE. 2002. The origin and spread of grass-dominated ecosystems in the late Tertiary of North America: Preliminary results concerning the evolution of hypsodonty. Palaeogeography, Palaeoclimatology, Palaeoecology 177: 59–75.

Strömberg CAE. 2006. Evolution of hypsodonty in equids: Testing a hypothesis of adaptation. Paleobiology 32: 236–258.

Strömberg CAE. 2011. Evolution of grasses and grassland ecosystems. Annual Review of Earth and Planetary Sciences 39: 517–544.

Tapaltsyan V, Eronen JT, Lawing AM, Sharir A, Janis C, Jernvall J, Klein OD. 2015. Continuously growing rodent molars result from a predictable quantitative

evolutionary change over 50 million years. Cell Reports 11: 673–680.

The NOW Community. 2019. New and Old Worlds Database of Fossil Mammals (NOW). (http://www.helsinki.fi/science/now/).

Toljagić O, Voje KL, Matschiner M, Liow LH, Hansen TF. 2018. Millions of years behind: Slow adaptation of ruminants to grasslands. Systematic Biology 67: 145–157.

Vermillion WA, Polly PD, Head JJ, Eronen JT, Lawing AM. 2018. Ecometrics: a trait-based approach to paleoclimate and paleoenvironmental reconstruction. Pages 373–394 in Croft DA, Su D, and Simpson SW, eds. Methods in Paleoecology: Reconstructing Cenozoic Terrestrial Environments and Ecological Communities. Springer.

Violle C, Navas ML, Vile D, Kazakou E, Fortunel C, Hummel I, Garnier E. 2007. Let the concept of trait be functional! Oikos 116: 882–892.

Williams SH, Kay RF. 2001. A comparative test of adaptive explanations for hypsodonty in ungulates and rodents. Journal of Mammalian Evolution 8: 207–229.

Wilson D, Reeder D. 2005. Mammal Species of the World: A Taxonomic and Geographic Reference. 3rd ed. Johns Hopkins University Press.

Wolfe JA. 1979. Temperature parameters of humid to mesic forests of Eastern Asia and relation to forests of other regions of the Northern Hemisphere and Australasia. U.S. Geological Survey Professional Paper 1106: 1–37.

Wuebbles D, Fahey D, Hibbard K, DeAngelo B, Doherty S, Hayhoe K, Horton R, Kossin J, Taylor P, Waple A, Weaver C. 2017. Executive summary. Pages 12–34 in Wuebbles D, Fahey D, Hibbard K, Dokken D, Stewart B, and Maycock T, eds. Climate science special report: Fourth national climate assessment, volume 1. U.S. Global Change Research Program.

Žliobaitė I, Rinne J, Tóth AB, Mechenich M, Liu L, Behrensmeyer AK, Fortelius M. 2016. Herbivore teeth predict climatic limits in Kenyan ecosystems. Proceedings of the National Academy of Sciences 113: 12751–12756.

# 3. GEOGRAPHIC VARIATION IN ARTIODACTYL LOCOMOTOR MORPHOLOGY AS AN ENVIRONMENTAL PREDICTOR

## 3.1. Introduction

Functional traits are measurable features that influence an organism's interaction with its environment (McGill et al. 2006, Violle et al. 2007), and, because of this relationship, the morphological composition of a community will change as environment changes (Violle et al. 2007, Enquist et al. 2015). Study of these functional trait-environment relationships over spatial and temporal scales and at the community level has come to be called "ecometrics" (Eronen et al. 2010a, Polly et al. 2011, Vermillion et al. 2018). Ecometric indices have been used to reconstruct paleoenvironment (Eronen et al. 2010b, Polly 2010, Lawing et al. 2012, Fortelius et al. 2016, Barr 2017), evaluate extinction risk (Polly and Sarwar 2014), to understand the impact of non-ecological processes on patterns of biodiversity (Lawing et al. 2017), and to estimate community vulnerability to environmental change (Polly and Head 2015, Barnosky et al. 2017). In ecometric studies, the focus on morphological change makes it possible to examine the diversity of associations between climates and biotas through time.

In faunal communities, hypsodonty (or, the ratio of tooth crown height to tooth root height) is commonly used as a functional trait because of its relationship with precipitation (Fortelius et al. 2002, Eronen et al. 2010c, 2012, Evans 2013, Meloro and Kovarovic 2013, Žliobaitė et al. 2016). Communities dominated by fauna with high-crowned teeth occur in drier, more open, grassland-like environments and communities

dominated by fauna with low-crowned teeth occur in wetter, more closed, forest-like environments (Janis et al. 2000, Fortelius et al. 2002, Eronen et al. 2010c). Higher-crowned teeth enable animals to tolerate high levels of environmental grit associated with arid environments (Damuth and Janis 2011, Jardine et al. 2012, Kaiser et al. 2013, Lucas et al. 2014, Semprebon et al. 2019) as well as increased roughage in a diet of primarily grass (Strömberg 2002, 2006, Erickson 2014, Merceron et al. 2016, Winkler et al. 2019).

In ecometric analyses of post-cranial skeletal elements, some traits are functionally related to an animal's locomotion strategy, which is directly linked to the landscape in which the animal moves and, thus, the environment in which they live. Previous research has established a relationship between the calcaneal gear ratio of carnivorans and ecoregion province, vegetation cover, and mean annual temperature (Polly 2010), but this work has not yet been applied to other taxonomic orders. Whereas carnivorans are the primary carnivores in most ecosystems, artiodactyls are the primary large herbivores. Artiodactyls are typically cursorial with limbs that are restricted to parasagittal movement by hinge joints (Hildebrand and Goslow Jr 2001, Foss and Prothero 2007). Although they are cursorial, there is still a reasonable degree of variation in their locomotor strategies producing functional trait variation in their tarsals and metatarsals that is related to vegetation cover (Barr 2017, 2020).

Mammalian hind limbs are responsible for net propulsion at all times (Dutto et al. 2006, Kilbourne and Hoffman 2013), and research has correlated calcaneal morphology and locomotor style, which, when averaged across a community, can be

indicative of habitat (Polly and MacLeod 2008, Panciroli et al. 2017). The calcaneum, or heel bone, is the primary lever in the hind limb and serves as the insertion point for the gastrocnemius muscle (Radinsky 1987). The calcaneal gear ratio is a measure of the overall calcaneal length relative to the length of the in-lever (i.e., the calcaneal tuber) (Polly 2010). Calcanea are excellent elements to use for paleobiological studies because they have strong trait-environment relationships and are likely to be preserved in the fossil record because they are relatively dense elements without much soft tissue (Hill 1996). These circumstances render an investigation of artiodactyl calcanea an important next step in building ecometric models to relate morphology to environment.

Here, we test whether the trait-environment relationship between calcaneal gear ratio and ecoregion that was documented in Carnivora by Polly (2010) is also present in Artiodactyla, and we explore other environmental variables that may also produce good ecometric models. We contribute and analyze newly collected data of functional-trait measurements on the calcanea of artiodactyls. Functional traits are analyzed for relationships to richness, taxonomic family, and environment, including precipitation, temperature, elevation, vegetation cover, and ecoregion division. All five environmental variables are expected to have a relationship with artiodactyl calcaneal gear ratio, because the environmental variables are closely related to vegetation, substrate, and topography. We expect that vegetation cover will have the strongest relationship with the gear ratios of artiodactyl communities because, as herbivores, artiodactyls have a direct reliance on vegetation.

### 3.2. Materials and methods

To investigate calcaneal gear ratio as an ecometric trait in artiodactyls, we collected gear ratio measurement from skeletal specimens preserved in museum collections and cross-referenced the spatial distributions of species to determine community composition. The variation in gear ratio, summarized at the community level, was evaluated for fit with five environmental variables.

#### 3.2.1. Study system

With 240 species in 89 genera in 10 families (Wilson and Reeder 2005), Artiodactyla has a nearly global distribution in nearly all ecosystems, and species frequently overlap geographically creating a myriad of unique communities. Specimens were examined from the Smithsonian National Museum of Natural History (Washington, DC, USA), the Denver Museum of Nature and Science (Denver, Colorado, USA), the Museum für Naturkunde (Berlin, Germany), the National Museums of Kenya (Nairobi, Kenya), the Museo di Storia Naturale (Florence, Italy), and the Natural History Museum (London, United Kingdom). Only adults were measured and, when possible, both male and female specimens were included to account for sexual dimorphism. We resolved any discrepancies in species taxonomy and followed Wilson and Reeder (2005). Domestic species were removed from analysis following Gentry et al. (2004). Species were retained in the analysis if the species are extant and native or reintroduced. In all, a total of 571 individuals were measured from 157 (65%) extant species of Artiodactyla. Number of individuals per species ranged from one to 13, and the proportion of males and females varied with many recorded as “unknown.”

Calcaneal gear ratio is a measurement of the overall length of a calcaneum divided by the length of its tuber, or in-lever (Polly 2010) (Figure 3.1). These two linear measurements were measured with calipers from the medial tubercle of the calcaneal tuber to the furthest extent of the cuboid facet and the furthest extent of the dorsal edge of the astragalar facet, respectively. The ratio of these measurements indicates the position of the sustentaculum, which articulates with the astragalus to form the ankle joint. A low gear ratio indicates a long in-lever and a more plantigrade stance whereas a high gear ratio indicates a short in-lever and a more unguligrade stance (Polly 2010). Gear ratios of individuals were used to calculate mean and standard deviation values for each species. Mean gear ratios were evaluated for differences at the family level.

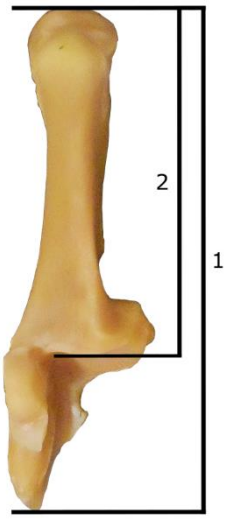


**Figure 3.1. Measurements used to calculate calcaneal gear ratio on a right calcaneum in dorsal view. 1, Greatest length of calcaneum. 2, Length of calcaneal tuber. The gear ratio is calculated by dividing measurement 1 by measurement 2 to represent the position of the sustentaculum. Measurements are modified from Polly (2010).**

### 3.2.2. Sampling strategy and environment

We downloaded species' geographic range maps from IUCN (2018) and sampled communities from overlapping range maps using a global 50 km grid of equidistant points (Polly 2010, Lawing et al. 2012; available at https://pollylab.indiana.edu/data/index.html). Evenly spaced points at this scale are representative of geographic mixing and the derived patterns are appropriate for comparing with samples from the fossil record (Polly 2010). Where Hurlbert and Jetz (2007) suggested to only use points of at least 200 km in distance when evaluating global trends, Lawing et al. (2017) showed that, in mammals, ecometric relationships do not change when evaluating records at 50, 100, or 250 km distance. Thus, we chose to use 50 km points to be consistent with previous ecometric studies. In total, there were 54,090 terrestrial global points after removing Antarctica from the dataset, with 47,420 being occupied by at least one artiodactyl species. For each community with three or more species, we calculated mean and standard deviation of calcaneal gear ratio from species' means.

We extracted environmental data, including mean annual temperature (C), annual precipitation (mm), elevation (m), vegetation cover, and ecoregion province, at each geographic point in our sampling scheme. Mean annual temperature (Figure 3.2A) and annual precipitation (Figure 3.2B) were sourced from weather stations for 1900-2014 and have been averaged and interpolated to a 0.5 x 0.5 degree raster layer (Matsuura and National Center for Atmospheric Research Staff 2017). Elevation was extracted from the GLOBE digital elevation model with a resolution of 30 arc-seconds (GLOBE Task

Team et al. 1999, Hastings and Dunbar 2008; Figure 3.2C). Matthews' vegetation cover was used to classify landscapes into one of 31 vegetation types; cultivation was excluded from this analysis (Matthews 1983, 1984, 1999; Figure 3.2D). Bailey's ecoregions define large-scale areas with similar ecosystem features, such as climate, physiography, and vegetation (Bailey and Hogg 1986, Bailey 1989, 1998, 2005; Figure 3.2E). Each ecoregion domain (n = 4) contains between four and 12 divisions for a total of 29 divisions that were used in this study; divisions are based on monthly measures of temperature and precipitation and are further divided based on vegetation (Bailey 2005).

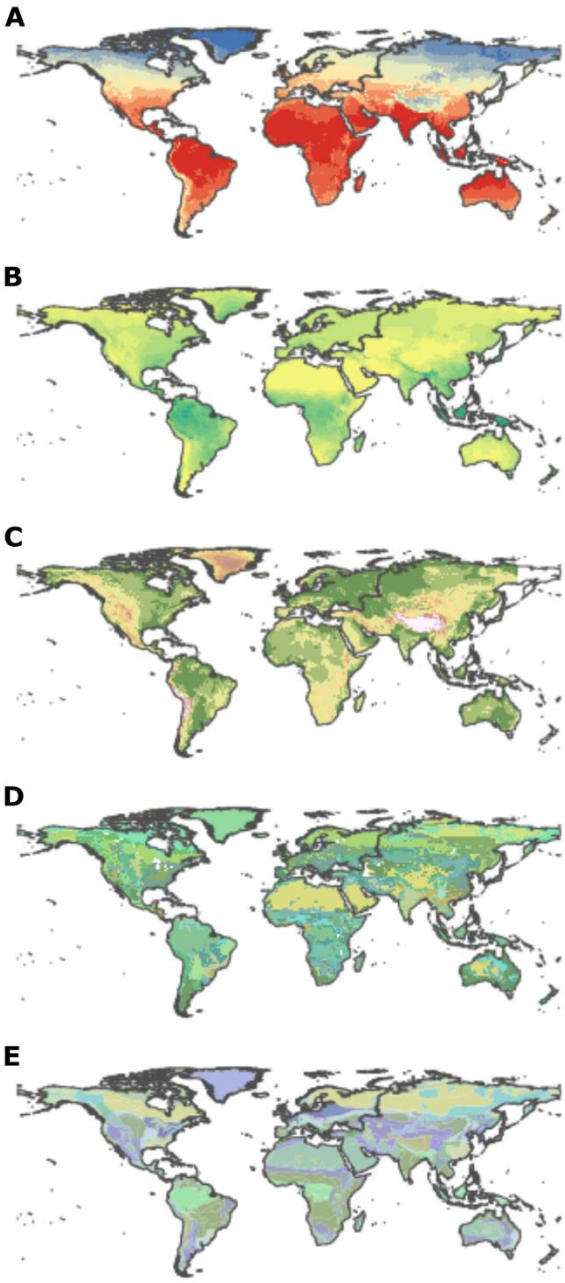


**Figure 3.2. Environmental variables used to test for trait-environment relationships. A, Mean annual temperature displayed in 10 color bins using Jenks Natural Breaks. Dark blue is the lowest temperature (-26.9 – -17.2°C) and dark red is the highest temperature (23.9 – 31.4°C); B, Annual precipitation displayed in 10 color bins using Jenks Natural Breaks. Bright yellow is the lowest precipitation (0 – 220 mm) and dark green is the highest precipitation (4,388 – 9,916 mm); C, Elevation displayed in 10 color bins using Jenks Natural Breaks. Dark green is the lowest elevation (-1,216 – 214 m) and white is the highest elevation (4,245 – 6,231**

**m); D, Bailey's ecoregion divisions. Colors are arbitrarily assigned to show variation; E. Matthews' vegetation cover. Colors are approximately aligned with vegetation so that dense vegetation is darker and sparse vegetation is lighter. Legend values are provided in Figure B-1.**

### 3.2.3. Ecometric summaries and analyses

Community means of calcaneal gear ratio were evaluated for relationships with species richness, and each of the five environmental variables. Continuous variables were transformed for normality as follows: cube root of richness and elevation, cube of mean annual temperature, and log of annual precipitation. Continuous variables were analyzed with a Pearson's correlation and categorical variables were analyzed with an ANOVA-derived $R^2$.

For environmental variables that were associated with a large amount of trait variation, an ecometric space was constructed following Lawing et al. (2012) and Vermillion et al. (2018). Trait values were binned into 25x25 cells by mean and standard deviation within an ecometric space. Short et al. (in review) showed that maximum likelihood had the smallest anomalies among four methods used to fit ecometric relationships. Thus, we used maximum likelihood to estimate the most likely environmental conditions for each trait bin. The ecometric models were then used to predict environments for the same dataset of communities. This enabled the models to be evaluated by comparing the observed environment to the predicted environment. Differences between the observed and predicted values were used to produce anomaly maps (Vermillion et al. 2018). Continuous variables were evaluated using numeric anomaly values. Categorical variables do not allow for numeric anomalies, so these were

evaluated using the percentage of predictions that were “correct” (i.e., matching the observed) or “incorrect” (i.e., not matching the observed).

### 3.3. Results

Species-level calcaneal gear ratios range from 1.40 (*Ammodorcas clarkei*, dibatag) to 1.74 (*Hexaprotodon liberiensis*, pygmy hippopotamus) ($\mu = 1.49$, SD = 0.051; Figure 3.3A). At the family level, gear ratio means are significantly different among taxonomic families ($R^2 = 0.473$, $p < 0.001$). Bovids and cervids make up most of the low gear ratios with the five lowest values from species of Antilopinae (Bovidae). There is more taxonomic diversity in the high gear ratios with the five highest values from different families, including Tragulidae, Suidae, Giraffidae, Camelidae, and Hippopotamidae (Figure 3.3B).

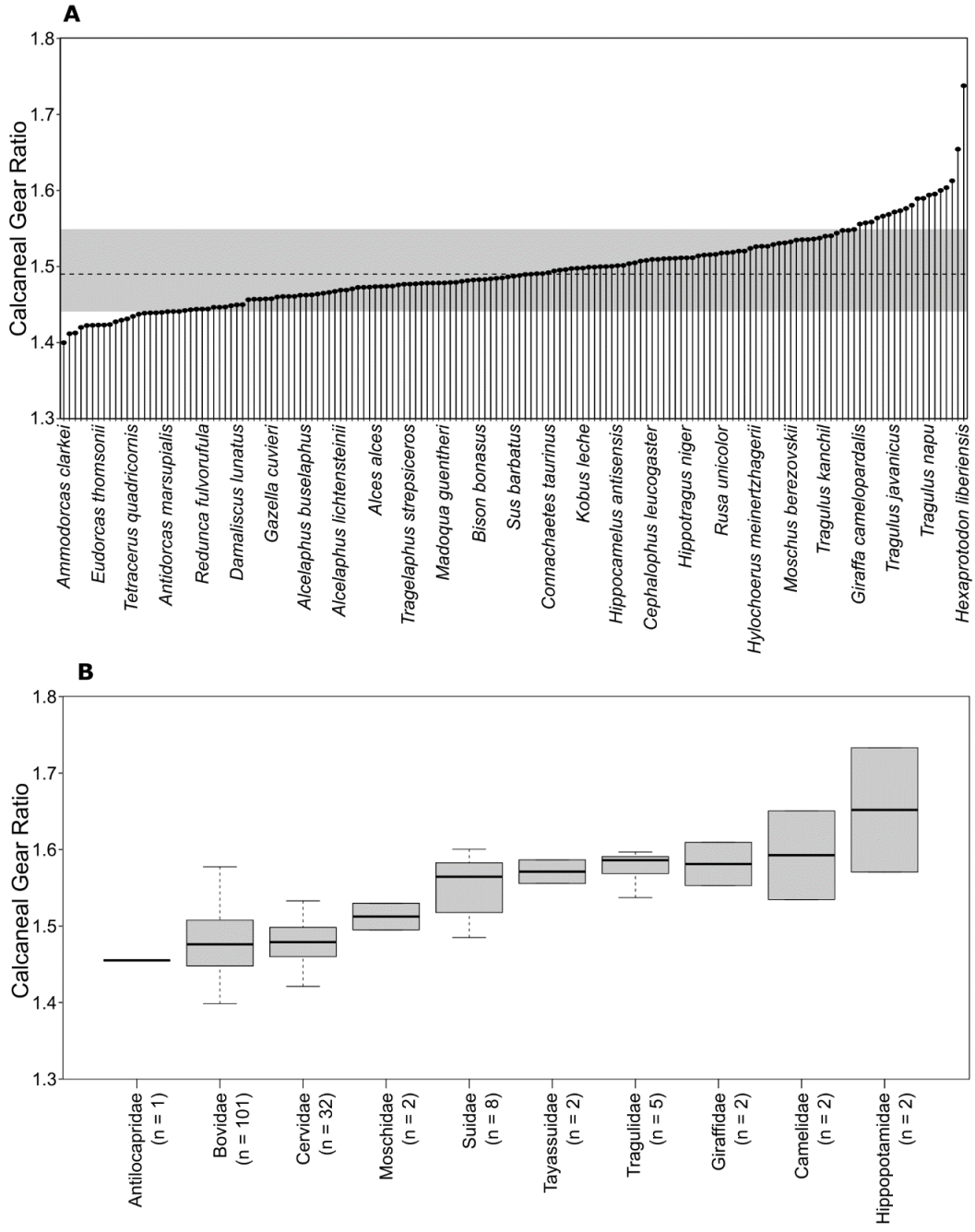


**Figure 3.3. Taxonomic distributions of calcaneal gear ratios. A, Rank order plot of gear ratios by species. The horizontal dashed line indicates the mean (μ = 1.49) and the gray shading includes one standard deviation (SD = 0.051) to either side of the mean. B, Boxplot of gear ratios by family.**

Community mean gear ratios range from 1.42 to 1.59 (μ = 1.48). Mean gear ratios are highest in the tropical regions and lowest in the mid-latitudes (Figure 3.4A). Community mean gear ratios are associated with community richness (R = 0.534, $R^2$ = 0.285, $p < 0.001$) so that communities with high species richness have gear ratio values near the mean of 1.48 (Figure 3.4B). Communities with low species richness have mean gear ratios across the range of trait values, but are on average lower than the mean.

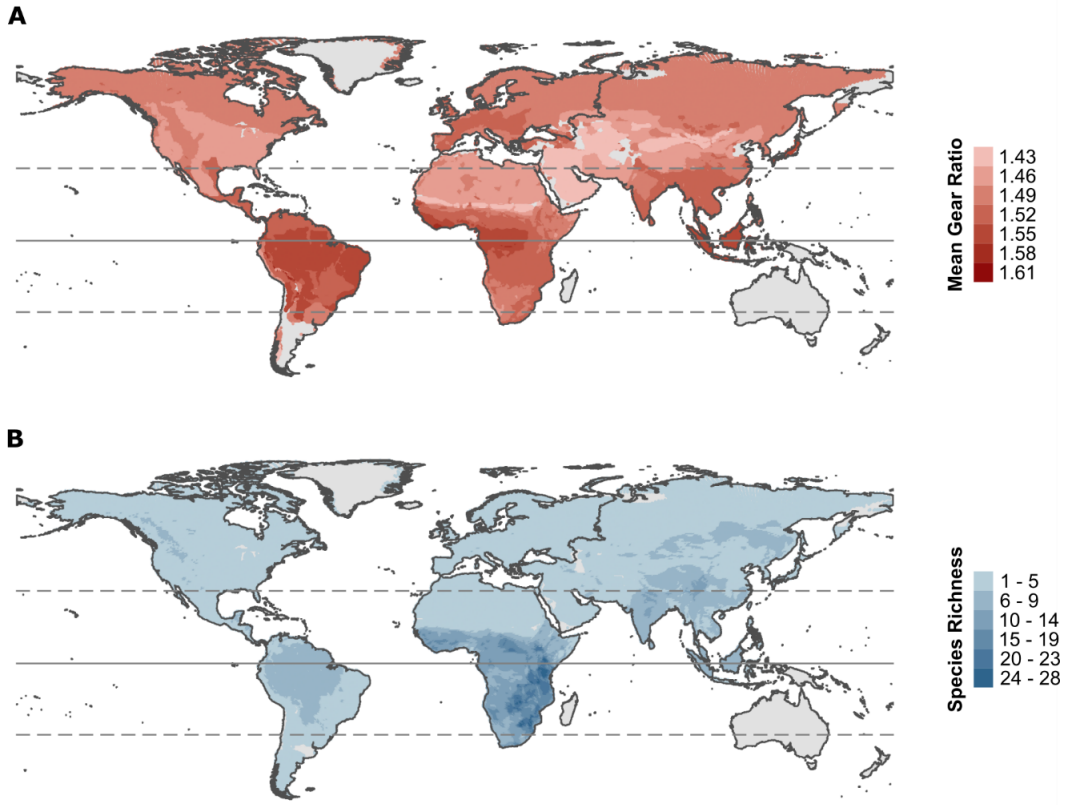


**Figure 3.4. Geography of artiodactyl community morphological composition. A, Mean calcaneal gear ratios; B, Species richness. Solid line is the equator (0°) and dotted lines are 30°N and 30°S.**

All five environmental variables are related to community mean calcaneal gear ratios (Table 1). Although, elevation explains little variation in community mean calcaneal gear ratio (1.6 %; Table 1). Ecoregion division is the most strongly correlated with gear ratio and explains 60.8% of the trait variance. Vegetation cover and annual precipitation are also strongly correlated with gear ratio and explain 57.6% and 44.1% of the variance, respectively. Because of their strong relationships with community mean calcaneal gear ratio, these three environmental variables are investigated further to produce ecometric spaces.

**Table 3.1. Relationships between mean gear ratio and environment. R is the Pearson's correlation coefficient and $R^2$ is the amount of variance explained by the environmental variable. All trait-environment relationships are significant at p < 0.001(***).**

| | R | $R^2$ | *p* |
|---|---|---|---|
| Mean annual temperature | 0.263 | 0.069 | *** |
| Annual precipitation | 0.664 | 0.441 | *** |
| Elevation | -0.125 | 0.016 | *** |
| Ecoregion division | | 0.608 | *** |
| Vegetation cover | | 0.576 | *** |

In the ecometric space of ecoregions, humid tropical savannas make up the largest division that is nearly centered in the ecometric space (Figure 3.5A). Communities in humid tropical divisions have mostly moderate calcaneal gear ratio means and low to moderate standard deviations. Communities in humid temperate divisions range from low mean and low standard deviation to high mean and high standard deviation. There are no humid temperate communities predicted to occur with a high standard deviation and low mean calcaneal gear ratio. Communities in dry divisions

have low to moderate calcaneal gear ratio means and occur across the range of standard deviation. Communities in polar divisions have moderate means and low standard deviations; these communities are mixed with humid tropical and humid temperate divisions.

When the ecometric model is used to predict the ecoregion division based on the community calcaneal gear ratio, the model is accurate for 60.5% of the communities (Figure 3.5B; Table S1). Ecoregion divisions can be grouped in to four, higher-level ecoregion domains. The model accurately predicts the ecoregion domains for 83.46% of the communities. This ecometric model is most accurate in the savannas and rainforests divisions (humid tropical domain) of South America and Africa, and the subarctic regime mountains division (polar domain) of North America and Asia. The model is also accurate for the temperate steppe division of North America and the tropical/subtropical desert regime mountains division of Asia; both of these are in the dry domain.

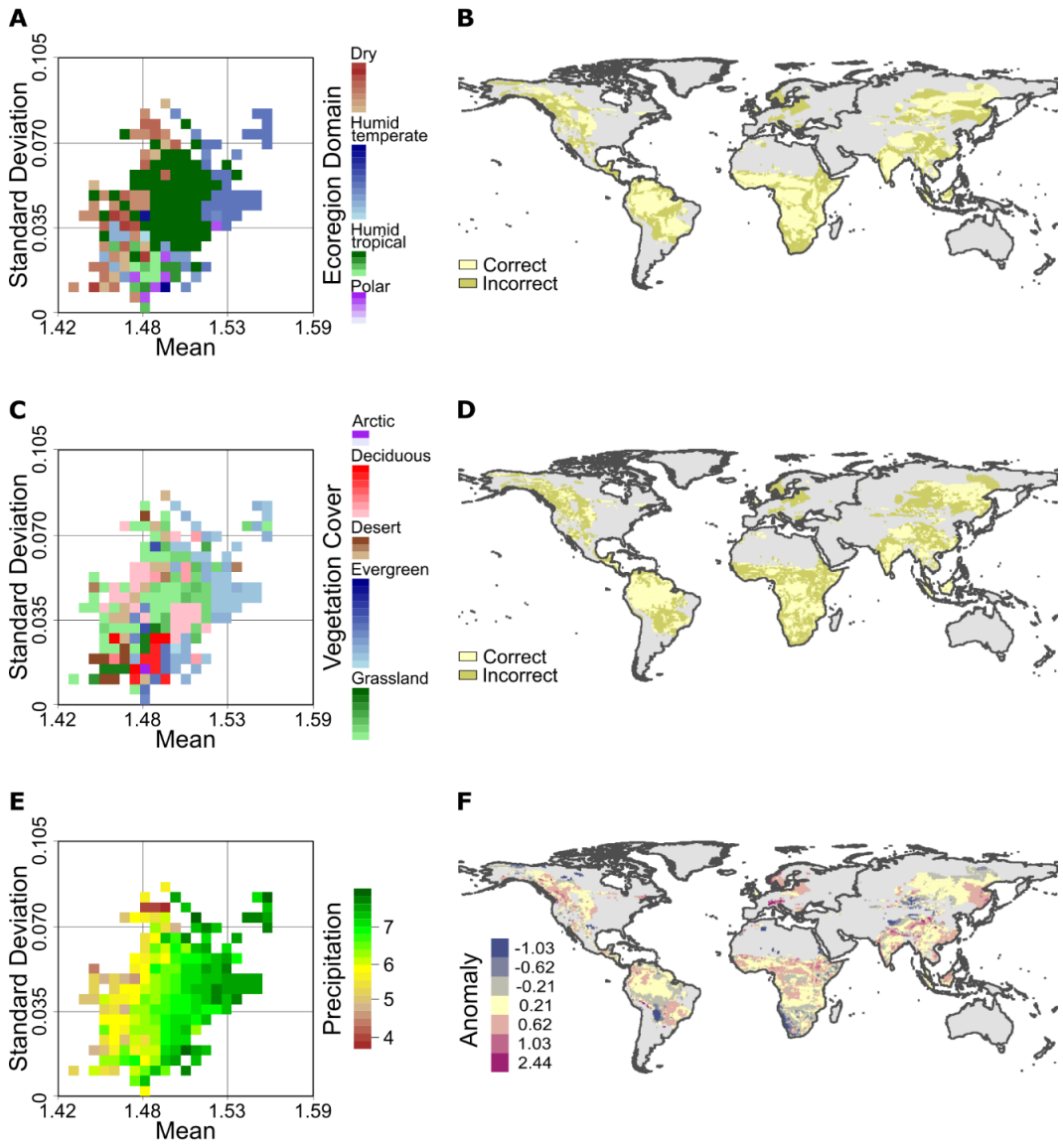


**Figure 3.5. Ecometric trait-environment relationships. A, Ecometric space showing the most likely ecoregion division given community level gear ratio means and standard deviations. Colors represent ecoregion domain groupings of ecoregion divisions. B, Anomaly map of ecoregion division predictions based on gear ratio. Light yellow locations are correct predictions in which the prediction accurately matches the observed (60.5%). Dark yellow locations are incorrect predictions in which the prediction does not accurately match the observed. C, Ecometric space showing the most likely vegetation cover given community level gear ratio means and standard deviations. Colors represent vegetation classes within five large-scale vegetation regimes. D, Anomaly map of vegetation cover predictions. Colors are as in B with 50.4% of locations predicted correctly. E, Ecometric space showing the most likely annual precipitation (log mm) given community level gear ratio means**

**and standard deviations. F, Anomaly map of annual precipitation predictions (log mm). Each color bin is equivalent to one standard deviation and values are the maximum for each bin. Precipitation is overpredicted in blue locations and underpredicted in pink locations.**

The ecometric space for vegetation cover is dominated by evergreen and grassland classes (Figure 3.5C). Both evergreen and grassland classes range from low mean and low standard deviation to high mean and high standard deviation, but communities in evergreen classes generally have higher gear ratio means than those in grassland classes. Communities in desert classes follow the same low-low to high-high pattern that evergreen and grassland communities do, but desert communities are consistently at a lower mean than most of the communities in evergreen or grassland communities. Communities in deciduous classes have low to moderate means and standard deviations. The only trait bin of arctic communities has a moderate mean and low standard deviation. In general, as density of vegetation cover increases, the mean gear ratio also increases.

When the ecometric model is used to predict vegetation cover based on community calcaneal gear ratio, the model is accurate for only 50.4% of the communities (Figure 3.5D; Table B-1). However, the model can accurately predict the five binned vegetation regimes for 65.9% of the communities. This ecometric model is most accurate in the cold-deciduous forest without evergreens in Europe and Asia, the tropical evergreen rainforests of South America, Africa, and Asia, and the deserts of Africa and Asia.

Annual precipitation is separated along the mean trait values so that communities with low calcaneal gear ratios have low precipitation and communities with high calcaneal gear ratios have high precipitation (Figure 3.5E). There is no separation of communities along standard deviation, so that low, moderate, and high standard deviations exist at all levels of precipitation. Precipitation anomalies range from -4.24 log mm – 2.44 log mm ($\mu$ = -0.002 log mm), and 84.5% of the communities have an anomaly value within 0.5 log mm of the mean (Figure 3.5F). The model overpredicts precipitation in dry areas, such as the North American desert region, the Himalayan Plateau, southern Africa, and central South America. The model underpredicts precipitation in wet areas, such as the Pacific Northwest, central Africa, and Southeast Asia.

### 3.4. Discussion

Here, we demonstrate the ecometric value of ungulate calcanea by quantifying the trait-environment relationship between mean gear ratio and five environmental variables, three of which make reasonably good ecometric models. Functionally, the calcaneum is directly related to an animal's locomotion strategy and, consequently, the environment in which the animal lives. In artiodactyls, this results in strong relationships between calcaneal morphology and taxonomic family (Figure 3.3B), species richness (Figure 3.4), and ecoregion division, vegetation cover, and precipitation (Figure 3.5, Table 3.1).

### 3.4.1. Community trait composition

Calcaneal gear ratio is a measure of foot posture. Animals range from plantigrade, or walking flat-footed on their metatarsals as in bears and humans, to digitigrade, or walking on their phalanges as in dogs and cats, to unguligrade, or walking on their distal-most phalanges as in deer and sheep. Lower calcaneal gear ratios are found in more plantigrade taxa, and higher gear ratios are found in more digitigrade taxa. Artiodactyls are unguligrade, and, in the data presented here, species-level mean gear ratios range from 1.40 to 1.74 (Figure 3.3A). Whereas the lowest gear ratios are found in stotting species, the highest gear ratios are found in plodding species. Stotting bovids also have longer calcanea tubers, possibly to facilitate upward propulsion and predator avoidance (Barr 2020).

In Polly's (2010) study of North American carnivorans, gear ratios range from 1.13 in *Ursus arctos* (brown bear) to 1.41 in *Puma concolor* (mountain lion). Globally, carnivoran gear ratios range from 1.08 in *Melursus ursinus* (sloth bear) to 1.46 in *Ichneumia albicauda* (white-tailed mongoose) (Polly 2010). Therefore, there is a continuous increase in gear ratio from the most plantigrade carnivorans through the progressive elevation of the foot to the most unguligrade artiodactyls. This continuum of foot position could be used to study community composition and interactions across taxonomic orders and trophic levels.

Community trait composition is expected to be related to taxonomic designations because of the constrained morphology that is typical within clades (Polly 2010, Lawing et al. 2012, Polly et al. 2017). In artiodactyls, species-level gear ratio has a strong

relationship with taxonomic family ($R^2 = 0.473$, $p < 0.001$). At the family level, Antilocapridae, represented only by *Antilocapra americana* (pronghorn), has the lowest gear ratio, but only slightly lower than bovids and cervids whereas hippopotamids and camelids have the highest gear ratios (Figure 3.3B). Bovids and cervids have a nearly global distribution and are also the artiodactyl families that have most recently diversified and radiated (Janis 2007). With a large number of species that are able to inhabit many different geographic locations, bovids and cervids have a larger range of gear ratios with a lower mean. Hippopotamuses, represented by *Hippopotamus amphibius* (hippopotamus) and *Hexaprotodon* (*Choeropsis*) *liberiensis* (pygmy hippopotamus), and camels, represented by *Camelus dromedarius* (dromedary camel) and *Vicugna vicugna* (vicuña), have many fewer, specialized species with much more restricted geographic ranges and higher gear ratios.

Communities with a high species richness have moderate gear ratio values whereas communities with low species richness have gear ratios across the range (Figure 3.4). As richness increases, the functional diversity of species also increases, and that diversity shifts the community trait value toward the mean (Petchey and Gaston 2002, 2006). This is particularly evident in eastern and southeastern Africa, which is where all communities with species richness greater than 18 occur. Although the richness is high in these communities, the mean gear ratio when richness is 18 or higher is 1.50, only slightly higher than the global average of 1.48. In areas of low richness, such as North and South America, mean gear ratio is either low (e.g., North America) or high (e.g., South America). Communities on both of these continents have cervids and tayassuids,

but North America also has *Antilocapra americana* and bovids while South America has *Vicugna vicugna*. Thus, the mean gear ratio is shifted to the low and high ends, respectively.

### 3.4.2. Trait-environment relationships

In ecometric spaces, ecoregion divisions and vegetation cover overlap (Figures 3.5A, 3.5C); humid tropical divisions overlap grassland vegetation, humid temperate divisions overlap evergreen vegetation, and dry divisions overlap desert, deciduous, and grassland vegetation cover. However, trait bins in the polar divisions mostly overlap evergreen vegetation rather than arctic vegetation; the one trait bin of arctic vegetation is in the humid tropical division. This mismatch highlights the need to consider more than one environmental variable. Ecoregion divisions and vegetation cover classes are consistently accurate across continents (Figures 3.5B, 3.5D). For instance, savannas and rainforests divisions are correctly classified in South America and Africa, and the subarctic regime mountains division is correctly classified in both North America and Asia. These geographically-widespread communities must have similar trait composition to produce these results. Thus, trait composition can be used in place of taxonomic composition to understand global patterns of ecoregions and vegetation.

Ecometric models accurately predicted ecoregion division for 60.5% of the communities and vegetation cover for 50.36% of the artiodactyl communities (Figures 3.5B, 3.5D). Incorrect predictions occur when trait bins include communities from more than one ecoregion, which is likely to happen given the amount of overlap between the ecoregion domains and divisions. However, for both variables, the ecometric models

more accurately predicted the higher-level groupings—ecoregion domain and binned vegetation regime—with accuracies of 83.5% and 71.6%, respectively. This is not unexpected because the models should be more accurate with fewer options, and there is potential to use these higher groupings as additional information when interpreting an unknown environment. For example, when a community has an incorrect prediction of ecoregion division, it is likely that the prediction is still from the correct ecoregion domain.

Ecologically, precipitation influences the ecoregion designations and vegetation cover. In Bailey's ecoregions, domains are first separated into "dry" and "humid, thermally differentiated"; then, the latter group is separated into humid temperate, humid tropical, and polar (Bailey 2005). This similar precipitation pattern is why ecoregion divisions in the dry domain appear less intermingled with the divisions in the humid temperate, humid tropical, and polar domains (Figures 3.5A). It also matches the distribution of precipitation values so that low precipitation largely occurs in communities with the same trait composition as those in the dry ecoregion divisions, and communities with high precipitation are in the same trait bins as those in the humid temperate ecoregion divisions. Precipitation has less of a relationship with the vegetation type categories. In ecometric spaces, the strongest match is between high precipitation and evergreen vegetation type, whereas low precipitation occurs across vegetation types (Figures 3.5C, 3.5E).

Precipitation differs from ecoregion division and vegetation cover in that it is a continuous variable and enables a numeric anomaly to evaluate model accuracy. Here,

84.5% of the communities have an anomaly value within 0.5 log mm of the mean ($\mu$ = -0.002 log mm). The ecometric model underpredicts precipitation in wet areas and overpredicts precipitation in dry areas. This tendency toward the mean is expected because maximum likelihood uses the most frequent precipitation of the communities in a trait bin to predict precipitation for all communities in that trait bin. However, the severely over- and underpredicted areas may also be highlighting areas of environmental change where the faunal community has not yet responded. Many of the areas that are overpredicted are also drylands that are or will be vulnerable to increased aridity by 2100 (Berdugo et al. 2020). In these areas, the fauna may be lagging aridification, and thus, the morphology of native, extant communities conveys past precipitation.

### 3.4.3. Conservation paleobiology

Ecometric methods have been developed to expand conservation paleobiology (Eronen et al. 2010a). Lawing et al. (2012) showed shifts in mean snake tail length in five North American assemblages over the last 100 years in response to changes in vegetation. Each of these assemblages were located in conservation areas that will benefit from knowing how their snake communities are changing through time. Similarly, Polly (2010) and Polly and Head (2015) each showed changes in the calcaneal gear ratios of four North American carnivore communities in response to shifts in ecoregions. Here, we demonstrate the application of community-level artiodactyl calcaneal gear ratios at six sites in Kenya from Tóth et al. (2014).

The six sites in Kenya are protected areas with historical (1896-1950) and modern (1950-2013) data on mammal composition (Tóth et al. 2014). Sites are from a

variety of habitats – Kakamega Forest Reserve (forest), Maasai Mara National Reserve (grassland), Nairobi National Park and Samburu Game Reserve (savanna), Lake Naivasha National Park (wetland), and Tsavo East and West National Parks (woodland/scrub). Kakamega is in western Kenya near Lake Victoria, Samburu is in central Kenya, and the other four sites are in southern Kenya along the Tanzania border. Tóth et al. (2014) found homogenization of community structure as beta-diversity decreased at all six sites; although, richness only decreased at Lake Naivasha.

With the published community species lists from Tóth et al. (2014), we used artiodactyl calcaneal gear ratios to investigate the trait and environment shifts at each of the six sites through time. Historical and modern means and standard deviations of community-level gear ratio were calculated at each site. According to their gear ratio values, communities were assigned historical and modern trait bins in ecometric spaces from Figure 3.5. Maximum likelihood was used to predict the most likely historical and modern environmental conditions for each site. Vectors were used to evaluate the direction of change from the historical time point to the modern time point in ecometric space.

Artiodactyl trait shifts support the homogenization of communities in Kenya (Figure 3.6). Nairobi National Park did not shift trait bins from historical to modern, but Maasai Mara, Lake Naivasha, and Tsavo East and West converged toward Nairobi. At Maasai Mara, the mean calcaneal gear ratio increased and at Lake Naivasha and Tsavo East and West, the mean and standard deviations decreased. Kakamega and Samburu

diverged from the other four sites. At Kakamega, the mean calcaneal gear ratio increased, and at Samburu, the standard deviation of the gear ratio increased.

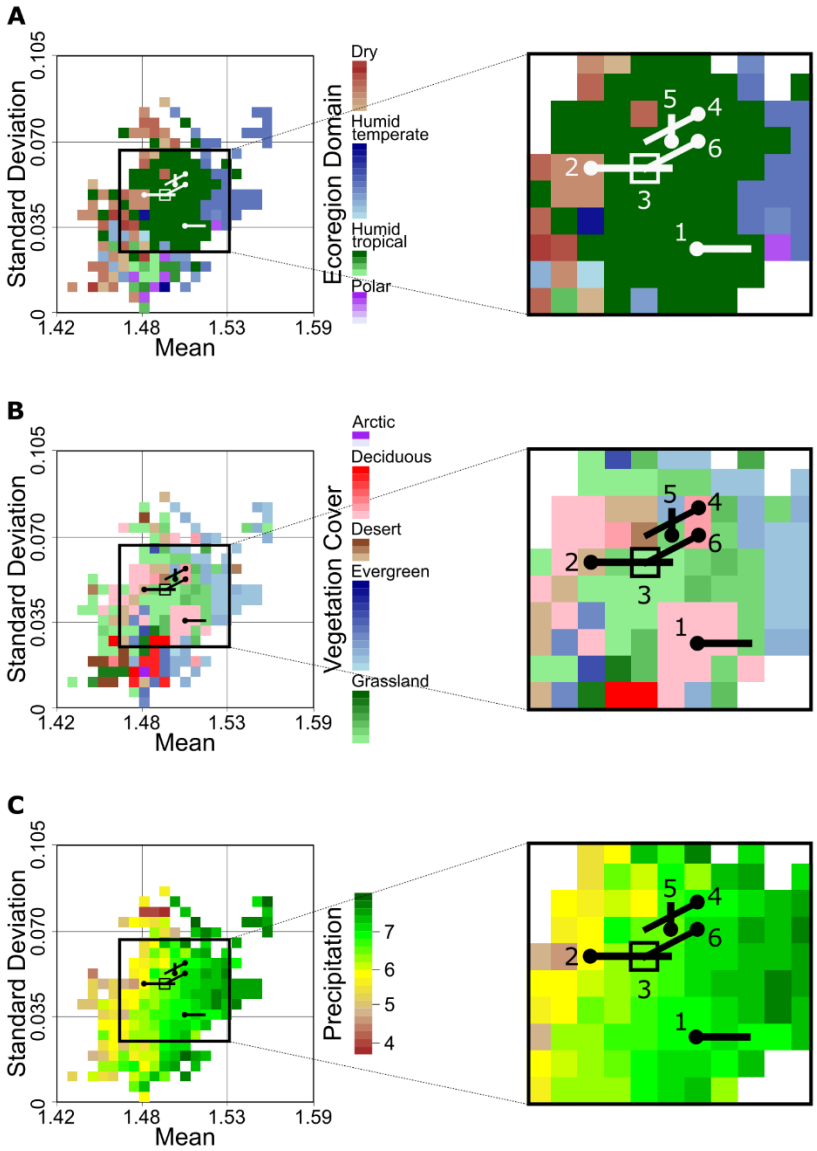


**Figure 3.6. Placement of Kenyan sites in ecometric space. A, Ecoregion divisions as in Figure 3.5A; B, Vegetation cover as in Figure 3.5C; and C, Precipitation as in Figure 3.5E. Sites are from Tóth et al. (2014): 1 – Kakamega Forest Reserve, 2 – Maasai Mara National Reserve, 3 – Nairobi National Park, 4 – Lake Naivasha National Park, 5 – Samburu Game Reserve, and 6 – Tsavo East and West National Parks. The box indicates no change in trait bin from historical to modern. Vectors**

**indicate change with the dotted end representing historical community traits and the end without a dot representing modern community traits.**

Historically, five sites were savanna, and only Maasai Mara changed ecoregion division from tropical/subtropical steppe to savanna (Figure 3.6A; Table B-3). All of the sites are in the savanna ecoregion division today. Vegetation cover at Kakamega, Tsavo East and West, and Maasai Mara shifted from woody or desert habitats to grassland habitats (Figure 3.6B; Table B-3). Lake Naivasha shifted from a tropical/subtropical drought-deciduous forest to a xeromorphic forest/woodland. Samburu shifted away from grassland to tropical/subtropical evergreen seasonal broad-leaved forest. Maasai Mara had the largest increase in precipitation (431.71 mm) from 5.80 log mm (329.55 mm) to 6.64 log mm (761.25 mm) (Figure 3.6C; Table B-3). Tsavo East and West had the largest decrease in precipitation (-527.96 mm) from 7.09 log mm (1193.90 mm) to 6.50 log mm (665.94 mm). This distribution of precipitation change is consistent with observed annual precipitation trends in Kenya (Gebrechorkos et al. 2019). Because trait composition at Nairobi National Park did not change, historical and modern environmental predictions did not shift either.

Nairobi National Park is centrally located among the six sites and did not display an environmental shift. In the last century, Maasai Mara, Lake Naivasha, and Tsavo East and West have converged toward Nairobi as Kenyan habitats have become more homogenized (Figure 3.6). Kakamega (furthest west) and Samburu (furthest north) do not show the same trend but diverge from the others. Tóth et al. (2014) document a similar homogenization pattern in the mammal communities, but argue against habitat

change as a possible driver for the stable or increasing richness and decreasing beta diversity. There is limited environmental data from the historical time interval, and the authors credit common species that can easily move between protected areas for the changes in community structure (Tóth et al. 2014). We posit that the environmental changes, captured in the ecometric spaces (Figure 3.6), enabled these common species to move between protected areas and facilitated the changes in community structures documented by Tóth et al. (2014).

### 3.4.4. Limitations

Ecometric methods are limited by incomplete datasets. Modern range maps overestimate the distribution of species and, therefore, bias the trait values of communities (Cantú-Salazar and Gaston 2013, Chen 2013). Trait data are limited by the availability of museum specimens and published datasets. Fossil sites are not always a complete record. However, Polly and Sarwar (2014) showed that only 25% of species within a community are needed to predict accurate ecometric relationships. As geographic ranges and trait databases become more commonplace, increased availability of data will increase the fit of trait-environment relationships.

No-analog communities include species that are extant today, yet they do not occur in the same combinations today as they did in the past (Williams and Jackson 2007). No-analog communities are expected to increase as species reshuffling occurs in response to climatic and environmental changes (Williams and Jackson 2007, Hobbs et al. 2018). Ecometrics provides a method for comparing no-analog communities with trait compositions within the modern trait bins of the ecometric spaces (Vermillion et al.

2018). Thus, maximum likelihood predictions are possible for no-analog communities, but this method is limited for communities with trait compositions that do not exist in the trait bins of the constructed ecometric spaces.

Community trait composition is likely to be impacted by domestics and other non-natives filling new ecological roles or replacing native fauna (Smith et al. 2016). Many domesticated and livestock animals are artiodactyls, and we have removed these species from the dataset used here following Gentry et al. (2004). We expect domestic species that are heavily managed may weaken the ecometric relationships because the species are not naturally interacting with their environment but are dependent on human activities. However, non-native species that are well-suited to their new environment and are not dependent on humans for survival may strengthen the ecometric relationships. As scientists consider agricultural land as a distinct system in the middle of a continuum ranging from unmanaged wilderness to human-dominated urban areas (Swinton et al. 2007), the impact of these species on community composition should be further investigated.

### 3.4.5. Conclusions

Here, we present a new application of ecometrics for studying short- and long-term change in the fossil record. These methods have been used before but have not been applied to artiodactyl post-crania or applied at a global scale. Ecometric models have the potential to be tools in understanding biodiversity responses to environmental change because of relationships between community calcaneal gear ratio and ecoregion division, vegetation cover, and precipitation. Artiodactyls make up a large proportion of the

world's megabiota, which is disproportionately threatened, yet critical for ecosystem health and resiliency (Enquist et al. 2020).

Ecometric models can be used in studies of conservation by providing a longer-term view of change when environmental data are not available. In the example of the Kenyan sites, detailed historical environmental data were not available, but with the trait-environment relationships, it becomes possible to track environmental changes using calcaneal gear ratios. With forward modeling, the same ecometric models can be used to predict how communities will continue to change and where they might be in danger of extirpation or extinction so conservation efforts can be directed appropriately. Vectors in Figure 6 could be extended to match expected environmental changes at each location, and trait values could be extracted from the appropriate trait bin to anticipate impacts on artiodactyl communities. For example, Wingard et al. (2017) described how paleoecological data were used to establish pre-anthropogenic trends and cycles in the Greater Everglades Ecosystem. With this data, they were able to predict future patterns and identify restoration targets for resource management efforts (Wingard et al. 2017).

In the past 50 years, biodiversity changed at a rate that was unprecedented during human history but is expected to accelerate in the future (Walther et al. 2002, Foley et al. 2005, Lipton et al. 2018). Ecometrics provides methods for understanding past trait-environment relationships so that future biodiversity responses can be better anticipated. For instance, in Kenya, as habitats changed, the communities of the protected areas were changed by the movement of common species between the protected areas. Yet, climate connectivity remains a challenge, so that species many not easily shift their ranges as

climate change continues (McGuire et al. 2016). With ecometric models, it will be possible to target areas for conservation efforts, such as increased connectivity, to facilitate community responses.

**References**


Bailey RG. 1989. Bailey's Ecoregions of the World. (16 April 2018; www.unep-wcmc.org/resources-and-data/baileys-ecoregions-of-the-world).

Bailey RG. 1998. Ecoregions map of North America explanatory note. USDA Forest Service Miscellaneous Publication 1548: .

Bailey RG. 2005. Identifying ecoregion boundaries. Environmental Management 34: 14–26.

Bailey RG, Hogg HC. 1986. A world ecoregions map for resource reporting. Environmental Conservation 13: 195–202.

Barnosky AD, Hadly EA, Gonzalez P, Head J, Polly PD, Lawing AM, Eronen JT, Ackerly DD, Alex K, Biber E, Blois J, Brashares J, Ceballos G, Davis E, Dietl GP, Dirzo R, Doremus H, Fortelius M, Greene HW, Hellmann J, Hickler T, Jackson ST, Kemp M, Koch PL, Kremen C, Lindsey EL, Looy C, Marshall CR, Mendenhall C, Mulch A, Mychajliw AM, Nowak C, Ramakrishnan U, Schnitzler J, Das Shrestha K, Solari K, Stegner L, Stegner MA, Stenseth NC, Wake MH, Zhang Z. 2017. Merging paleobiology with conservation biology to guide the future of terrestrial ecosystems. Science 355: eaah4787.

Barr WA. 2017. Bovid locomotor functional trait distributions reflect land cover and annual precipitation in sub-Saharan Africa. Evolutionary Ecology Research 18: 253–269.

Barr WA. 2020. The morphology of the bovid calcaneus: Function, phylogenetic signal, and allometric scaling. Journal of Mammalian Evolution 27: 111–121.

Berdugo M, Delgado-Baquerizo M, Soliveres S, Hernández-Clemente R, Zhao Y, Gaitán JJ, Gross N, Saiz H, Maire V, Lehman A, Rillig MC, Solé R V., Maestre FT. 2020. Global ecosystem thresholds driven by aridity. Science 367: 787–790.

Cantú-Salazar L, Gaston KJ. 2013. Species richness and representation in protected areas of the Western hemisphere: Discrepancies between checklists and range maps. Diversity and Distributions 19: 782–793.

Chen Y. 2013. Species-area relationship is overestimated using distributional range

maps. Theoretical Biology Forum 106: 17–21.

Damuth J, Janis CM. 2011. On the relationship between hypsodonty and feeding ecology in ungulate mammals, and its utility in palaeoecology. Biological Reviews 86: 733–758.

Dutto DJ, Hoyt DF, Clayton HM, Cogger EA, Wickler SJ. 2006. Joint work and power for both the forelimb and hindlimb during trotting in the horse. Journal of Experimental Biology 209: 3990–3999.

Enquist BJ, Abraham AJ, Harfoot MBJ, Malhi Y, Doughty CE. 2020. The megabiota are disproportionately important for biosphere functioning. Nature Communications 11: 1–11.

Enquist BJ, Norberg J, Bonser SP, Violle C, Webb CT, Henderson A, Sloat LL, Savage VM. 2015. Scaling from traits to ecosystems: Developing a general trait driver theory via integrating trait-based and metabolic scaling theories. Advances in Ecological Research 52: 249–318.

Erickson KL. 2014. Prairie grass phytolith hardness and the evolution of ungulate hypsodonty. Historical Biology 26: 737–744.

Eronen JT, Fortelius M, Micheels A, Portmann FT, Puolamäki K, Janis CM. 2012. Neogene aridification of the northern hemisphere. Geology 40: 823–826.

Eronen JT, Polly PD, Fred M, Damuth J, Frank DC, Mosbrugger V, Scheidegger C, Stenseth NC, Fortelius M. 2010a. Ecometrics: The traits that bind the past and present together. Integrative Zoology 5: 88–101.

Eronen JT, Puolamäki K, Liu L, Lintulaakso K, Damuth J, Janis C, Fortelius M. 2010b. Precipitation and large herbivorous mammals II: Application to fossil data. Evolutionary Ecology Research 12: 235–248.

Eronen JT, Puolamäki K, Liu L, Lintulaakso K, Damuth J, Janis C, Fortelius M. 2010c. Precipitation and large herbivorous mammals I: Estimates from present-day communities. Evolutionary Ecology Research 12: 217–233.

Evans AR. 2013. Shape descriptors as ecometrics in dental ecology. Hystrix 24: .

Foley JA, DeFries R, Asner GP, Barford C, Bonan G, Carpenter SR, Chapin FS, Coe MT, Daily GC, Gibbs HK, Helkowski JH, Holloway T, Howard EA, Kucharik CJ, Monfreda C, Patz JA, Prentice IC, Ramankutty N, Snyder PK. 2005. Global consequences of land use. Science 309: 570–574.

Fortelius M, Eronen J, Jernvall J, Liu L, Pushkina D, Rinne J, Tesakov A, Vislobokova

I, Zhang Z, Zhou L. 2002. Fossil mammals resolve regional patterns of Eurasian climate change over 20 million years. Evolutionary Ecology Research 4: 1005–1016.

Fortelius M, Žliobaitė I, Kaya F, Bibi F, Bobe R, Leakey L, Leakey M, Patterson D, Rannikko J, Werdelin L. 2016. An ecometric analysis of the fossil mammal record of the Turkana Basin. Philosophical Transactions of the Royal Society B: Biological Sciences 371: 20150232.

Foss S, Prothero D. 2007. Introduction. Pages 1–3 in Prothero D and Foss S, eds. The Evolution of Artiodactyls. Johns Hopkins University Press.

Gebrechorkos SH, Hülsmann S, Bernhofer C. 2019. Long-term trends in rainfall and temperature using high-resolution climate datasets in East Africa. Scientific Reports 9: 1–9.

Gentry A, Clutton-Brock J, Groves CP. 2004. The naming of wild animal species and their domestic derivatives. Journal of Archaeological Science 31: 645–651.

GLOBE Task Team, others (Hastings, David A., Paula K. Dunbar, Gerald M. Elphingstone, Mark Bootz, Hiroshi Murakami, Hiroshi Maruyama, Peter Holland, John Payne, Nevin A. Bryant, Thomas L. Logan, J.-P. Muller, Gunter Schreier, and John S. MacDonald) E. 1999. The Global Land One-kilometer Base Elevation (GLOBE) Digital Elevation model, Version 1.0. (16 April 2018; www.ngdc.noaa.gov/mgg/topo/globe.html).

Hastings DA, Dunbar PK. 2008. Global Land One-kilometer Base Elevation (GLOBE), Digital Evelation Model, Version 1.0. Key to Geophysical Records Documentation (KGRD) 34.

Hildebrand M, Goslow Jr G. 2001. Analysis of Vertebrate Structure. 5th ed. John Wiley and Sons Inc.

Hill MG. 1996. Size comparison of the Mill Iron site bison calcanea. Pages 231–237 in Frison GC, ed. The Mill Iron Site. University of New Mexico Press.

Hobbs RJ, Valentine LE, Standish RJ, Jackson ST. 2018. Movers and stayers: Novel assemblages in changing environments. Trends in Ecology and Evolution 33: 116–128.

Hurlbert AH, Jetz W. 2007. Species richness, hotspots, and the scale dependence of range maps in ecology and conservation. Proceedings of the National Academy of Sciences 104: 13384–13389.

[IUCN] International Union for Conservation of Nature and Natural Resources. 2018.

The IUCN Red List of Threatened Species. (16 April 2018; www.iucnredlist.org).

Janis CM. 2007. Artiodactyl Paleoecology and Evolutionary Trends. Pages 292–302 in Prothero DR and Foss SE, eds. The Evolution of Artiodactyls. Johns Hopkins University Press.

Janis CM, Damuth J, Theodor JM. 2000. Miocene ungulates and terrestrial primary productivity: Where have all the browsers gone? Proceedings of the National Academy of Sciences 97: 7899–7904.

Jardine PE, Janis CM, Sahney S, Benton MJ. 2012. Grit not grass: Concordant patterns of early origin of hypsodonty in Great Plains ungulates and Glires. Palaeogeography, Palaeoclimatology, Palaeoecology 365–366: 1–10.

Kaiser TM, Müller DWH, Fortelius M, Schulz E, Codron D, Clauss M. 2013. Hypsodonty and tooth facet development in relation to diet and habitat in herbivorous ungulates: Implications for understanding tooth wear. Mammal Review 43: 34–46.

Kilbourne BM, Hoffman LC. 2013. Scale effects between body size and limb design in quadrupedal mammals. PLoS ONE 8: e78392.

Lawing AM, Eronen JT, Blois JL, Graham CH, Polly PD. 2017. Community functional trait composition at the continental scale: The effects of non-ecological processes. Ecography 40: 651–663.

Lawing AM, Head JJ, Polly PD. 2012. The ecology of morphology: The ecometrics of locomotion and macroenvironment in North American snakes. Pages 117–146 in Louys J, ed. Paleontology in Ecology and Conservation. Springer-Verlag Berlin Heidelberg.

Lipton D, Rubenstein M, Weiskopf SR, Carter SL, Peterson J, Crozier LG, Fogarty M, Gaichas S, Hyde KJW, Morelli TL, Morisette J, Moustahfid H, Muñoz R, Poudel R, Staudinger MD, Stock CA, Thompson LM, Waples R, Weltzin JF. 2018. Ecosystems, ecosystem services, and biodiversity. Pages 259–312 in Reidmiller DR, Avery CW, Easterling KE, Kunkel KE, Lewis KLM, Maycock TK, and Stewart BC, eds. Impacts, Risks, and Adaptation in the United States: Fourth National Climate Assessment, Volume II. U.S.Global Change Research Program.

Lucas PW, Casteren A Van, Al-fadhalah K, Almusallam AS, Henry AG, Michael S, Watzke J, Reed D a, Diekwisch TGH, Strait DS, Atkins AG. 2014. The role of dust, grit and phytoliths in tooth wear. Annales Zoologici Fennici 2450: 143–152.

Matsuura K, National Center for Atmospheric Research Staff. 2017. The climate data guide: Global (land) precipitation and temperature. (16 April 2018;

https://climatedataguide.ucar.edu/climate-data/global-land-precipitation-and-temperature-willmott-matsuura-university-delaware).

Matthews E. 1983. Global vegetation and land use: New high-resolution data bases for climate studies. Journal of Climate and Applied Meteorology 22: 474–487.

Matthews E. 1984. Prescription of Land-Surface Boundary Conditions in GISS GCM II: A Simple Method Based on High-Resolution Vegetation Data Bases. NASA Tech. Memo 86096.

Matthews E. 1999. Global Vegetation Types, 1971-1982 (Matthews). Data set. (16 April 2018; http://daac.ornl.gov).

McGill BJ, Enquist BJ, Weiher E, Westoby M. 2006. Rebuilding community ecology from functional traits. Trends in Ecology and Evolution 21: 178–185.

Meloro C, Kovarovic K. 2013. Spatial and ecometric analyses of the Plio-Pleistocene large mammal communities of the Italian peninsula. Journal of Biogeography 40: 1451–1462.

Merceron G, Ramdarshan A, Blondel C, Boisserie JR, Brunetiere N, Francisco A, Gautier D, Milhet X, Novello A, Pret D. 2016. Untangling the environmental from the dietary: Dust does not matter. Proceedings of the Royal Society B: Biological Sciences 283: .

Panciroli E, Janis CM, Stockdale M, Martín-Serra A. 2017. Correlates between calcaneal morphology and locomotion in extant and extinct carnivorous mammals. Journal of Morphology 278: 1333–1353.

Petchey OL, Gaston KJ. 2002. Functional diversity (FD), species richness and community composition. Ecology Letters 5: 402–411.

Petchey OL, Gaston KJ. 2006. Functional diversity: Back to basics and looking forward. Ecology Letters 9: 741–758.

Polly PD. 2010. Tiptoeing through the trophics: Geographic variation in carnivoran locomotor ecomorphology in relation to environment. Pages 374–410 in Goswami A and Friscia A, eds. Carnivoran Evolution: New Views on Phylogeny, Form, and Function. Cambridge University Press.

Polly PD, Eronen JT, Fred M, Dietl GP, Mosbrugger V, Scheidegger C, Frank DC, Damuth J, Stenseth NC, Fortelius M. 2011. History matters: Ecometrics and integrative climate change biology. Proceedings of the Royal Society B: Biological Sciences 278: 1131–1140.

Polly PD, Fuentes-Gonzalez J, Lawing AM, Bormet AK, Dundas RG. 2017. Clade sorting has a greater effect than local adaptation on ecometric patterns in Carnivora. Evolutionary Ecology Research 18: .

Polly PD, Head JJ. 2015. Measuring Earth-life transitions: Ecometric analysis of functional traits from late Cenozoic vertebrates. Pages 21–46 in Polly PD, Head JJ, and Fox DL, eds. Earth-Life Transitions: Paleobiology in the Context of Earth System Evolution, vol. 21. The Paleontological Society.

Polly PD, MacLeod N. 2008. Locomotion in fossil Carnivora: An application of eigensurface analysis for morphometric comparison of 3D surfaces. Palaeontologia Electronica 11: 10A:13p.

Polly PD, Sarwar S. 2014. Extinction, extirpation, and exotics: Effects on the correlation between traits and environment at the continental level. Annales Zoologici Fennici 51: 209–226.

Radinsky L. 1987. The Evolution of Vertebrate Design. University of Chicago Press.

Semprebon G, Rivals F, Janis CM. 2019. The role of grass vs. exogenous abrasives in the paleodietary patterns of North American ungulates. Frontiers in Ecology and Evolution 7: 1–23.

Short RA, Pinson K, Lawing AM. In review. Comparison of environmental inference approaches for ecometric analyses: Using hypsodonty to estimate precipitation. Methods in Ecology and Evolution.

Smith FA, Doughty CE, Malhi Y, Svenning JC, Terborgh J. 2016. Megafauna in the Earth system. Ecography 39: 99–108.

Strömberg CAE. 2002. The origin and spread of grass-dominated ecosystems in the late Tertiary of North America: Preliminary results concerning the evolution of hypsodonty. Palaeogeography, Palaeoclimatology, Palaeoecology 177: 59–75.

Strömberg CAE. 2006. Evolution of hypsodonty in equids: Testing a hypothesis of adaptation. Paleobiology 32: 236–258.

Swinton SM, Lupi F, Robertson GP, Hamilton SK. 2007. Ecosystem services and agriculture: Cultivating agricultural ecosystems for diverse benefits. Ecological Economics 64: 245–252.

Tóth AB, Lyons SK, Behrensmeyer AK. 2014. A century of change in Kenya's mammal communities: Increased richness and decreased uniqueness in six protected areas. PLoS ONE 9: e93092.

Vermillion WA, Polly PD, Head JJ, Eronen JT, Lawing AM. 2018. Ecometrics: a trait-based approach to paleoclimate and paleoenvironmental reconstruction. Pages 373–394 in Croft DA, Su D, and Simpson SW, eds. Methods in Paleoecology: Reconstructing Cenozoic Terrestrial Environments and Ecological Communities. Springer.

Violle C, Navas ML, Vile D, Kazakou E, Fortunel C, Hummel I, Garnier E. 2007. Let the concept of trait be functional! Oikos 116: 882–892.

Walther GR, Post E, Convey P, Menzel A, Parmesan C, Beebee TJC, Fromentin JM, Hoegh-Guldberg O, Bairlein F. 2002. Ecological responses to recent climate change. Nature 416: 389–395.

Williams JW, Jackson ST. 2007. Novel climates, no-analog communities, and ecological surprises. Frontiers in Ecology and the Environment 5: 475–482.

Wilson D, Reeder D. 2005. Mammal Species of the World: A Taxonomic and Geographic Reference. 3rd ed. Johns Hopkins University Press.

Wingard GL, Bernhardt CE, Wachnicka AH. 2017. The role of paleoecology in restoration and resource management-the past as a guide to future decision-making: Review and example from the Greater Everglades ecosystem, U.S.A. Frontiers in Ecology and Evolution 5: 1–24.

Winkler DE, Schulz-Kornas E, Kaiser TM, De Cuyper A, Clauss M, Tütken T. 2019. Forage silica and water content control dental surface texture in Guinea pigs and provide implications for dietary reconstruction. Proceedings of the National Academy of Sciences 116: 1325–1330.

Žliobaitė I, Rinne J, Tóth AB, Mechenich M, Liu L, Behrensmeyer AK, Fortelius M. 2016. Herbivore teeth predict climatic limits in Kenyan ecosystems. Proceedings of the National Academy of Sciences 113: 12751–12756.

# 4. ADDITIONS TO THE PLEISTOCENE MAMMALIAN FAUNA OF TÉRAPA, SONORA, MEXICO

## 4.1. Introduction

At San Clemente de Térapa (hereafter, Térapa), Sonora, Mexico, a rich fossil deposit records a late Pleistocene mesic marsh savanna in an area that is now xeric desert chaparral. Northern Mexico contains a boundary zone between the Nearctics and the Neotropics; however, relatively few sites are known from the Pleistocene (Rancholabrean North American Land Mammal Age; LMA) of the region (Ceballos et al. 2010). Overall, our knowledge of the fossil mammals of Mexico is biased toward taxa of larger sizes and younger geological ages, possibly because of collection methods (Montellano-Ballesteros and Jiménez-Hidalgo 2006, Ferrusquía-Villafranca et al. 2010). White et al. (2010) reviewed 64 Neogene sites from Sonora, Mexico, but only three sites have considerable, detailed faunal records—El Golfo (Sussman et al. 2016), Térapa (Mead et al. 2006), and Rancho la Brisca (Van Devender et al. 1985) (Figure 4.1).

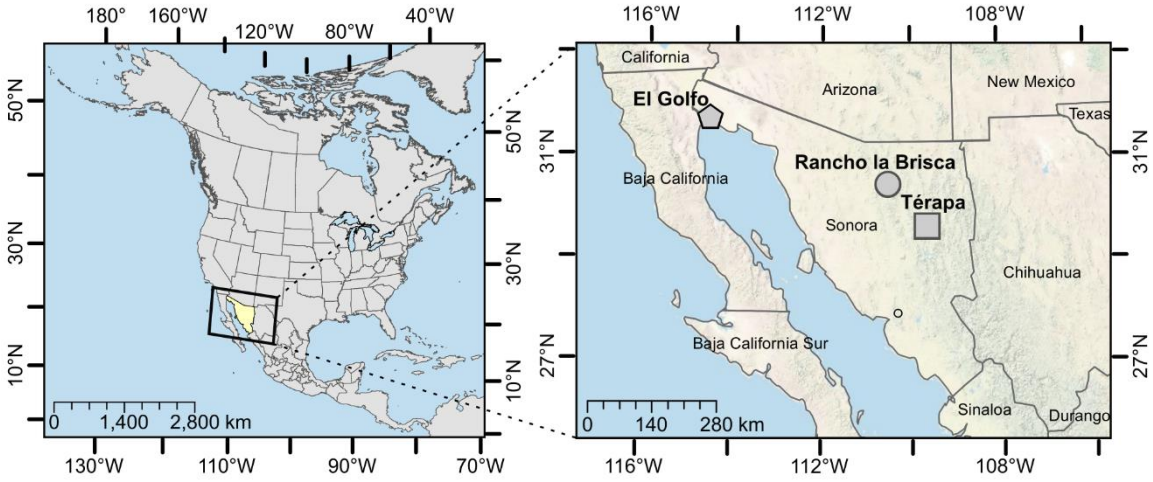


**Figure 4.1. Geography of Sonora, Mexico (yellow; left) and selected fossil sites (right). Terrain basemap is from the US National Park Service.**

Rancho La Brisca is known to be Rancholabrean, but this site has a slightly different fauna than is preserved at Térapa and other sites in the region because the record is biased toward small and medium fish, amphibians, and reptiles (Van Devender et al. 1985). La Playa has the first record of *Cynomys* in Sonora, which was found alongside *Bison, Platygonus*, *Mammuthus, Equus,* camelids, and other large mammals (Mead et al. 2010). Fossils found at other sites, including La Botana, Llano Prieto, and Chinobampo, are primarily large mammals, such as *Bison*, *Equus*, *Mammuthus*, *Glyptotherium*, and *Camelops* (White et al. 2010, Cruz-y-Cruz et al. 2018). These taxonomic occurrences support the interpretation of a more equable climate during the Rancholabrean as seen today (Nunez et al. 2010). It is probable that more sites exist in this region and can contribute to our understanding of the paleontological record but have yet to be found, fully analyzed, and reported upon.

With *Bison* present throughout the stratigraphic profile, Térapa represents one of the few Rancholabrean LMA sites studied in detail in Sonora (Mead et al. 2006). Within the Térapa basin, fossils of more than 60 taxa, many with tropical affinities, have been recovered; a preliminary faunal list is provided in Mead et al. (2006) and an updated list is provided in White et al. (2010). More recent publications have described *Mammuthus* and *Cuvieronius* (Mead et al. 2019), *Glyptotherium cylindricum* and *Pampatherium* cf. *P. mexicanum* (Mead et al. 2007), shrews and bats (Czaplewski et al. 2014), and 39 species of birds (Steadman and Mead 2010, Oswald and Steadman 2011). Here, we add to the growing list of fossil vertebrates recovered from Térapa that have detailed descriptions regarding the identifications.

Térapa is located along the Río Moctezuma, and a riparian corridor most likely existed from the Gulf of Mexico up the Río Yaqui and Río Moctezuma to Térapa where a basalt flow created a shallow lake and marsh environment (Mead et al. 2006). Stable isotope analyses of carbon and oxygen from fossil material at Térapa suggest that marsh and grasslands were likely present in the basin (Nunez et al. 2010, Bright et al. 2016). The basin created a shallow pond environment and began to fill with sediment at 40 ± 3 ka (Bright et al. 2010). Today, there is an 11 m-thick sequence of medium- to fine-grained sediments; details of the geology are provided in Mead et al. (2006) and Bright et al. (2016).

Fossils found at Térapa were deposited during the Wisconsinan Glacial period when the climate of Sonora was more equable than today with cooler, drier summers and wetter winters (Metcalfe 2006, Van Devender 2007, Nunez et al. 2010, Bright et al.

2016). As global temperatures increased and precipitation decreased, Sonora became more arid, and species were forced to shift their ranges in response. Thus, Térapa provides a unique opportunity to further investigate the mammals and increase our understanding of the late Pleistocene of northern Mexico.

Here, we describe specimens from eight mammalian species and discuss their geographic distribution in the North American desert region. Though previous work has included most of these genera on a faunal list (Mead et al. 2006), this is the first attempt to provide detailed descriptions. In doing so, we identify three species for which Térapa fills a geographic gap in their previously known occurrences.

**4.2. Materials and methods**

Specimens from Térapa are housed temporarily at The Mammoth Site, Hot Springs, South Dakota, USA, and are curated with numbers prefixed with TERA. We used primarily comparative reference specimens to determine taxonomic assignments. Specimens were from the Florida Museum of Natural History (FLMNH) and the East Tennessee Museum of Natural History (ETMNH). When possible, linear measurements and the related citations were provided within the taxonomic descriptions. Geographic occurrences were determined using online databases and literature.

Species identifications for equid post-crania were determined using a quadratic discriminant analysis implemented in R (R Core Team 2016) using the package MASS (R Core Team 2016). Training data used in the analyses are from McHorse et al. (2016) and Sertich et al. (2014). For analysis of the phalanx, training data included *Equus occidentalis, E. conversidens, E. lambei, E. scotti,* and a northwest stilt-legged taxon.

For analysis of the metacarpal, training data included *Equus complicatus, E. conversidens, E. occidentalis,* and *E. scotti*.

### 4.3. Results

Among the mammalian fauna from Térapa, we provide descriptions for members of seven genera, including *Equus*, *Platygonus*, *Camelops*, *Palaeolama*, *Canis*, *Procyon*, *Lynx,* and *Smilodon.* Additional large-bodied mammalian remains have been excluded from this analysis and will appear elsewhere. Cervids and antilocaprids are being described in a forthcoming publication, and *Bison* will be presented in an upcoming review of the taxon's presence in the southwestern US and northwestern Mexico.

#### 4.3.1. Systematic paleontology

Class Mammalia

Order Perissodactyla

Family Equidae

*Equus* Linnaeus 1758

*Equus scotti* Gidley 1900

Material: Left distal metacarpal (TERA 313), left partial phalanx 1 (TERA 320), phalanx 2 and sesamoid (TERA 319).

Description: The left metacarpal (TERA 313) is broken transversely across the diaphysis, but the distal end is complete (Figure 4.2A). The left partial first phalanx (TERA 320) is missing the lateral, distal portion (Figure 4.2B). The metacarpal and phalanx articulate. The second phalanx is complete (TERA 319; Figure 4.2C) and articulates with a sesamoid. The first and second phalanges do not articulate.

Identification: In quadratic discriminant analyses, the second phalanx (TERA 319) was identified to species level with 87.5% confidence, and the distal metacarpal (TERA 313) was identified with 100% confidence (Figure C-1).

Remarks: *Equus* is widespread across the US and Mexico during the Rancholabrean (Ferrusquía-Villafranca et al. 2010, 2017), including in Sonora (Cruz-y-Cruz et al. 2018). Taxonomy of *Equus* introduces complex questions surrounding species identifications. *Equus scotti* is a stout-legged horse that has been documented across the North American desert region during the Rancholabrean (Harris 2014). Recent efforts to revise equid taxonomy have considered *E. scotti* to be synonymous with *E. mexicanus* (Alberdi et al. 2014) and *E. excelsus* (Priego-Vargas et al. 2017), but there is discussion on the correct nomenclature (Harris 2014). Previous work identified *E. excelsus* at Térapa (Carranza-Castañeda and Roldán-Quintana 2007), and it is likely the same as our *E. scotti*. However, equid taxonomy needs to be thoroughly and formally evaluated before these issues can be confidently resolved.

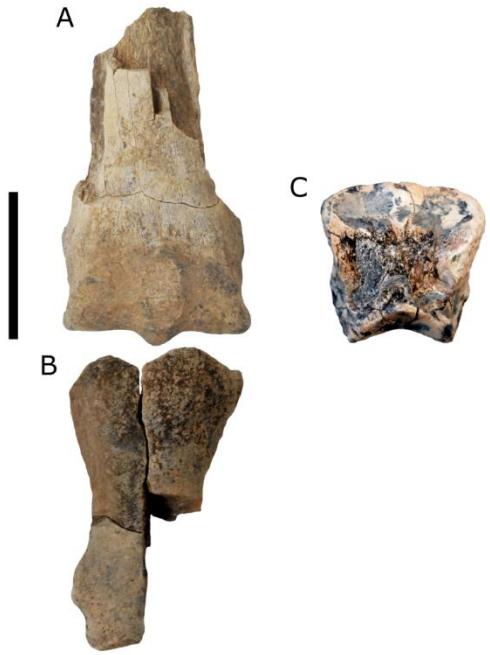


**Figure 4.2. *Equus scotti* specimens. A, left distal metacarpal (TERA 313); B, left partial phalanx (TERA 320); C, second phalanx (TERA 319). A and B articulate. Scale bar equals 5 cm.**

*Equus* cf. *E. scotti* Gidley 1900

Material: Right P4 (TERA 284), right M2 (TERA 287), right M3 (TERA 285), right P4 and M1 (TERA 291), right P3 and P4 (TERA 168), left P2 (TERA 282, 289), left P4 (TERA 290), left M2 (TERA 286, 288), left M3 (TERA 283), right p4 (TERA 310), lower left tooth (TERA 308), upper left tooth and lower right tooth (TERA 266).

Description: Most of the teeth are complete with moderate wear. These teeth (Figures 4.3A-D) are larger and have more complex enamel patterns than the teeth assigned to *Equus* sp. (Figures 4.3E-H).

Identification: We hypothesize that the teeth are from the same species as the postcranial elements previously identified as *Equus scotti* because of their large size.

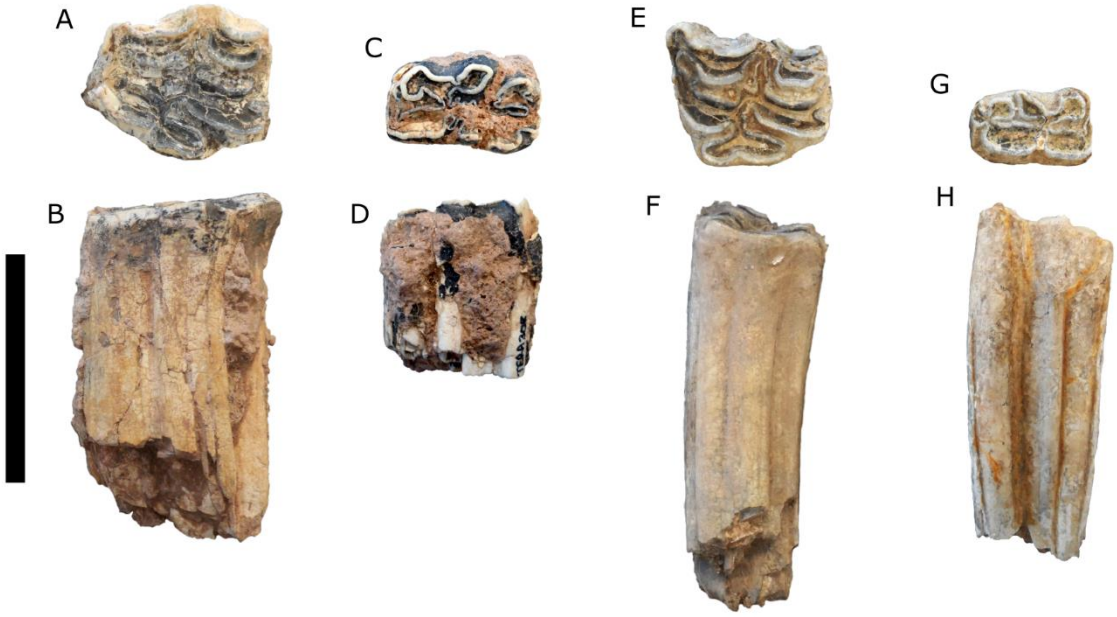


**Figure 4.3. *Equus* spp. teeth. A-B, *Equus* cf. *E. scotti*, upper left molar (TERA 286); C-D, *Equus* cf. *E. scotti*, lower left molar (TERA 308); E-F, *Equus* sp., upper left molar (TERA 303); G-H, *Equus* sp., lower right molar (TERA 295). A, C, E, and G are in occlusal view. B, D, F, and H are in lingual view. Scale bar equals 5 cm.**

*Equus* sp.

Material: Right P3 (TERA 166), right M1 (TERA 263), right M2 (TERA 157, 169, 296, 300), right M3 (TERA 298), left M2 (TERA 303), left P4 and M1 (TERA 293), left P3-M1 and right M1 (TERA 297), upper right tooth (TERA 299, 307), upper tooth (TERA 267), right m2 (TERA 295), right m3 (TERA 262, 305, 306), left m2 with fragment (TERA 312), left m3 (TERA 322), lower left molar (TERA 301, 302), lower

right tooth (TERA 309), lower left tooth (TERA 311), lower tooth fragment (TERA 264, 265, 304), mandibular symphysis (TERA 294), left partial distal humerus (TERA 314), left magnum (TERA 318), right distal tibia (TERA 317), left partial calcaneum (TERA 315, 316), right cuneiform and lunar (TERA 321).

Description: The postcranial elements are slight compared to extant *Equus caballus* and the Térapa specimens conferred to *Equus scotti*, and the teeth (Figures 4.3E-H) are noticeably smaller and have less complex enamel patterns than those assigned to *E.* cf. *E. scotti* (Figures 4.3A-D).

Identification: It is unknown if the post-cranial elements are of the same species as the dentition. At this time, there are no morphological features to confirm species designations.

Remarks: Previous work on different specimens also identified *E. conversidens* at Térapa (Carranza-Castañeda and Roldán-Quintana 2007), and, because of the smaller size, it is possible that our *Equus* sp. refers to the same taxon. Occurrence of both *E. scotti* and a smaller-sized horse is common at Rancholabrean sites, and the small horse is often identified as *E. conversidens* (Harris 2014).

Mead et al. (2006) listed *Tapirus* sp. among the taxa found at Térapa based on a mandibular symphysis (TERA 294; Figure 4.4). However, this specimen is now identified as *Equus* sp. Depth of the mandible suggests hypsodont teeth as in *Equus*. The narrow intermandibular space extends anterior to the second premolar as in *Equus*; in *Tapirus*, this space is closed at the anterior end of the second premolar. The mandibular

foramen is located well anterior to the tooth row as in *Equus*; in *Tapirus*, the mandibular foramen is inferior to the anterior second premolar.


**Figure 4.4. *Equus* spp. mandible fragments. A, *Equus* sp. (TERA 294) previously identified as *Tapirus*; B, *Equus caballus* (ETMNH-Z 15462).**

Order Artiodactyla

Family Tayassuidae

*Platygonus* LeConte 1848

*Platygonus compressus* LeConte 1848

Material: Molar fragments (TERA 167), deciduous upper premolar (TERA 280), right upper canine (TERA 281).

Description: The molar fragments (TERA 167) are hypsodont and zygodont (Figure 4.5A). The deciduous tooth (TERA 280) is complete and more bunodont than

the molar fragments (Figure 4.5B). The canine is complete (TERA 281) and has an anterior occlusal surface (Figure 4.5C).

Identification: This specimen was initially identified as cf. *Platygonus* by Mead et al. (2006). Comparisons with fossil material at FLMNH suggest that these teeth are *Platygonus* because the cusps are more zygolophodont as in *Platygonus* than bunodont as in *Mylohyus*. Because *Platygonus* is monotypic in the middle and late Rancholabrean (Kurtén and Anderson 1980, Wright 1998), these specimens are assigned to *P. compressus.*

Remarks: *Platygonus compressus* is known from the Rancholabrean of Arizona (Murray et al. 2005), New Mexico, and eastern Texas as well as the Central Plateau and Trans-Mexican Volcanic Belt (Ferrusquía-Villafranca et al. 2010, 2017). In Sonora, *Platygonus* sp. is known from La Playa and Bajimari (White et al. 2010) and *P.* cf. *P. vetus* is known from El Golfo (Croxen et al. 2007). Térapa provides the first record of *P. compressus* in Sonora, but it is not unexpected.

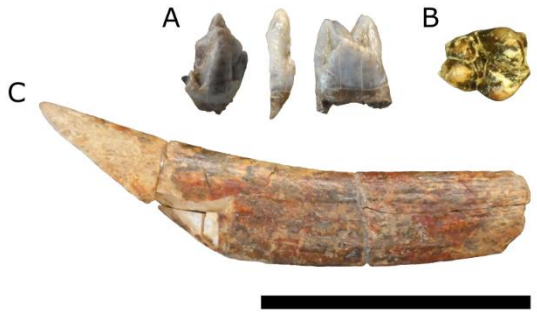


**Figure 4.5. *Platygonus compressus* specimens. A, molar fragments (TERA 167); B, deciduous upper tooth in occlusal view (TERA 280); C, right upper canine in labial view (TERA 281). Scale bar equals 5 cm.**

Family Camelidae

*Camelops* Leidy, 1854

*Camelops hesternus* (Leidy, 1873)

Material: Left mandibular fragment with roots of m1-2 (TERA 278); left partial distal phalanx (TERA 279).

Description: The partial distal phalanx (TERA 279) has splayed ventral trochlea (Figure 4.6A). This specimen is not a metapodial because of the lack of a condylar keel (Zazula et al. 2016). The mandibular fragment (TERA 278) has the roots of large selenodont molars (Figure 4.6B). At its base, the m2 measures 43.28 mm.

Identification: These specimens were initially identified as "*Camelops*-sized" by Mead et al. (2006). The m2 measurement is within the range of *Camelops* provided by Honey et al. (1998) and Baskin and Thomas (2016). The mandible is also substantially larger than comparative material of *Palaeolama* and *Hemiauchenia*. The phalanx was also compared to phalanges of *Palaeolama* and *Hemiauchenia*, but it is considerably larger than specimens within both genera. *Camelops* is the only other Rancholabrean camelid, and it was large enough to have mandibles and phalanges of the size found at Térapa (Baskin and Thomas 2016). The most recent review of *Camelops* described two species – *C. hesternus* in the Rancholabrean and *C. minidokae* in the Irvingtonian (Baskin and Thomas 2016). Because *Camelops* is considered monotypic in the Rancholabrean and the specimens are consistent with the morphology, these specimens are assigned to *C. hesternus.*

Remarks: *Camelops hesternus* is widespread across the US and northern Mexico (Ferrusquía-Villafranca et al. 2010, 2017), including in Sonora (Cruz-y-Cruz et al. 2018).

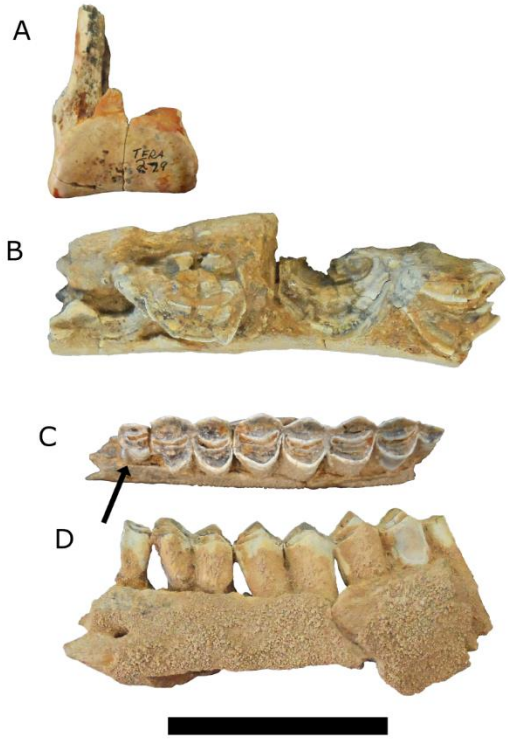


**Figure 4.6. Camelidae specimens. A, *Camelops hesternus*, partial left distal phalanx in anterior view (TERA 279); B, *C. hesternus*, left mandible fragment, including roots of first and second molars, in occlusal view (TERA 278); C, *Palaeolama mirifica*, right mandible fragment with a partial fourth premolar and three molars in occlusal view (TERA 156); D, *P. mirifica*, TERA 156 in labial view. Black arrow indicates the infolding on the p4 that is characteristic of *Palaeolama.* Scale bar equals 5 cm.**

*Palaeolama* Gervais, 1867

*Palaeolama mirifica* (Simpson, 1929)

Material: Left mandible fragment with partial p4-m3 (TERA 156).

Description: The mandibular fragment (TERA 156) has a partial p4 and m1-3 with brachydont, selenodont dentition (Figures 4.6C-D). The p4 has a vertical groove just posterior to the break. The m2 measures 19.18 mm at the base and 21.25 mm at the occlusal surface.

Identification: This specimen was initially identified as "*Hemiauchenia*-sized" by Mead et al. (2006). The groove on the p4 is indicative of the "complex infolding" seen in *Palaeolama* (Figure 4.6C; Honey et al., 1998, p. 454; Kurtén and Anderson, 1980). Both m2 measurements are within the range of *Palaeolama* provided by Honey et al. (1998). Because *Palaeolama* is monotypic in the Rancholabrean of North America (Honey et al. 1998) and the specimens fit the morphology, these specimens are assigned to *P. mirifica.*

Remarks: *Palaeolama mirifica* is found at Rancholabrean sites in Florida, California, and Texas (Kurtén and Anderson 1980), South Carolina (Sanders 2002), Costa Rica (Pérez 2011), and in the Mexican state of Puebla (Bravo-Cuevas and Jiménez-Hidalgo 2015). However, it has not been documented in Arizona (Mead et al. 2005). *Palaeolama* sp. is documented at Irvingtonian sites at El Golfo in northwestern Sonora (Croxen et al. 2007) and Rio Tomayate in El Salvador (Cisneros 2005), and from the Rancholabrean of Guatemala (Dávila et al. 2019). Térapa is the first Rancholabrean occurrence of *P. mirifica* in northwestern Mexico.

Order Carnivora

Family Canidae

*Canis* Linnaeus, 1758

*Canis dirus* Leidy, 1858

Material: Left mandible with c1-m2 (TERA 154), left maxilla and jugal with P3-M1, left mandible with partial c1-partial m2, right mandible with p4-m2, four incisors, two upper canines, two lower canines, one M1, one m3, and two unidentified fragments (TERA 450), distal left humerus (TERA 155).

Description: The left mandible with c1-m2 (TERA 154) and the distal humerus (TERA 155) were previously described in detail (Hodnett et al. 2009); the remaining specimens (TERA 450) are described here. All teeth in the maxilla and both mandibles are in an advanced stage of wear. The left maxilla is articulated with the left jugal, and the P3 is broken between the anterior and posterior roots (Figures 4.7A-B). The left mandible is missing the coronoid process and angular process; the condyle is complete (Figure 4.7C). There is no evidence of an alveolus for a p1 on the mandible. The anterior mental foramen is inferior to the anterior p2, and the posterior mental foramen is inferior to the posterior p3. The right mandible is broken between the p4 and m1 and along the inferior masseter fossa (Figure 4.7D). Only the anterior root of the m2 is present and the alveolus for a single-rooted m3 is broken. Cranial and dental measurements suggest a larger than average *C. dirus* (Table C-1, Figure 4.8; Tedford et al., 2009).

Identification: Mead et al. (2006) initially identified *Canis dirus* at Térapa, and Hodnett et al. (2009) agreed for TERA 154 and TERA 155. Measurements on the left

mandible indicate that this specimen is too large to be a different Rancholabrean-age canid, such as *C. latrans* or *C. lupus* (Figure 4.8). *Canis armbrusteri* was also a large canid in the late Irvingtonian (Kurtén and Anderson 1980, Harris 2014) and is thought to have given rise to *C. dirus* (Tedford et al. 2009). The Térapa teeth are too worn to examine the cusp patterns, but the upper molars have reduced labial cingula as in *C. dirus* rather than *C. armbrusteri* (Tedford et al. 2009).

Remarks: *Canis dirus* is considered "one of the most common mammalian species in the Rancholabrean" and is found across the US and Mexico (Kurtén and Anderson, 1980, p. 171; Harris, 2014; Ferrusquia-Villafranca et al., 2017). However, Térapa is the first occurrence of *C. dirus* in Sonora (Hodnett et al. 2009). There are at least three individuals of *C. dirus* found at Térapa based on lower left canines. The maxilla and mandibles of TERA 450 are likely from the same individual because of the similar degree of wear on the teeth. The extensive wear on the teeth and the large size suggests one older individual.

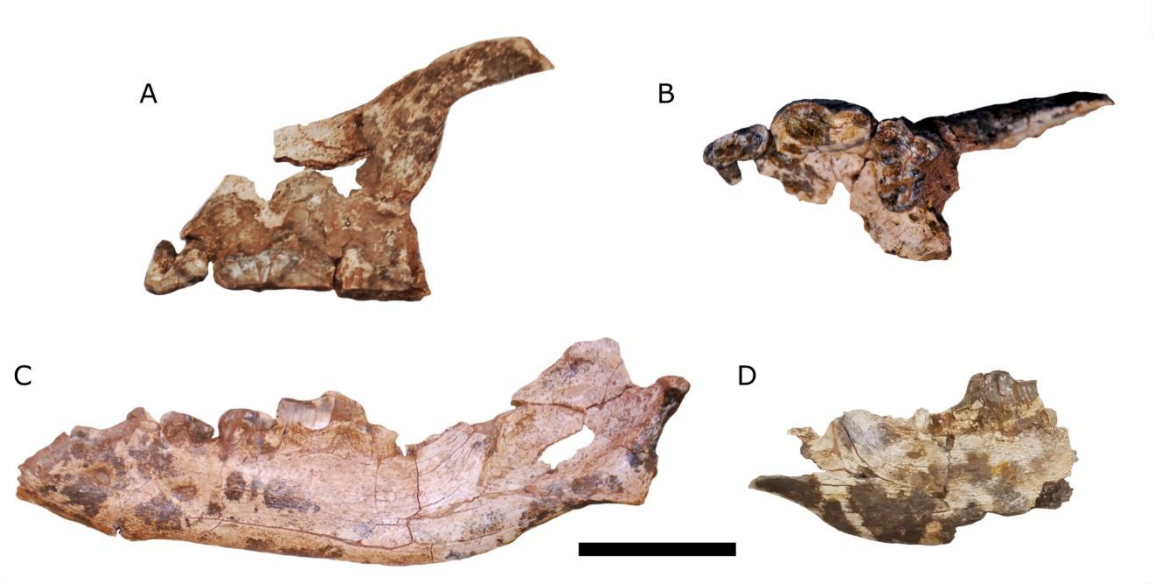


**Figure 4.7. *Canis dirus* specimens (TERA 450). A, left maxilla and jugal with P3-M1 in lateral view; B, left maxilla and jugal with P3-M1 in occlusal view; C, left mandible with partial c1-partial m2 in buccal view; D, right mandible with p4-m2 in buccal view. Scale bar equals 5 cm.**

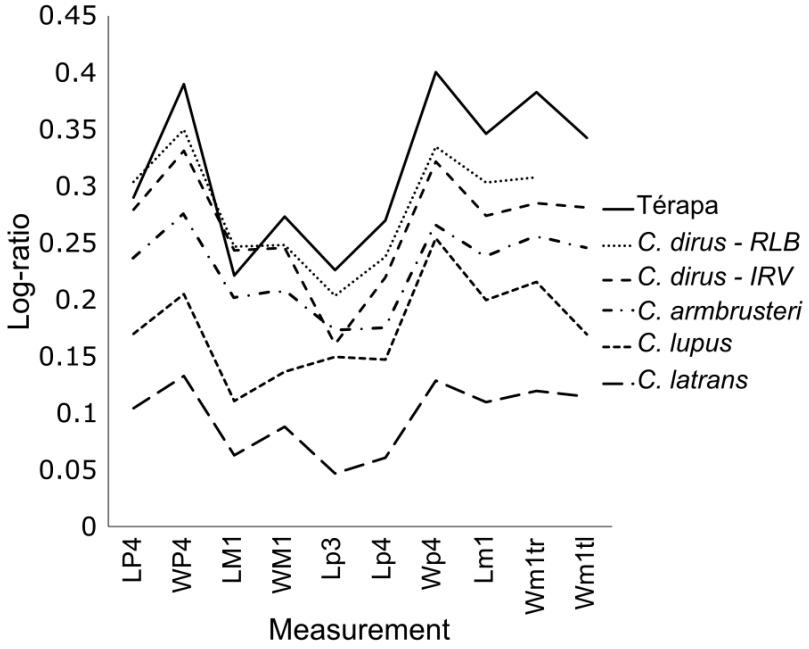


**Figure 4.8. Log-ratios of Térapa *Canis dirus* (TERA 450) compared to *Canis dirus* from the Rancholabrean (RLB) and Irvingtonian (IRV), *C. armbrusteri, C. lupus,* and *C. latrans.* Measurements are relative to *Eucyon davisi.* Methods and reference data from Tedford et al. (2009); data are available in Table A-1.**

Family Procyonidae

*Procyon* Storr, 1780

*Procyon lotor* (Linnaeus, 1758)

Material: Left calcaneum (TERA 453).

Description: The calcaneum (TERA 453) is complete (Figure 4.9A). There is no knob present on the trochlear process, which has a minimal groove, and the calcaneum does not have an accessory surface between the anterior articular surface and the cuboid facet; the latter has a point on its dorsal edge. The greatest length of the calcaneum is 28.03 mm and the transverse breadth of the sustentaculum is 14.49 mm.

Identification: The calcaneum was previously identified as *Procyon* sp. (Mead et al. 2006). Following descriptions provided by Stains (1973; lack of a knob on the trochlear process), the calcaneum is now referred to *P. lotor*. Within *Procyon*, the calcaneum is assigned to *P. lotor* instead of *P. cancrivorous* because of the minimal trochlear groove, the cuboid facet, and the lack of an accessory surface between the anterior articular surface and the cuboid facet (Stains 1973). In addition, the length and breadth measurements are within the range of *P. lotor* provided by Stains (1973). Additional Pleistocene species of *Procyon* have been synonymized with *P. lotor* because the morphology was within the range of intraspecific variation (Kurtén and Anderson 1980). Kurtén and Anderson (1980) recognized only one other fossil species, *P. rexroadensis*, which was limited to the Blancan LMA. Emmert and Short (2018) recommended synonymizing *P. rexroadensis* with *P. lotor* because of a lack of distinct morphological characters.

Remarks: Pleistocene-age *Procyon* has been found across North America and into northern South America (Kurtén and Anderson 1980), but the fossil record is sparse (Harris 2014). In Mexico, *Procyon* sp. is at the Irvingtonian-age El Golfo (Croxen et al. 2007), and *Procyon lotor* is known from the Rancholabrean in California and New Mexico (Harris 2014) as well as the Chihuahua-Coahuila Plateaus and Ranges, the Sierra Madre Oriental, the Trans Mexican Volcanic Belt and the Yucatan Platform (Ferrusquía-Villafranca et al. 2010), so it is expected in the northwest of Mexico although it is not reported from the Rancholabrean of Arizona (Mead et al. 2005).

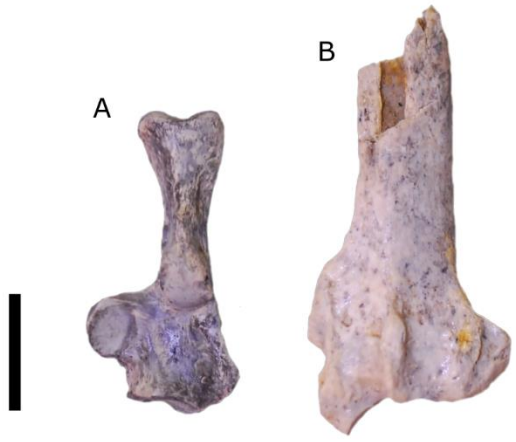


**Figure 4.9. Carnivora specimens. A, *Procyon lotor*, left calcaneum in anterior view (TERA 453); B, *Lynx rufus*, left distal radius in anterior view (TERA 451). Scale bar equals 1 cm.**

Family Felidae

*Lynx* Kerr, 1792

*Lynx rufus* (Schreber, 1777)

Material: Distal left radius (TERA 451).

Description: The radius (TERA 451) is broken transversely across the diaphysis, which is compressed anteroposteriorly (Figure 4.9B). The styloid process, dorsal tubercle, and lateral tuberosity are angular and pronounced. The greatest breadth of the distal end (Bd; von den Driesch, 1976) measures 19.41 mm.

Identification: This radius was initially reported as *Lynx rufus* by Mead et al. (2006), and the identification is confirmed here. The distinct features are as in Felidae rather than Canidae, and the anteroposterior compression excludes *Felis* (Kelson 1946). As in *L. rufus*, there is a distinct horizontal ridge superior to the distal articulation on the posterior surface and a lack of mediolateral constriction between the diaphysis and

epiphysis. *Lynx rufus* is known from the Rancholabrean of Mexico (Ferrusquía-Villafranca et al. 2010) and Arizona (Mead et al. 2005), whereas *Lynx canadensis* has not been found south of Utah (Lavoie et al. 2019).

Remarks: *Lynx rufus* is frequently found at North American Pleistocene sites (Kurtén and Anderson 1980), and is known across northern and central Mexico during the Rancholabrean (Ferrusquía-Villafranca et al. 2010, 2017). In Mexico, *L. rufus* is also known from the Irvingtonian of Cedazo (Mooser and Dalquest 1975), and the latest Pleistocene or early Holocene of Jimenez Cave (Messing 1986).

*Smilodon* Lund 1842

*Smilodon* cf. *S. fatalis* (Leidy 1869)

Material: Fragment of right dP3 including ectoparastyle and parastyle (TERA 452).

Description: The tooth fragment (TERA 452) is mediolaterally compressed and has a distinct parastyle and ectoparastyle (Figure 4.10). The tooth fragment is lacking a distinct protocone and preserves no evidence of any lingual flaring that would indicate a protocone had been present. There is a minimal anterior cingulum on the tooth. Diagnostic measurements are not possible because of the fragmented nature of the specimen.

Identification: This specimen was initially identified as *Canis latrans* by Mead et al. (2006). However, the mediolateral compression and parastyle suggest this tooth is from Felidae and not Canidae. The size suggests a large cat, possibly *Panthera, Puma*, or *Smilodon.* The lack of protocone excludes *Panthera* and *Puma* (Cherin et al. 2013,

Babiarz et al. 2018), and the ectoparastyle and cingulum are as in *Smilodon* (Christiansen 2013). Therefore, we confer the tooth fragment to *Smilodon*. Because *Smilodon fatalis* is common during the Rancholabrean, *S. populator* has not been found in North America, and *S. gracilis* is from the early Irvingtonian, we confer the specimen to *S. fatalis.*

Remarks: *Smilodon* is known extensively throughout North America from the Irvingtonian and Rancholabrean LMAs (Kurtén and Anderson 1980, Babiarz et al. 2018), but this is the first record from the northwest of Mexico. In Mexico, *S. fatalis* has been found at Pleistocene sites across the Central Plateau, the Trans-Mexico Volcanic Belt, and the Sierra Madre Oriental (Ferrusquía-Villafranca et al. 2010, 2017). In the United States, *S. fatalis* is known from the Rancholabrean of eastern New Mexico and southern California (Kurtén and Anderson 1980, Morgan and Lucas 2001, Harris 2014), so its presence in northwestern Mexico is novel but not wholly unexpected, although it is not reported from the Rancholabrean of Arizona (Mead et al. 2005).

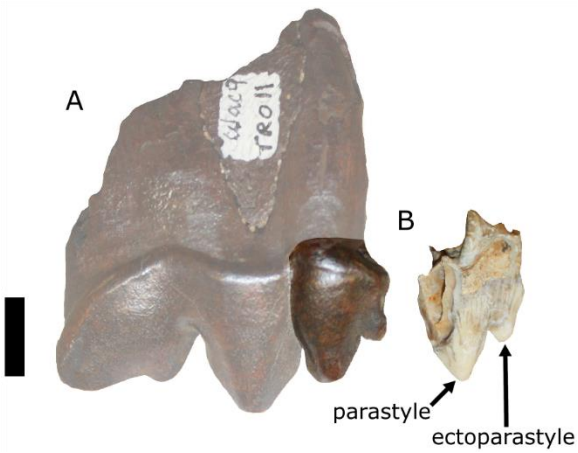

**Figure 4.10. *Smilodon* carnassials. A, *S. fatalis* adult right P4 (UF/TRO 11) with parastyle and ectoparastyle more opaque; B, *S.* cf. *S. fatalis* fragment of right deciduous P3 in labial view (TERA 452). Scale bar equals 1 cm.**

### 4.4. Discussion

This detailed description advances the understanding of the Pleistocene fauna of northwest Mexico by revising taxonomic designations at Térapa (Table C-2). Térapa provides the first Rancholabrean occurrences of *Palaeolama*, *Procyon,* and *Smilodon* in northwest Mexico and the first records of *Platygonus compressus* and *Canis dirus* in Sonora. *Equus*, *Camelops*, and *Canis* are well-represented in sites across the North American desert region and, although *Platygonus* and *Lynx* are sparsely represented in northern Mexico, they have extensive records in the southwestern US making them expected at Térapa during the Rancholabrean. It is worth noting that, during the Pleistocene, the Rancholabrean LMA is defined by the presence of *Bison* (Bell et al. 2004). The Holarctic genus did not arrive in Mexico until much later than they appear in the northern part of the continent. This biochronological delay complicates assigning LMA ages to Mexican sites but also illustrates the need to further explore Mexico for fossil sites that can provide insight on North American fauna during the Pleistocene.

Sonora has been considered an ecotone between the northern Nearctic climate and the southern Neotropical climate (Mead et al. 2007) because of shifting habitats during glacial and interglacial periods. Modern (i.e., interglacial) Sonoran and Chihuahuan deserts are typified by scrubland ecosystems with warm tropical-subtropical climates, whereas this geographic region was more temperate during glacial periods and

were typified with pinyon-juniper-oak woodlands (Van Devender 2007). During the glacial period, lower global temperatures produced a more constricted Intertropical Convergence Zone (ITCZ) and increased precipitation in northwestern Mexico (Metcalfe 2006). As temperatures increased into the modern interglacial period, the ITCZ expanded poleward and shifted the mid-latitude jet stream—and associated precipitation—poleward (Metcalfe 2006). The poleward shift of the ITCZ and mid-latitude jet stream also shifted the biodiversity-rich savanna habitats and left the scrubland habitats of today (Metcalfe 2006).

Climatically-driven habitat changes have been shown to affect the distribution ranges of carnivoran species and the richness of carnivoran communities in North and South America during the Pleistocene (Arias-Alzate et al. 2017, 2020). Inferred faunal corridors would have allowed for temperate species to move south and tropical-subtropical species to move north, and "holding pen" areas would have been inhabited by taxa until more preferred environments allowed further migration (Ceballos et al. 2010, Woodburne 2010). Térapa lies along the Pleistocene Sonora – Central America Pacific lowlands corridor and the Rocky Mountains – Sierra Madre Occidental corridor (Ceballos et al. 2010). The former allowed dispersal of tropical taxa north and the latter permitted the movement of temperate taxa south (Ceballos et al. 2010); therefore, northern Mexico likely acted as a region of faunal exchange during environmental shifts between glacial and interglacial periods. For instance, *Palaeolama* originated in South America (Webb 1974), and researchers postulate that *P. mirifica* used tropical corridors

along the Sonora-Central America Pacific lowlands and the Tamaulipas-Central America Gulf lowlands to move across Mexico (Bravo-Cuevas and Jiménez-Hidalgo 2015).

Study of past fauna can have great implications for wildlife conservation because of the biodiversity shifts expected as a consequence of impending climate change (Walther et al. 2002, Foley et al. 2005, Lipton et al. 2018). The Sonoran Desert is expected to expand north as climate projections include a 1–3°C increase in temperature and up to a 20% decrease in precipitation by the mid-21$^{st}$ century, resulting in an increasingly arid climate (Magaña et al. 2012). But, only 41% of natural areas in the U.S. demonstrate climate connectivity, so that species can shift their ranges as climate change continues (McGuire et al. 2016). Térapa and other similar fossil sites provide a record that informs anticipation of climate change consequences across an increasingly xeric landscape. Future fossil recovery may help provide more details about the fauna at Térapa and in Sonora but also allow for study of habitat and biodiversity shifts.

**References**

Alberdi MT, Arroyo-Cabrales J, Marín-Leyva AH, Polaco OJ. 2014. Study of Cedral Horses and their place in the Mexican Quaternary. Revista Mexicana de Ciencias Geologicas 31: 221–237.

Arias-Alzate A, González-Maya JF, Arroyo-Cabrales J, Martínez-Meyer E. 2017. Wild felid range shift due to climatic constraints in the Americas: A bottleneck explanation for extinct felids? Journal of Mammalian Evolution 24: 427–438.

Arias-Alzate A, González-Maya JF, Arroyo-Cabrales J, Medellín RA, Martínez-Meyer E. 2020. Environmental drivers and distribution patterns of Carnivoran assemblages (Mammalia: Carnivora) in the Americas: Past to present. Journal of Mammalian Evolution 1–16.

Babiarz JP, Wheeler HT, Knight JL, Martin LD. 2018. *Smilodon* from South Carolina: Implications for the taxonomy of the genus. Pages 76–107 in Werdelin L, McDonald HG, and Shaw CA, eds. *Smilodon*: The Iconic Sabertooth. Johns

Hopkins University Press.

Baskin J, Thomas R. 2016. A review of *Camelops* (Mammalia, Artiodactyla, Camelidae), a giant llama from the Middle and Late Pleistocene (Irvingtonian and Rancholabrean) of North America. Historical Biology 28: 120–127.

Bell CJ, Lundelius Jr. EL, Barnosky AD, Graham RW, Lindsay EH, Ruez Jr. DR, Semken Jr. HA, Webb SD, Zakrzewski RJ. 2004. The Blancan, Irvingtonian, and Rancholabrean Mammal Ages. Pages 232–314 in Woodburne MO, ed. Late Cretaceous and Cenozoic Mammals of North America: Biostratigraphy and Geochronology. Columbia University Press.

Bravo-Cuevas VM, Jiménez-Hidalgo E. 2015. First reported occurrence of *Palaeolama mirifica* (Camelidae, Lamini) from the late Pleistocene (Rancholabrean) of Puebla, central Mexico. Boletin de la Sociedad Geologica Mexicana 67: 13–20.

Bright J, Kaufman DS, Forman SL, McIntosh WC, Mead JI, Baez A. 2010. Comparative dating of a *Bison*-bearing late-Pleistocene deposit, Térapa, Sonora, Mexico. Quaternary Geochronology 5: 631–643.

Bright J, Orem CA, Mead JI, Baez A. 2016. Late Pleistocene (OIS 3) paleoenvironmental reconstruction for the Térapa vertebrate site, northcentral Sonora, Mexico, based on stable isotopes and autecology of ostracodes. Revista Mexicana de Ciencias Geologicas 33: 239–253.

Carranza-Castañeda O, Roldán-Quintana J. 2007. Mastofaunula de la cuenca de Moctezuma, Cenozoico tardío de Sonora, México. Revista Mexicana de Ciencias Geologicas 24: 81–88.

Ceballos G, Arroyo-Cabrales J, Ponce E. 2010. Effects of Pleistocene environmental changes on the distribution and community structure of the mammalian fauna of Mexico. Quaternary Research 73: 464–473.

Cherin M, Iurino DA, Sardella R. 2013. Earliest occurrence of *Puma pardoides* (Owen, 1846) (Carnivora, Felidae) at the Plio/Pleistocene transition in western Europe: New evidence from the Middle Villafranchian assemblage of Montopoli, Italy. Comptes Rendus - Palevol 12: 165–171.

Christiansen P. 2013. Phylogeny of the sabertoothed felids (Carnivora: Felidae: Machairodontinae). Cladistics 29: 543–559.

Cisneros JC. 2005. New Pleistocene vertebrate fauna from El Salvador. Revista Brasileira de Paleontologia 8: 239–255.

Croxen FW, Shaw CA, Sussman DR. 2007. Pleistocene geology and paleontology of the

Colorado River Delta at Golfo de Santa Clara, Sonora, Mexico. Wild, Scenic and Rapid: a Trip Down the Colorado River Trough: The 2007 Desert Symposium Field Guide and Abstracts from Proceedings. Desert Studies Consortium, California State University, Fullerton.

Cruz-y-Cruz T, Sánchez-Miranda G, Carpenter J, Terrazas-Mata A, Sedov S, Solleiro-Rebolledo E, Benavente-Sanvicente ME. 2018. Pleistocene paleosols associated with megafauna in northwestern Mexico: Paleoecological inferences. Spanish Journal of Soil Science 8: 130–147.

Czaplewski NJ, Morgan GS, Arroyo-Cabrales J, Mead JI. 2014. Late Pleistocene shrews and bats (Mammalia: Soricomorpha and Chiroptera) from Térapa, a neotropical–nearctic transitional locality in Sonora, Mexico. The Southwestern Naturalist 59: 489–501.

Dávila SL, Stinnesbeck SR, Gonzalez S, Lindauer S, Escamilla J, Stinnesbeck W. 2019. Guatemala's Late Pleistocene (Rancholabrean) fauna: Revision and interpretation. Quaternary Science Reviews 219: 277–296.

von den Driesch A. 1976. A guide to the measurement of animal bones from archaeological sites. Peabody Museum Bulletins 1: 1–137.

Van Devender TR. 2007. Ice ages in the Sonoran Desert: Pinyon pines and Joshua trees in the Dry Borders Region. Pages 58–68 in Felger RS and Broyles B, eds. Dry Borders: Great Natural Reserves of the Sonoran Desert. University of Utah Press.

Van Devender TR, Rea AM, Smith ML. 1985. The Sangamon interglacial vertebrate fauna from Rancho la Brisca, Sonora, Mexico. Transactions of the San Diego Society of Natural History 21: 23–55.

Emmert LG, Short RA. 2018. Three new procyonids (Mammalia, Carnivora) from the Blancan of Florida. Bulletin of the Florida Museum of Natural History 55: 157–173.

Ferrusquía-Villafranca I, Arroyo-Cabrales J, Martínez-Hernández E, Gama-Castro J, Ruiz-González J, Polaco OJ, Johnson E. 2010. Pleistocene mammals of Mexico: A critical review of regional chronofaunas, climate change response and biogeographic provinciality. Quaternary International 217: 53–104.

Ferrusquía-Villafranca I, Lundelius EL, Ruiz-Gonzalez JE. 2017. Pleistocene radiometric geochronology and vertebrate paleontology in Mexico: overview and critical appraisal. Natural History Museum of LA County Contributions in Science 525: 1–23.

Foley JA, DeFries R, Asner GP, Barford C, Bonan G, Carpenter SR, Chapin FS, Coe

MT, Daily GC, Gibbs HK, Helkowski JH, Holloway T, Howard EA, Kucharik CJ, Monfreda C, Patz JA, Prentice IC, Ramankutty N, Snyder PK. 2005. Global consequences of land use. Science 309: 570–574.

Harris AH. 2014. Pleistocene Vertebrates of Southwestern USA and Northwestern Mexico. University of Texas at El Paso.

Hodnett J-PM, Mead JI, Baez A. 2009. Dire wolf, *Canis dirus* (Mammalia; Carnivora; Canidae), from the Late Pleistocene (Rancholabrean) of east-central Sonora, Mexico. The Southwestern Naturalist 54: 74–81.

Honey J, Harrison J, Prothero D, Stevens M. 1998. Camelidae. Pages 439–462 in Janis CM, Scott KM, Jacobs LL, Gunnell GF, and Uhen MD, eds. Evolution of Tertiary Mammals of North America, vol. 1: Terrestrial Carnivores, Ungulates, and Ungulatelike Mammals. Cambridge University Press.

Kelson KR. 1946. Notes on the comparative osteology of the bobcat and the house cat. Journal of Mammalogy 27: 255–264.

Kurtén B, Anderson E. 1980. Pleistocene Mammals of North America. Columbia University Press.

Lavoie M, Renard A, Larivière S. 2019. *Lynx canadensis* (Carnivora: Felidae). Mammalian Species 51: 136–154.

Lipton D, Rubenstein M, Weiskopf SR, Carter SL, Peterson J, Crozier LG, Fogarty M, Gaichas S, Hyde KJW, Morelli TL, Morisette J, Moustahfid H, Muñoz R, Poudel R, Staudinger MD, Stock CA, Thompson LM, Waples R, Weltzin JF. 2018. Ecosystems, ecosystem services, and biodiversity. Pages 259–312 in Reidmiller DR, Avery CW, Easterling KE, Kunkel KE, Lewis KLM, Maycock TK, and Stewart BC, eds. Impacts, Risks, and Adaptation in the United States: Fourth National Climate Assessment, Volume II. U.S.Global Change Research Program.

Magaña V, Zermeño D, Neri C. 2012. Climate change scenarios and potential impacts on water availability in northern Mexico. Climate Research 51: 171–184.

McGuire JL, Lawler JJ, McRae BH, Nuñez TA, Theobald DM. 2016. Achieving climate connectivity in a fragmented landscape. PNAS 113: 7195–7200.

McHorse BK, Davis EB, Scott E, Jenkins DL. 2016. What species of horse was coeval with North America's earliest humans in the Paisley Caves? Journal of Vertebrate Paleontology 36: e1214595.

Mead JI, Arroyo-Cabrales J, Swift SL. 2019. Late Pleistocene *Mammuthus* and *Cuvieronius* (Proboscidea) from Térapa, Sonora, Mexico. Quaternary Science

Reviews 223: 105949.

Mead JI, Baez A, Swift SL, Carpenter MC, Hollenshead M, Czaplewski NJ, Steadman DW, Bright J, Arroyo-Cabrales J. 2006. Tropical marsh and savanna of the Late Pleistocene in northeastern Sonora, Mexico. The Southwestern Naturalist 51: 226–239.

Mead JI, Czaplewski NJ, Agenbroad LD. 2005. Rancholabrean (Late Pleistocene) mammals and localities of Arizona. Mesa Southwest Museum Bulletin 11: 139–180.

Mead JI, Swift SL, White RS, McDonald HG, Baez A. 2007. Late Pleistocene (Rancholabrean) Glyptodont and Pampathere (Xenarthra, Cingulata) from Sonora, Mexico. Revista Mexicana de Ciencias Geologicas 24: 439–449.

Mead JI, White RS, Baez A, Hollenshead MG, Swift SL, Carpenter MC. 2010. Late Pleistocene (Rancholabrean) *Cynomys* (Rodentia, Sciuridae: prairie dog) from northwestern Sonora, Mexico. Quaternary International 217: 138–142.

Messing HJ. 1986. A Late Pleistocene-Holocene fauna from Chihuahua, Mexico. The Southwestern Naturalist 31: 277–288.

Metcalfe SE. 2006. Late Quaternary environments of the Northern Deserts and Central Transvolcanic Belt of Mexico. Annals of the Missouri Botanical Garden 93: 258–273.

Montellano-Ballesteros M, Jiménez-Hidalgo E. 2006. Mexican fossil mammals, who, where, and when? Pages 249–273 in Vega FJ, Nyborg TG, Del Carmen Perrilliat M, Montellano-Ballesteros M, Cevallos-Ferriz SRS, and Quiroz-Barroso SA, eds. Studies on Mexican Paleontology. Springer Netherlands.

Mooser O, Dalquest WW. 1975. Pleistocene mammals from Aguascalientes, Central Mexico. Journal of Mammalogy 56: 781–820.

Morgan GS, Lucas SG. 2001. The sabertooth cat *Smilodon fatalis* (Mammalia: Felidae) from a Pleistocene (Rancholabrean) site in the Pecos River valley of Southeastern New Mexico/Southwestern Texas. New Mexico Geology 23: 130–133.

Murray LK, Bell CJ, Dolan MT, Mead JI. 2005. Late Pleistocene fauna from the southern Colorado Plateau, Navajo County, Arizona. The Southwestern Naturalist 50: 363–374.

Nunez EE, Macfadden BJ, Mead JI, Baez A. 2010. Ancient forests and grasslands in the desert: Diet and habitat of Late Pleistocene mammals from northcentral Sonora, Mexico. Palaeogeography, Palaeoclimatology, Palaeoecology 297: 391–400.

Oswald JA, Steadman DW. 2011. Late Pleistocene passerine birds from Sonora, Mexico. Palaeogeography, Palaeoclimatology, Palaeoecology 301: 56–63.

Pérez EA. 2011. Los mamíferos fósiles de la localidad de Puente de Piedra (Xenarthra, Glyptodontidae; Artiodactyla, Camelidae, Lamini) Grecia, Provincia de Alajuela, Costa Rica. Revista Geológica de América Central 49: 33–44.

Priego-Vargas J, Bravo-Cuevas VM, Jiménez-Hidalgo E. 2017. Revisión taxonómica de los équidos del Pleistoceno de México con base en la morfología dental. Revista Brasileira de Paleontologia 20: 239–268.

R Core Team. 2016. R: A language and environment for statistical computing. .

Sanders AE. 2002. Additions to the Pleistocene mammal faunas of South Carolina, North Carolina, and Georgia. Transactions of the American Philosophical Society 92: 1–152.

Sertich JJW, Stucky RK, McDonald HG, Newton C, Fisher DC, Scott E, Demboski JR, Lucking C, McHorse BK, Davis EB. 2014. High-elevation late Pleistocene (MIS 6-5) vertebrate faunas from the Ziegler Reservoir fossil site, Snowmass Village, Colorado. Quaternary Research 82: 504–517.

Stains HJ. 1973. Comparative study of the calcanea of members of the Ursidae and Procyonidae. Bulletin of the Southern California Academy of Sciences 72: 137–148.

Steadman DW, Mead JI. 2010. A Late Pleistocene bird community at the northern edge of the tropics in Sonora, Mexico. American Midland Naturalist 163: 423–441.

Sussman DR, Croxen FW, McDonald HG, Shaw CA. 2016. Fossil porcupine (Mammalia, Rodentia, Erethizontidae) from El Golfo de Santa Clara, Sonora, Mexico, with a review of the taxonomy of the North American erethizontids. Natural History Museum of LA County Contributions in Science 524: 1–29.

Tedford RH, Wang X, Taylor BE. 2009. Phylogenetic systematics of the North American Fossil Caninae (Carnivora: Canidae). Bulletin of the American Museum of Natural History 325: 1–218.

Walther GR, Post E, Convey P, Menzel A, Parmesan C, Beebee TJC, Fromentin JM, Hoegh-Guldberg O, Bairlein F. 2002. Ecological responses to recent climate change. Nature 416: 389–395.

Webb SD. 1974. Pleistocene llamas of Florida, with a brief review of the Lamini. Pages 170–213 in Webb SD, ed. Pleistocene mammals of Florida. University Press of Florida.

White RS, Mead JI, Baez A, Swift SL. 2010. Localidades de vertebrados fósiles del Neógeno (Mioceno, Plioceno y Pleistoceno): Una evaluación preliminar de la biodiversidad del pasado. Pages 51–72 in. Diversidad biológica de Sonora.

Woodburne MO. 2010. The Great American Biotic Interchange: Dispersals, tectonics, climate, sea level and holding pens. Journal of Mammalian Evolution 17: 245–264.

Wright DB. 1998. Tayassuidae. Pages 389–401 in Janis CM, Scott KM, Jacobs LL, Gunnell GF, and Uhen MD, eds. Evolution of Tertiary Mammals of North America, vol. 1: Terrestrial Carnivores, Ungulates, and Ungulatelike Mammals. Cambridge University Press.

Zazula GD, MacPhee RDE, Hall E, Hewitson S. 2016. Osteological assessment of Pleistocene *Camelops* hesternus (Camelidae: Camelinae: Camelini) from Alaska and Yukon. American Museum Novitates 3866: 1–45.

# 5. SPATIAL INEQUALITIES LEAVE MICROPOLITAN AREAS AND INDIGENOUS POPULATIONS UNDERSERVED BY INFORMAL STEM LEARNING INSTITUTIONS

## 5.1. Introduction

Public understanding of science requires more than content knowledge, it also requires knowledge of the nature of science, positive beliefs about science, and scientific literacy (Sinatra and Hofer 2016). A comprehensive understanding of science supports a better informed public that can make evidence-based decisions (Sinatra et al. 2014) and contributes to a healthier population, greater interest in STEM careers, and higher earnings (Darling-Hammond 2001, NRC 2009, NASEM 2016). Unfortunately, access to information is unequal; rural and poor communities receive the fewest programs for public education in science (Calabrese Barton 1998, Bevan et al. 2018, Rogers and Sun 2018). When there have been investments in improving public science literacy, it has historically focused in the classroom (Falk et al. 2018); yet, with most people spending 95% of their lives outside of classroom settings (Falk and Dierking 2010), informal learning experiences can be more valuable for science literacy, especially for adults (Falk and Needham 2011, Zarestky et al. 2018).

In contrast to a classroom's formality, sites of informal learning provide opportunities for visitors to learn through inquiry (Spector et al. 2012) and educate the public through engaging experiences (Falk and Needham 2011). Informal learning institutions (ILIs), such as museums and science centers, increase appreciation for

science (Diamond et al. 2012), increase understanding of the nature of science (Spector et al. 2012), and positively influence attitudes and beliefs about science and technology (Falk and Needham 2011). These ILIs also provide learning opportunities for populations underrepresented in the sciences to make STEM knowledge relevant, accessible, and meaningful (Institute of Medicine 2011). Other STEM-related ILIs include botanical gardens and arboretums, zoos and aquariums, public libraries, National Park Service lands, and biological field stations and marine laboratories. Together, ILIs comprise a geographic landscape of informal learning opportunities available to the general public.

This is especially important for members of underrepresented groups in the sciences who may feel excluded from informal STEM learning (Dawson 2014) or who may not recognize the viability of STEM careers (NASEM 2016, Fuesting et al. 2017). Minorities, girls and women, and rural and poor populations are persistently underrepresented in the sciences (Garrison 2013, NCSES 2017, Rogers and Sun 2018). Creating informal STEM education opportunities within underserved areas and for underrepresented groups can reduce barriers, promote scientific literacy, and contribute to better representation in STEM careers (NRC 2009). Although it does not ensure equity or even accessibility, close proximity removes a sizeable barrier. Many people visit ILIs annually (Schwan et al. 2014) and are willing to travel to do so (Yucelt 2001), but structural barriers, such as entry and day trip costs, and socially-exclusive practices related to class and ethnicity limit the diversity of ILI audiences (Dawson 2017). Therefore, to understand where ILIs can most broaden participation in STEM, we first

need to know the populations who are least able to participate in informal STEM learning opportunities because of proximity.

Here, we map ILIs in the United States and explore their relative densities in the informal learning landscape to determine the national geographic distribution of each type. We identify ILI "deserts" where there are currently fewer sites for informal STEM education and more opportunities for ILI development, collaboration, and expansion of existing resources. We expect counties with higher population densities to have more ILIs because of larger potential audiences, and counties with higher poverty to have fewer ILIs because of fewer financial resources. In addition, we explore the racial and ethnic demographics of those underserved counties to determine if populations with few informal learning opportunities are also those populations who are underrepresented in STEM careers.

**5.2. Materials and methods**

To map US informal learning institutions (ILIs), we extracted locality data from the Institute of Museum and Library Services' Museum Universe Data File (Grimes et al. 2014). Records were cleaned to remove duplicates and were maintained for different institutions at the same geographic location, e.g., Southwest Minnesota State University (SMSU) Museum of Natural History and SMSU Planetarium.We compiled data on 2962 STEM-related ILIs were compiled, including 1010 arboretums, botanical gardens, and nature centers (BOT), 1490 children's museums, natural history museums, natural science museums, science and technology museums, and planetariums (MUS), and 462 zoos, aquariums, and wildlife conservation centers (ZOO). Additional ILIs in our

analysis included 16720 public central and branch libraries (LIB) extracted from the Public Library Survey's Outlet Data File (Pelczar et al. 2019). Libraries were removed if they were listed as bookmobiles or books-by-mail only, reported as temporary or permanent closure, or located in outlying territories of the United States. National Park Service (NPS) lands included 167 national parks, national monuments, national preserves, and national seashores (NPS 2019). Centroid points were used to represent national park lands because informal learning activities are often available throughout the park. Finally, 435 biological field stations and marine labs (FSML) were compiled from the Organization of Biological Field Stations (OBFS 2016) and National Association of Marine Laboratories (NAML 2016). In all, 20,284 ILIs were included in this study, and all ILI data are available in Appendix D.

We sourced population data at the county level from the American Community Survey (ACS) 2017 5-year estimate dataset (USCB 2018) and included population density, measures of poverty, and populations of racial and ethnic groups. Population density was calculated as the census number divided by the land area for each county (individuals per $km^2$) and was transformed to natural log for analysis. For each county, we extracted a Rural-Urban Continuum Code (RUCC; USDA ERS 2013a). Nine RUCC categories are based on county population density and metropolitan influence (USDA ERS 2013b). The first three categories (RUCC 1-3) are metro counties, and the remaining six (RUCC 4-9) are non-metro counties that are either adjacent or not adjacent to a metro area (USDA ERS 2013b; Table D-1). Adjacency is defined as a shared border with a metro area and at least 2% of workers commuting into the central counties of the

larger metro area (USDA ERS 2013b). Poverty was determined at the family level by comparing income over the previous 12 months to set thresholds that vary depending on the size of the family (USCB 2017). Percentage of poverty was binned into six categories from lowest (1) to highest (6) using Jenks Natural Breaks (Jenks 1977; Table D-2). Racial and ethnic data from the ACS 2017 5-year estimate dataset (USCB 2018) were used to calculate population percentages. All county-level data are available in Appendix D.

### 5.2.1. Analyses

To determine the density of ILIs, we calculated a kernel density surface of ILIs per $km^2$ with a cell size of 1000 within a World Geodetic System 1984 (WGS84) spatial reference system. At each ILI location, the ILI kernel density was extracted from the kernel density surface to calculate the mean density, standard deviation, and standard error for all ILIs and for each ILI type (BOT, FSML, LIB, MUS, NPS, and ZOO). The ILI densities for each type were compared using a one-way ANOVA test to determine statistical differences between the types.

Next, we calculated a simple density surface of ILIs per county area ($km^2$) that we could compare to county population density and to percentage of poverty. We modeled the influence of log population density and poverty percentage on ILI density with a generalized linear model that included log population density, poverty percentage, and their interaction as factors, along with a rational quadratic correlation structure to account for spatial autocorrelation of the variables. McFadden's pseudo-$R^2$ was used to evaluate the models. This statistic indicates a good fit when $0.2 <= R^2 <= 0.4$ (McFadden

1979). We compared the residuals of this model across RUCCs to determine the geographic element of equality of access relative to population density. We also compared the residuals across poverty categories. Residuals were evaluated across RUCC categories and poverty categories using analyses of variance.

Three strategies were then used to identify groups of counties most underserved in the ILI landscape: 1) counties with no ILIs, 2) 0.5% of counties with the greatest negative residuals defined as more than 2.5 standard deviations below the mean (i.e., they had the fewest ILIs relative to their expected number), and 3) counties in the RUCC or poverty category with the greatest mean negative residual. The greatest mean negative residual indicates the group with the fewest opportunities relative to the expected. We calculated the percentages of the US population and racial and ethnic groups in each of the three groups of underserved counties ((group population of underserved counties/total group population of US) * 100). All analyses were performed in ArcMap and R (R Core Team 2016, ESRI 2017).

**5.3. Results**

Our results document the landscape of ILIs across the US and indicate geographic gaps across the West, Midwest, and South (Figure 5.1A). National Park Service (NPS) lands and biological field stations and marine laboratories (FSMLs) occur in areas with lower ILI densities than other types; botanical gardens occur in areas with the highest ILI densities ($F(5,20278) = 22.37$, $p < 0.001$; Figure 5.1B). Geographic distributions vary depending on the type of ILI (Figures 5.1C-H); NPS lands (Figure

5.1C) are much denser in western states and along the East Coast, whereas botanical gardens (Figure 5.1H) are sparse across the west and dense on the coasts.

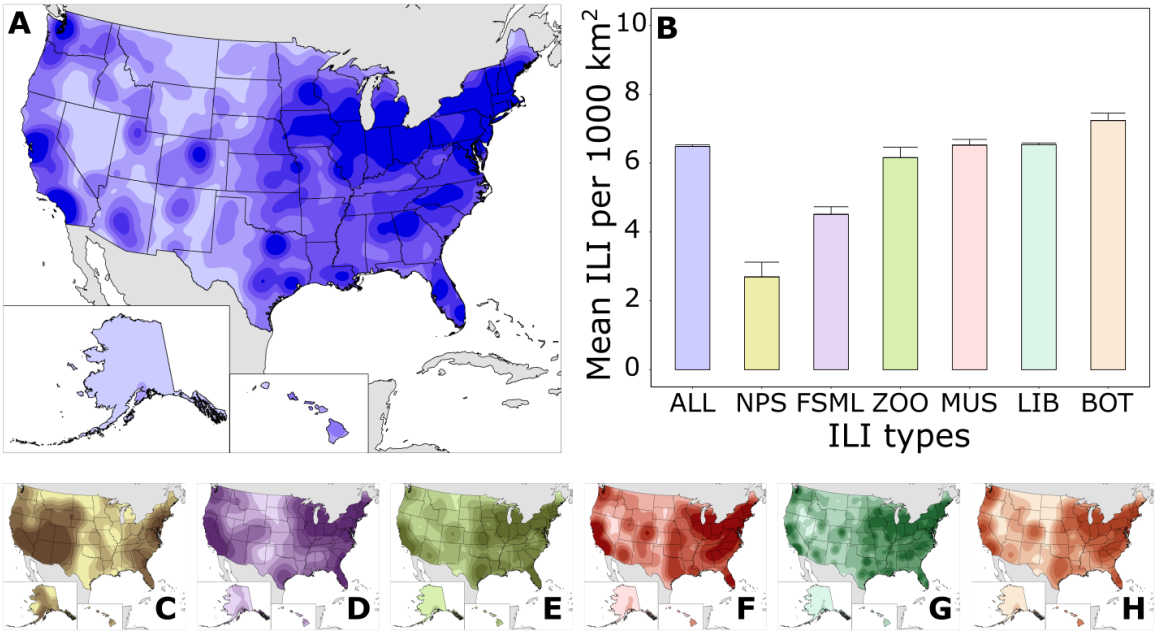


**Figure 5.1. Landscape of ILIs in the US (density per 1000 km$^2$). A, Kernel density surface of all ILIs displayed as six quantiles (cell size = 1000 m$^2$; μ = 6.5 ILI per 1000 km$^2$), B, Mean density of ILIs per 1000 km$^2$ at each type (abbreviations follow) with standard error bars (colors correspond to A, C-H), C, National Park Service lands (NPS), D, Biological field stations and marine laboratories (FSML), E, Zoos, aquariums, and wildlife conservation (ZOO), F, Science museums, children's museums, and planetariums (MUS), G, Libraries (LIB), H, Botanical gardens, arboretums, and nature centers (BOT). All densities are displayed as six quantiles and values associated with each break are in Table D-3. Mean values for the bar plot are provided in Table D-4. All ILI point data are in Appendix D.**

There are 48 counties with no ILIs, and these counties are primarily in the middle part of the country from North Dakota to Texas (Figure 5.2A), which leaves 327,121 people underserved (0.10% of the US population). Low densities of ILIs are in the southeast and the intermountain west (Figure 5.1A), and high densities of ILIs are in the

Northeast, near the Great Lakes in the Midwest, and along the west coast. These geographic patterns may be related to population density and poverty levels in those areas. When considered together, population density and poverty maintain a significant relationship with ILI density, and the interaction of population density and poverty percentage is also significantly related to ILI density ($R^2_{McFadden} = 0.322$; Table 5.1). With lower population density and higher poverty, a county is expected to have fewer ILIs than counties with higher population density and lower poverty.

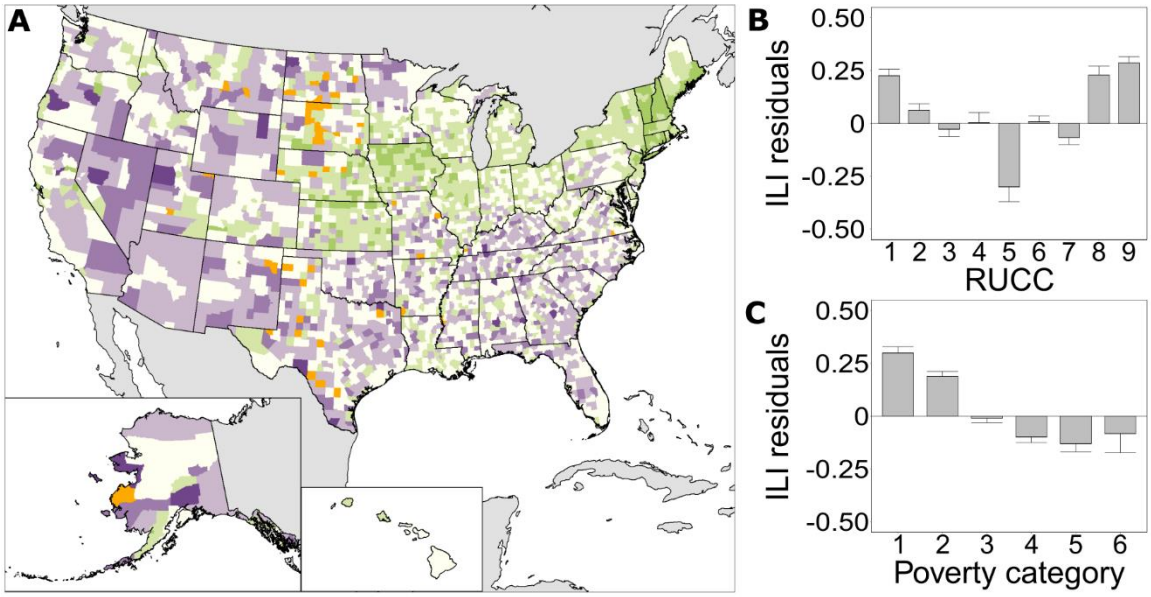


**Figure 5.2. Distribution of ILIs among the US population summarized at the county level. A, Standard deviation of ILI residuals with the darkest purple indicating the fewest number of ILIs (σ < -2.5) and the darkest green indicating the most ILIs (σ > 1.5) relative to the number expected. Blue counties have no ILIs. B, ILI residuals grouped by Rural-Urban Continuum Codes with standard error bars; C, ILI residuals grouped by poverty categories with standard error bars; ILI residuals are from a spatially-corrected regression between log ILI density and the interaction of log population density and poverty percentage. Standard deviation values are in Table D-5 and county data are in Appendix D.**

**Table 5.1. Summary of the generalized linear model that included log population density, poverty percentage, and their interaction as factors.**

| Factor | Co-efficient | *t*-value | *p*-value |
|---|---|---|---|
| Intercept | -7.63 | -74.9 | 0 |
| Log population density | 0.468 | 26.9 | 0 |
| Poverty percentage | -0.014 | -4.35 | 0 |
| Log population density * Poverty percentage | 0.006 | 6.46 | 0 |

Geographically, the residuals between log ILI density and the interaction between log population density and poverty percentage are higher than expected in the northeast and across the central Midwest, and residuals are lower than expected in the southeast and the intermountain west (Figure 5.2A). There are 21 counties in the lowest 0.5% of ILI residuals ($\sigma < -2.5$), and these counties are primarily in the southeast and northwest (Figure 5.2A). These counties have a total of 29 ILIs ($\mu = 1.4$ ILIs per county) and include 1,372,650 people or 0.43% of the US population.

ILI density residuals of the interaction between log population density and poverty percentage were further used to investigate which groupings based on Rural-Urban Continuum Codes (RUCCs) or poverty percentages are more underserved by ILIs than expected. RUCC 1 includes counties in the largest metro areas (more than one million people) and has residual values higher than expected, which indicates these counties have more ILIs than expected for their population densities and poverty levels (Figure 5.2B). Other metro counties with 250,000 to 1,000,000 residents (RUCC 2) and fewer than 250,000 (RUCC 3) have nearly as many ILIs as expected. Counties that are completely rural or urban with less than 2,500 people have more ILIs than expected regardless of if they are adjacent (RUCC 8) or not adjacent to a metro area (RUCC 9).

Most non-metro counties have nearly as many ILIs as expected. This occurs in counties with an urban area of 20,000 people or more that are adjacent to a metro area (RUCC 4), and counties with an urban area of 2,500 to 19,999 that are either adjacent (RUCC 6) or not adjacent (RUCC 7) to a metro area. The exception is RUCC 5, which includes counties with an urban area of 20,000 people or more that are not adjacent to a metro area and has the lowest ILI residuals ($\mu = -0.30$, $\sigma = 0.67$). Therefore, RUCC 5 counties have the fewest ILIs relative to the expected for their population densities and poverty levels. The 92 RUCC 5 counties include 5,028,805 people (1.6% of the US population).

There is an inverse relationship between ILI residuals and poverty, so that counties with a low poverty percentage (poverty category 1) have higher ILI residuals and more ILIs than expected, whereas counties with a high poverty percentage (poverty category 6) have lower residuals and fewer ILIs than expected (Figure 5.2B). Poverty category 5 (23.6 – 31.4% poverty) has the lowest residuals and fewer ILIs than expected; this group includes 1,229,241 people (0.38% of the US population). None of the poverty categories have a mean residual value as low as RUCC 5 counties (Figures 5.2A-B).

### 5.3.1. Underserved counties

We further examined the demographics of the counties identified as underserved. There are 48 counties with no ILIs (Figure 5.3A), 21 counties in the lowest 0.5% of ILI residuals (Figure 5.3B), and 92 counties in RUCC 5 (Figure 5.3C). Five RUCC 5 counties also have residuals in the lowest 0.5%. These counties are Campbell, WY, Garfield, OK, Lamar, TX, Val Verde, TX, and Laurens, GA. They include a total of 256,365 people, and each occurs in a different poverty category from 1 to 5,

respectively. In all, these 156 underserved counties (5.0%) are home to 6,472,211 people (2.0% of the population).

Underserved counties occur across the Rural-Urban Continuum depending on the group. Counties without ILIs are mostly (48%) in RUCC 9 – completely rural or urban with less than 2,500 people and not adjacent to a metro area. Counties with ILI residuals in the lowest 0.5 are mostly the mid-metro counties with 250,000 to 1,000,000 residents (RUCC 2; 24%) or the largest non-metro counties with an urban area of 20,000 people that are not adjacent to a metro area (RUCC 5; 24%). Counties in RUCC 5 are micropolitan areas with urban cores of 10,000-50,000 people (USOMB 2010), such as Gillette, WY, Carlsbad, NM, and Elko, NV.

All underserved counties occur across the poverty categories. Most counties without ILIs (40%) are in poverty category 1 (0-10.1% poverty) with a mean poverty of 17%. Most counties with ILI residuals in the lowest 0.5% (29%) and counties in RUCC 5 (39%) are in poverty category 3 (14.2-18.4% poverty). Both of these groups have a mean poverty of 18%.

The three underserved groups of counties include a small percentage of the overall US population, but larger percentages of indigenous populations (Figure 5.3D; Table D-6). Counties without ILIs include just 0.10% of the US population but 0.95% of the American Indian or Alaskan Native populations. Only 0.43% of the US population lives in counties with ILI residuals in the lowest 0.5%, yet 1.0% of the American Indian or Alaskan Native population and 0.79% of the Native Hawaiian and Other Pacific Islander population reside in these counties. Similarly, although 1.6% of the US

population lives in RUCC5 counties, 5.3% of the American Indian or Alaskan Native population and 6.5% of the Native Hawaiian and Other Pacific Islander population live in RUCC5 counties.

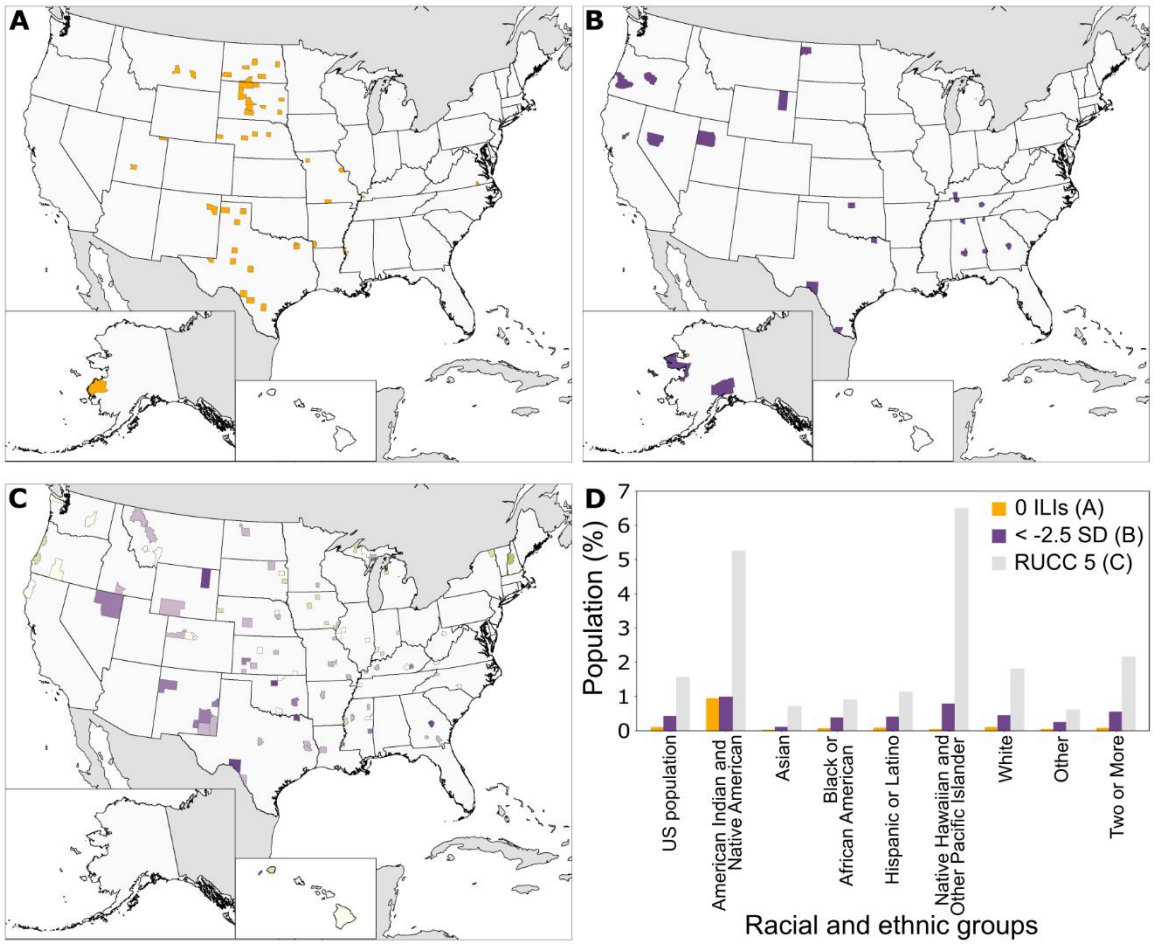


**Figure 5.3. Counties that are the most underserved by informal learning institutions (ILIs). A, Counties that do not have ILIs; B, Counties with ILI residuals in the lowest 0.5% (σ < -2.5); C, Non-metro, not adjacent counties with urban populations over 20,000 (RUCC 5) with standard deviations of log ILI residuals and the interaction of log population density and poverty percentage as in Figure 5.2A; D, Racial and ethnic percentages in underserved counties. US population is the percentage of the general population in each underserved group of counties for comparison with the racial and ethnic groups. Bar plot values are in Table D-6.**

## 5.4. Discussion

Many of the counties underserved by ILIs, unsurprisingly, are in regions of low ILI density, and the largest counties by area also occur in areas of lowest ILI density (Figure 5.4). This increases the challenge of providing informal STEM learning opportunities in these areas. Some of the underserved counties, particularly in the eastern part of the county, are in regions with neighboring counties with high ILI density; residents of these underserved counties may take advantage of informal learning resources in nearby counties. Conversely, ILI practitioners may be able to use these resources to target nearby counties with fewer ILIs and increase opportunities for participation closer to home for neighboring county residents.

NPS lands and FSMLs play a unique role in the spatial distribution of ILIs by reaching geographic areas with fewer ILIs of other types (Figure 5.1B). These institutions use their resources to provide place-based informal STEM education to the public (Novey and Hall 2007, Karlstrom et al. 2008, Billick et al. 2013, Struminger et al. 2018). FSMLs are also unique because they can easily incorporate scientists in their outreach programming (Billick et al. 2013, Struminger et al. 2018). Unlike marine laboratories, primarily located along the coast, biological field stations occur across the country's interior and can reach more geographically widespread populations (Struminger et al. 2018). Even at National Parks, scientists are more able to interact with visitors at field stations within the parks than at visitor centers (Stevens and Gilson 2016). Interacting with a scientist or STEM professional can result in positive learning

outcomes for participants, such as increased interest in science, learning of content, and awareness of STEM careers (Wiehe 2014, Boyette and Ramsey 2019).

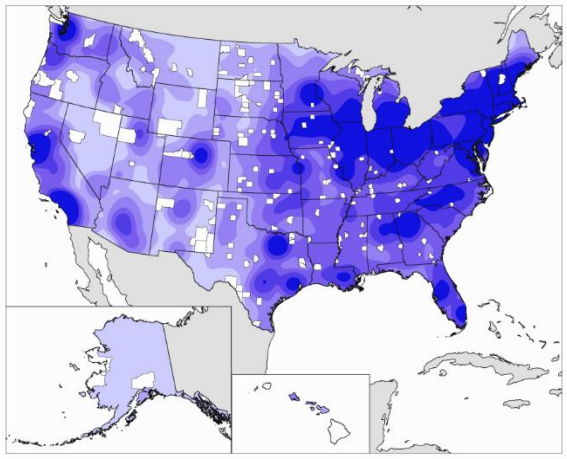

**Figure 5.4. ILI density from Figure 5.1A with underserved counties from Figure 5.3A-C highlighted in white.**

Gaps in the ILI landscape represent opportunities for resource investment and capacity building in informal STEM education (NRC 2015). Establishment of ILIs in these gaps will result in more programming, which will lead to improved public understanding of science (NRC 2009, Falk and Dierking 2019). We recommend targeted efforts to reach counties that are in the three groups of underserved counties – without ILIs, with too few ILI opportunities, and outside of metro areas but not completely rural. These counties have fewer than expected ILIs and larger percentages of indigenous groups (Figure 5.3) than counties that are not underserved. Indigenous students engage with STEM at lower rates than nonindigenous students and are less likely to pursue STEM careers (Abrams et al. 2013), and Native American students have difficulty

perceiving themselves as scientists (Laubach et al. 2012). Community-based and place-based learning may be more engaging for indigenous populations because these approaches to learning can more easily be intercultural (Bang and Medin 2010, Abrams et al. 2013). Underserved counties would benefit from increased investment in informal STEM learning opportunities that meaningfully integrate cultural practices with effective learning (Windchief and Brown 2017).

Partnerships between educational and community organizations can broaden participation of underserved populations (Penuel 2017), and ILIs are well-situated to play a role in these partnerships because of their geographically-widespread distributions. In particular, libraries occur in nearly every county and are 75% of the ILIs found in RUCC5 counties. When other ILIs, such as museums and botanical gardens, are further away, collaborations with libraries can facilitate STEM learning in these underserved communities (LaConte and Dusenbery 2016, Shtivelband et al. 2019, Wilhelm and Jones 2019). By providing engaging learning experiences for surrounding communities, ILIs can foster an increase in underrepresented groups in STEM careers and, more broadly, a more scientifically-literate population that can rely on scientific findings to inform decision-making and influence policies in areas such as health, technology, and the environment (NASEM 2016, Sinatra and Hofer 2016).

**References**

Abrams E, Taylor PC, Guo CJ. 2013. Contextualizing culturally relevant science and mathematics teaching for indigenous learning. International Journal of Science and Mathematics Education 11: 1–21.

Bang M, Medin D. 2010. Cultural processes in science education: Supporting the navigation of multiple epistemologies. Science Education 94: 1008–1026.

Bevan B, Calabrese Barton A, Garibay C. 2018. Broadening Perspectives on Broadening Participation in STEM: Critical Perspectives on the Role of Science Engagement.

Billick I, Babb I, Kloeppel B, Leong JC, Hodder J, Sanders J, Swain T. 2013. Field Stations and Marine Laboratories of the Future: A Strategic Vision.

Boyette T, Ramsey JR. 2019. Does the messenger matter? Studying the impacts of scientists and engineers interacting with public audiences at science festival events. Journal of Science Communication 18: 1–16.

Calabrese Barton A. 1998. Reframing 'Science for All' through the politics of poverty. Educational Policy 12: 525–541.

Darling-Hammond L. 2001. Inequality in teaching and schooling: How opportunity is rationed to students of color in America. Pages 208–233 in Institute of Medicine, ed. The Right Thing to Do, The Smart Thing to Do: Enhancing Diversity in Health Professions. National Academies Press.

Dawson E. 2014. 'Not designed for us': How science museums and science centers socially exclude low-income, minority ethnic groups. Science Education 98: 981–1008.

Dawson E. 2017. Social justice and out-of-school science learning: Exploring equity in science television, science clubs and maker spaces. Science Education 101: 539–547.

Diamond J, Evans EM, Spiegel AN. 2012. Walking whales and singing flies: An evolution exhibit and assessment of its impact. Pages 389–409 in Rosengren KS, Brem SK, Evans EM, and Sinatra GM, eds. Evolution Challenges: Integrating Research and Practice in Teaching and Learning about Evolution. Oxford University Press.

ESRI. 2017. ArcGIS Desktop: Release 10.6.1.

Falk JH, Dierking LD. 2010. School is not where most Americans learn most of their science. American Scientist 98: 486–493.

Falk JH, Dierking LD. 2019. Reimagining public science education: The role of lifelong free-choice learning. 1: 1–10.

Falk JH, Needham MD. 2011. Measuring the impact of a science center on its community. Journal of Research in Science Teaching 48: 1–12.

Falk JH, Pattison S, Meier D, Bibas D, Livingston K. 2018. The contribution of science-rich resources to public science interest. Journal of Research in Science Teaching

55: 422–445.

Fuesting MA, Diekman AB, Hudiburgh L. 2017. From classroom to career: The unique role of communal processes in predicting interest in STEM careers. Social Psychology of Education 20: 875–896.

Garrison H. 2013. Underrepresentation by race-ethnicity across stages of U.S. science and engineering education. CBE Life Sciences Education 12: 357–363.

Grimes J, Manjarrez CA, Miller KA, Swan DW. 2014. Museum Universe Data File: Documentation. Report no. IMLS-2014-MUDF-01.

Institute of Medicine. 2011. Expanding Underrepresented Minority Participation: America's Science and Technology Talent at the Crossroads.

Jenks GF. 1977. Optimal data classification for chloropleth maps. University of Kansas Department of Geography Occasional Papers 2: 1–24.

Karlstrom K, Semken S, Crossey L, Perry D, Gyllenhaal ED, Dodick J, Williams M, Hellmich-Bryan J, Crow R, Watts NB, Ault C. 2008. Informal geoscience education on a grand scale: The trail of time exhibition at Grand Canyon. Journal of Geoscience Education 56: 354–361.

LaConte K, Dusenbery P. 2016. STEM learning in public libraries: New perspectives on collaboration from a national conference. Informal Learning Review September: 21–27.

Laubach TA, Crofford GD, Marek EA. 2012. Exploring Native American students' perceptions of scientists. International Journal of Science Education 34: 1769–1794.

McFadden D. 1979. Quantitative methods for analyzing travel behaviour of individuals: Some recent developments. Pages 279–318 in Hensher DA and Stopher PR, eds. Behavioural Travel Modelling. Croom-Helm.

[NASEM] National Academies of Sciences Engineering and Medicine. 2016. Science Literacy: Concepts, Contexts, and Consequences. The National Academies Press.

[NAML] National Association of Marine Laboratories. 2016. Directory. (27 November 2019; http://www.naml.org/members/directory.php).

[NCSES] National Center for Science and Engineering Statistics. 2017. Women, minorities, and persons with disabilities in science and engineering: 2017. Special Report NSF 17-310.

[NPS] National Park Service. 2019. Administrative boundaries centroids of National Park System units 09/30/19. (27 November 2019;

https://irma.nps.gov/DataStore/Reference/Profile/2225714).

[NRC] National Research Council. 2009. Learning Science in Informal Environments: People, Places, and Pursuits. National Academies Press.

[NRC] National Research Council. 2015. Identifying and Supporting Productive STEM Programs in Out-of-School Settings. National Academies Press.

Novey LT, Hall TE. 2007. The effect of audio tours on learning and social interaction: An evaluation at Carlsbad Caverns National Park. Science Education 91: 260–277.

[OBFS] Organization of Biological Field Stations. 2016. Station directory. (27 November 2019; www.obfs.org/directories#/).

Pelczar M, Frehill LM, Williams K, Nielsen E. 2019. Public Libraries Survey Fiscal Year 2011: Data File Documentation and User's Guide.

Penuel WR. 2017. Research–practice partnerships as a strategy for promoting equitable science teaching and learning through leveraging everyday science. Science Education 101: 520–525.

R Core Team. 2016. R: A language and environment for statistical computing.

Rogers RRH, Sun Y. 2018. Engaging STEM Students from Rural Areas: Emerging Research and Opportunities. IGI Global.

Schwan S, Grajal A, Lewalter D. 2014. Understanding and engagement in places of science experience: Science museums, science centers, zoos, and aquariums. Educational Psychologist 49: 70–85.

Shtivelband A, Spahr KS, Jakubowski R, LaConte K, Holland A. 2019. Exploring "STEM-readiness" in public libraries. Journal of Library Administration 59: 854–872.

Sinatra GM, Hofer BK. 2016. Public understanding of science: Policy and educational implications. Policy Insights from the Behavioral and Brain Sciences 3: 245–253.

Sinatra GM, Kienhues D, Hofer BK. 2014. Addressing challenges to public understanding of science: Epistemic cognition, motivated reasoning, and conceptual change. Educational Psychologist 49: 123–138.

Spector BS, Burkett R, Leard C. 2012. Derivation and implementation of a model teaching the nature of science using informal science education venues. Science Educator 21: 51–61.

Stevens MT, Gilson GG. 2016. An exploration of field-station partnerships: University-

operated field stations located in US national parks. BioScience 66: 693–701.

Struminger R, Zarestky J, Short RA, Lawing AM. 2018. A framework for informal STEM education outreach at field stations. BioScience 68: 969–978.

[USCB] United States Census Bureau. 2017. American Community Survey and Puerto Rico Community Survey: 2017 Subject Definitions. 1–165.

[USCB] United States Census Bureau. 2018. ACS Demographic and Housting Estimates: 5-year estimates. (27 November 2019; https://data.census.gov/cedsci/table?q=population&hidePreview=false&table=DP05&tid=ACSDP5Y2017.DP05&lastDisplayedRow=33).

[USDA ERS] United States Department of Agriculture Economic Research Service. 2013a. Rural-Urban Continuum Codes. (27 November 2019; https://www.ers.usda.gov/data-products/rural-urban-continuum-codes.aspx).

[USDA ERS] United States Department of Agriculture Economic Research Service. 2013b. Rural-Urban Continuum Codes Documentation. (27 November 2019; https://www.ers.usda.gov/data-products/rural-urban-continuum-codes/documentation/).

[USOMB] United States Office of Management and Budget. 2010. 2010 standards for delineating metropolitan and micropolitan statistical areas. Federal Register 75: 37246–37252.

Wiehe B. 2014. When science makes us who we are: Known and speculative impacts of science festivals. Journal of Science Communication 13: .

Wilhelm J, Jones J. 2019. Adults need STEM, too: An assessment of one public library's experiment with STEM programming for adults. The Journal of Creative Library Practice 15 December 2019.

Windchief S, Brown B. 2017. Conceptualizing a mentoring program for American Indian/Alaska Native students in the STEM fields: A review of the literature. Mentoring and Tutoring: Partnership in Learning 25: 329–345.

Yucelt U. 2001. Marketing museums: An empirical investigation among museum visitors. Journal of Nonprofit & Public Sector Marketing 8: 3–13.

Zarestky J, Struminger R, Rodriguez J, Short RA, Lawing AM. 2018. Perspectives on informal learning: Cross-disciplinary concepts and a new venue for adult education. Paper presented at the 59th Adult Education Research Conference; 7–10 June 2018, Victoria, BC, Canada.

# 6. CONCLUSIONS

This interdisciplinary dissertation contributes to scientific efforts by: 1) providing confidence in analytical method selection for researchers using trait-environment relationships; 2) developing a new trait-environment relationship for ecometric analyses; 3) filling a geographic gap in our knowledge of Pleistocene mammals in the northwestern Mexico; and 4) identifying underserved counties and populations in the informal STEM learning landscape. From each of these chapters, I draw conclusions and make recommendations to inform scientists, as well as non-scientists, about community responses to climate change.

Of four analytical methods used to predict precipitation from hypsodonty, maximum likelihood produces more accurate predictions than linear regression, polynomial regression, and nearest neighbor (Figure 2.4). All four methods produce results that are highly correlated with log precipitation and predictions from the other methods ($p < 0.001$; Table 2.1). When applied to paleontological sites, paleoprecipitation predictions align more closely with glacial global climate models than with interglacial models regardless of the age of the site (Figures 2.5-2.6). It is unexpected that the interglacial paleoprecipitation predictions closely match glacial global climate models. I posit this is likely because of the anthropogenic effects on community reassembly in the Holocene following the last glacial period.

Calcaneal gear ratio data from 571 individuals in 157 (65%) artiodactyl species were measured to develop a new model of trait-environment relationship. At the

community-level, variance in mean calcaneal gear ratio is most explained by ecoregion division (60.8%), vegetation cover (57.6%), and precipitation (44.1%) (Table 3.1; Figure 3.5). Community gear ratio measures were applied to six sites in Kenya with historical and modern fauna records. Morphology captures habitat homogenization in the southwestern portion of Kenya and matches mammal community patterns described by previous researchers (Figure. 3.6; Tóth et al. 2014). With this ecometric framework, fossils of artiodactyl postcrania can be used to interpret paleoenvironment for a more comprehensive understanding of the past.

A new, detailed description of the mammals at Térapa provides a more thorough understanding of the Rancholabrean fauna of northern Mexico (Table C-1). It is important to document the past because it provides a baseline record that enriches our understanding of interactions between fauna and environment. It is now recognized that there are two distinct morphotypes of *Equus*, including *E. scotti* and a smaller species. Also present in the fauna are *Platygonus compressus, Camelops hesternus, Canis dirus*, and *Lynx rufus*, and the first regional records of *Palaeolama mirifica*, *Procyon lotor*, and *Smilodon* cf. *S. fatalis*. The faunal record documents biotic responses to environmental changes in an increasingly xeric landscape.

Among informal learning institutions (ILIs), National Park Service lands, biological field stations, and marine laboratories occur in areas with the fewest informal learning opportunities and have the greatest potential to reach populations underserved by ILIs (Figure 5.1). Most counties that are underserved occur in the Great Plains, the southeast, and the northwest. Furthermore, the counties that are most underserved also

have higher than expected indigenous populations who are underrepresented in STEM careers (Figure 5.3). These gaps represent opportunities for national investments in ILI offerings through new infrastructure and expansion of existing resources as well as collaborations with facilities in neighboring counties.

### 6.1. Recommendations

Conservation paleobiology is an emerging field that aims to use the fossil record to anticipate potential responses of species to future environmental changes (Dietl et al. 2015, Barnosky et al. 2017). Conservation paleobiology will benefit from further development of ecometrics, including additional analyses of the methods used in these studies but also development of new trait-environment models. Expansion of ecometric methods will improve the utility of the models and their application to biodiversity conservation. In the development of these models, I recommend using maximum likelihood to ensure the least biased predictions (Chapter 2). I also recommend using caution with models constructed with trait data from extant fauna because of possible anthropogenic effects on community assembly (Chapter 2).

Additional models will be informative, but existing models should be integrated to develop multi-trait models. For instance, with the new development of an ecometric model for the artiodactyl calcaneal gear ratio (Chapter 3), the data could be integrated with the carnivoran gear ratio models (Polly 2010) to include a larger segment of the mammalian community and improve environmental interpretation. These ecometric models can be applied to past and modern fauna to determine a directional vector of environmental change (Chapter 3). I recommend extending these vectors based on

projected climatic and environmental change to inform anticipatory management of biodiversity.

As ecometric models become incorporated in conservation paleobiology, the field will benefit from more detailed descriptions of fossil assemblages (Chapter 4) as well as increased sharing of trait data. Traits of fossil assemblages can be used for paleoenvironmental interpretation but much of this data remains undiscovered in museum collections or in unexcavated sediments (Uhen et al. 2013, Bell and Mead 2014). Collecting and sharing this original data contributes to the effort to build functional trait databases for modern and extinct organisms (Jones et al. 2009, The NOW Community 2019); thus, advancing the study of trait-environment relationships. While an ecometric analysis of Térapa would have been advantageous, the available data did not allow for it at this time. With more trait data from more fossil species, it will be possible to include more fossil sites in ecometric studies.

Ecometric models have the potential to influence environmental stewardship and inform conservation and management efforts for Earth's threatened biodiversity. However, effective decision-making relies on a well-informed public with increased scientific literacy. I recommend more scientists associate with informal learning institutions (ILIs) to engage with the public and increase public understanding of science (Chapter 5). Interactions with scientists contribute to positive learning outcomes, such as increased interest in science and science careers (Wiehe 2014, Boyette and Ramsey 2019). In underserved counties, this is even more important because of the lack of informal learning opportunities that are largely affecting groups already

underrepresented in STEM careers. This will require increased investments in resources and partnerships with nearby ILIs to fill the geographic gaps in the informal learning landscape.

**References**


Barnosky AD, Hadly EA, Gonzalez P, Head J, Polly PD, Lawing AM, Eronen JT, Ackerly DD, Alex K, Biber E, Blois J, Brashares J, Ceballos G, Davis E, Dietl GP, Dirzo R, Doremus H, Fortelius M, Greene HW, Hellmann J, Hickler T, Jackson ST, Kemp M, Koch PL, Kremen C, Lindsey EL, Looy C, Marshall CR, Mendenhall C, Mulch A, Mychajliw AM, Nowak C, Ramakrishnan U, Schnitzler J, Das Shrestha K, Solari K, Stegner L, Stegner MA, Stenseth NC, Wake MH, Zhang Z. 2017. Merging paleobiology with conservation biology to guide the future of terrestrial ecosystems. Science 355: eaah4787.

Bell CJ, Mead JI. 2014. Not enough skeletons in the closet: Collections-based anatomical research in an age of conservation conscience. Anatomical Record 297: 344–348.

Boyette T, Ramsey JR. 2019. Does the messenger matter? Studying the impacts of scientists and engineers interacting with public audiences at science festival events. Journal of Science Communication 18: 1–16.

Dietl GP, Kidwell SM, Brenner M, Burney DA, Flessa KW, Jackson ST, Koch PL. 2015. Conservation paleobiology: Leveraging knowledge of the past to inform conservation and restoration. Annual Review of Earth and Planetary Sciences 43: 79–103.

Jones KE, Bielby J, Cardillo M, Fritz SA, O'Dell J, Orme CDL, Safi K, Sechrest W, Boakes EH, Carbone C, Connolly C, Cutts MJ, Foster JK, Grenyer R, Habib M, Plaster CA, Price SA, Rigby EA, Rist J, Teacher A, Bininda-Emonds ORP, Gittleman JL, Mace GM, Purvis A. 2009. PanTHERIA: a species-level database of life history, ecology, and geography of extant and recently extinct mammals. Ecology 90: 2648–2648.

Polly PD. 2010. Tiptoeing through the trophics: Geographic variation in carnivoran locomotor ecomorphology in relation to environment. Pages 374–410 in Goswami A and Friscia A, eds. Carnivoran Evolution: New Views on Phylogeny, Form, and Function. Cambridge University Press.

The NOW Community. 2019. New and Old Worlds Database of Fossil Mammals (NOW). (30 March 2019; www.helsinki.fi/science/now/).

Tóth AB, Lyons SK, Behrensmeyer AK. 2014. A century of change in Kenya's mammal communities: Increased richness and decreased uniqueness in six protected areas. PLoS ONE 9: e93092.

Uhen MD, Barnosky AD, Bills B, Blois J, Carrano MT, Carrasco MA, Erickson GM, Eronen JT, Fortelius M, Graham RW, Grimm EC, Oleary MA, Mast A, Piel WH, Polly PD, Säilä LK. 2013. From card catalogs to computers: Databases in vertebrate paleontology. Journal of Vertebrate Paleontology 33: 13–28.

Wiehe B. 2014. When science makes us who we are: Known and speculative impacts of science festivals. Journal of Science Communication 13: C02.

# APPENDIX A

## SUPPLEMENTAL MATERIAL FOR CHAPTER 2

**Table A-1. Fossil sites used for analysis of paleoprecipitation predictions. Site ID numbers correspond to x-axis labels in Figure 2.6.**

| Site ID | Site Name | Longitude | Latitude | Country | State | TimeBin |
|---|---|---|---|---|---|---|
| 1 | Riddell | -106.70 | 52.20 | CA | Saskatchewan | interglacial |
| 2 | Silver Creek Junction | -111.20 | 40.90 | US | Utah | interglacial |
| 3 | Harrodsburg Crevice | -86.50 | 39.00 | US | Indiana | interglacial |
| 4 | Eagle Cave | -79.28 | 38.83 | US | West Virginia | interglacial |
| 5 | Melrose Caverns | -78.89 | 38.48 | US | Virginia | interglacial |
| 6 | Mesa de Maya | -105.00 | 37.30 | US | Colorado | interglacial |
| 7 | Island Ford Cave | -81.34 | 37.10 | US | Virginia | interglacial |
| 8 | Coppel | -96.60 | 32.80 | US | Texas | interglacial |
| 9 | Mayfair | -81.10 | 32.00 | US | Georgia | interglacial |
| 10 | Isle of Hope | -81.07 | 31.98 | US | Georgia | interglacial |
| 11 | Arredondo IIA | -82.42 | 29.60 | US | Florida | interglacial |
| 12 | Rock Springs | -81.45 | 28.72 | US | Florida | interglacial |
| 13 | Lost Chicken Creek (Purdy Collection) | -141.88 | 64.05 | US | Alaska | glacial |
| 14 | January Cave | -114.52 | 50.18 | CA | Alberta | glacial |
| 15 | Shelton | -83.36 | 42.81 | US | Michigan | glacial |
| 16 | Little Box Elder Cave | -105.68 | 42.78 | US | Wyoming | glacial |
| 17 | Ravine South of Fairfield Creek | -100.08 | 42.78 | US | Nebraska | glacial |
| 18 | Sheriden Cave | -83.45 | 40.97 | US | Ohio | glacial |
| 19 | Samwel Cave No. 1 | -122.23 | 40.92 | US | California | glacial |
| 20 | Potter Creek Cave | -122.28 | 40.78 | US | California | glacial |
| 21 | Mandy Walters Cave | -79.30 | 38.83 | US | West Virginia | glacial |
| 22 | Hoffman School Cave | -79.36 | 38.58 | US | West Virginia | glacial |
| 23 | Haystack Cave (Upper Levels 1-3) | -107.15 | 38.48 | US | Colorado | glacial |
| 24 | Natural Chimneys | -79.08 | 38.36 | US | Virginia | glacial |
| 25 | Strait Canyon | -79.57 | 38.33 | US | Virginia | glacial |
| 26 | Clark's Cave | -79.66 | 38.09 | US | Virginia | glacial |
| 27 | Gregg Ranch Site | -100.70 | 36.78 | US | Oklahoma | glacial |
| 28 | White Mesa Mine Fissure 1 | -106.80 | 35.53 | US | New Mexico | glacial |

| | | | | | | |
|---|---|---|---|---|---|---|
| 29 | Isleta Caves | -106.88 | 34.88 | US | New Mexico | glacial |
| 30 | Ladd's Quarry | -84.80 | 34.20 | US | Georgia | glacial |
| 31 | Moore Pit | -96.71 | 32.71 | US | Texas | glacial |
| 32 | Dry Cave | -104.45 | 32.37 | US | New Mexico | glacial |
| 33 | Burnet Cave | -104.78 | 32.35 | US | New Mexico | glacial |
| 34 | U-Bar Cave | -108.40 | 31.57 | US | New Mexico | glacial |
| 35 | Fowlkes Cave | -104.20 | 31.18 | US | Texas | glacial |
| 36 | Avenue Area A | -98.26 | 30.27 | US | Texas | glacial |
| 37 | Ichetucknee River | -82.79 | 29.95 | US | Florida | glacial |
| 38 | Friesenhahn Cave | -98.40 | 29.58 | US | Texas | glacial |
| 39 | Vero | -80.40 | 27.64 | US | Florida | glacial |
| 40 | West Palm Beach Site | -80.17 | 26.70 | US | Florida | glacial |
| 41 | Cutler Hammock | -80.40 | 25.70 | US | Florida | glacial |
| 42 | San Josecito Cave | -99.82 | 24.10 | MX | Nuevo Leon | glacial |
| 43 | Barranca Piedras Negras | -98.62 | 20.05 | MX | Hidalgo | glacial |

## Code

```
#all maps were made in ArcMap using point data from R code
#links to data sources are provided
#data available on request

#set working directory and install required packages
install.packages(c("sp", "raster", "ggplot2", "class", "caret", "FNN",
"maps"))
library(sp)
library(raster)
library(ggplot2)
library(class)
library(caret)
library(FNN)
library(maps)

################prepare data################
#grid points with precipitation from WorldClim
points <- read.csv("samplingpointsNOGRNLND.csv")

#transform precipitation for normality
points$LogPrecip <- 2 * (log1p(points$BIO12) - min(log1p(points$BIO12),
na.rm = T)) + 1
h <- hist(points$LogPrecip, breaks = 10, xlab = "Annual Precipitation",
col = "gray")
hbreaksmod <- ((expm1(h$breaks) - 1)/2) + min(expm1(h$breaks), na.rm =
T)

#traits data
traits <- read.csv("NA_hypsodonty.csv", header = T)
rownames(traits) <- traits$SCI_NAME

#geographic ranges from NatureServe
#available: https://www.natureserve.org/conservation-tools/digital-
distribution-maps-mammals-western-hemisphere
#download data and read as a shapefile
mammals <- shapefile("natureservemammals.shp")
geography <- subset(mammals, PRESENCE == 1 & (subset = ORIGIN == 1 |
ORIGIN == 2 | ORIGIN == 3 | ORIGIN == 4 | ORIGIN == 5 | ORIGIN == 8))

#convert sampling points to spatial points
sp <- SpatialPoints(points[ , 2:3], proj4string =
CRS(proj4string(geography)))

#sample species at each sampling locality
o <- over(sp, geography, returnList = T)

#calculate sample size at each point
richness <- unlist(lapply(o, function(x) length(traits[x$SCI_NAME,
"hypsodonty"])))
points$richness <- richness
```

```
#summarize traits for community level distributions
ecometric_hypsodonty <- unlist(lapply(o, function(x)
mean(traits[x$SCI_NAME, "hypsodonty"], na.rm = T)))
points$hypmean <- ecometric_hypsodonty

#restrict data for analysis
restricted <- richness >= 5 & ecometric_hypsodonty <= 3 &
ecometric_hypsodonty >= 1 & !is.na(ecometric_hypsodonty) &
!is.na(points$LogPrecip)
x <- ecometric_hypsodonty[restricted]
y <- points[restricted,"LogPrecip"]

#################analysis 1################
#################linear regression################
linreg <- lm(y~x)
summary(linreg)

#calculate anomaly
anom_lin <- points$LogPrecip[restricted] -
predict(linreg,data.frame(x=x))
max(anom_lin, na.rm = T)
min(anom_lin, na.rm = T)
mean(anom_lin, na.rm = T)

#################polynomial regression################
model_hyp <- lm(y ~ poly(x,3))
summary(model_hyp)

#calculate anomaly
anom_poly <- points$LogPrecip[restricted] -
predict(model_hyp,data.frame(x=x))
max(anom_poly, na.rm = T)
min(anom_poly, na.rm = T)
mean(anom_poly, na.rm = T)

#################maximum likelihood################
#calculate standard deviation
sd_ecometric_hypsodonty <- unlist(lapply(o, function(x)
sd(traits[x$SCI_NAME, "hypsodonty"], na.rm = T)))
points$hypsd <- sd_ecometric_hypsodonty

#group the community trait distributions in 25 x 25 bins
mhyp <- range(ecometric_hypsodonty, na.rm = T)
sdhyp <- range(sd_ecometric_hypsodonty, na.rm = T)
#get the break points for sd and mean
mbrks <- seq(mhyp[1]-0.001, mhyp[2]+0.001, diff(mhyp)/25)
sdbrks <- seq(sdhyp[1]-0.001, sdhyp[2]+0.001, diff(sdhyp)/25)
#assign bin codes
mbc <- .bincode(ecometric_hypsodonty, breaks = mbrks)
sdbc <- .bincode(sd_ecometric_hypsodonty, breaks = sdbrks)
#limit bin designations to restricted communities
mbc[!restricted] <- NA
sdbc[!restricted] <- NA
```

```
#calculate the data for the raster
obj <- array(NA, dim = c(25, 25))
for (i in 1:25) {
  for (j in 1:25) {
    dat <- points$LogPrecip[which(mbc == i & sdbc == j)]
    obj[26 - j, i] <- mean(dat, na.rm = T)
  }
}

#calculate maximum likelihood for all bins
modmax <- array(NA, dim = length(points[ , 1]))
mod <- list()
for (i in 1:length(points[ , 1])) {
  if(!(is.na(mbc[i]) | is.na(sdbc[i]))) {
    dat <- points$LogPrecip[which(mbc == mbc[i] & sdbc == sdbc[i])]
    mod[[i]] <- density(dat[!is.na(dat)], bw = 1)
    modmax[i] <- mod[[i]]$x[which.max(mod[[i]]$y)]
  }
}

#calculate anomaly
anom_maxlik <- points$LogPrecip - modmax ##observed - predicted
max(anom_maxlik, na.rm = T)
min(anom_maxlik, na.rm = T)
mean(anom_maxlik, na.rm = T)
anom_maxlik_csv <-cbind(points[ , 2:3], anom_maxlik)
anom_maxlik_csv <-
anom_maxlik_csv[!(is.na(anom_maxlik_csv$anom_maxlik)), ]

###################nearest neighbor######################
#partition training and testing data
#training and testing data provided to match manuscript results
#near <- data.frame(x, y)
#colnames(near)[colnames(near)==c("x", "y")] <- c("Hypsodonty",
"LogPrecip")
#near$ID = rownames(near)
#inTrain <- createDataPartition(y = near$Hypsodonty, p = 0.2, list =
FALSE)
#training <- near[inTrain, ] #training dataset, small (p) of whole data
#testing <- near[-inTrain, ] #testing dataset, large of whole data
#write.csv(training, file = "training.csv")
#write.csv(testing, file = "testing.csv")
training <- read.csv("training_data.csv")
testing <- read.csv("testing_data.csv")

#calculate nearest neighbor
#k = 15
pred_nn <- knn.reg(train = data.frame(training$Hypsodonty), test =
data.frame(testing$Hypsodonty), y = training$LogPrecip, k = 15)

#calculate anomaly
anom_nn <- testing$LogPrecip - pred_nn$pred
max(anom_nn, na.rm = T)
min(anom_nn, na.rm = T)
```

```
mean(anom_nn, na.rm = T)
anom_nn_csv <- cbind(testing, anom_nn)
points$rows <- as.numeric(rownames(points))
anom_nn_csv <-merge(points, anom_nn_csv[ , 4:5], by.x = "rows", by.y =
"ID")

######################Figure 2.4######################
k <- density(anom_lin)
l <- density(anom_poly)
m <- density(anom_nn)
n <- density(anom_maxlik, na.rm = T)
plot(k, col = "black", xlim = c(-5, 5), ylim = c(0, 0.6), yaxs = "i",
main = " ", xlab = "Anomaly")
abline(v = 0, lwd = 2)
polygon(k, border = "black", col = adjustcolor("#969696", alpha = 0.5),
lty = 1, lwd= 2)
polygon(l, border = "black", col = adjustcolor("#bdbdbd", alpha = 0.5),
lty = 2, lwd= 2)
polygon(m, border = "black", col = adjustcolor("#d9d9d9", alpha = 0.5),
lty = 3, lwd= 2)
polygon(n, border = "black", col = adjustcolor("#f7f7f7", alpha = 0.5),
lty = 6, lwd= 2)
legend("topright", c("Linear regression", "Polynomial regression",
"Nearest neighbor", "Maximum likelihood"), bty = "n", col = "black",
lty = c(1, 2, 3, 6), lwd = 2)

###################correlations################
#compile paleoprecipitation predictions into one dataframe
pointsdata <- points
pointsdata$rownames <- as.numeric(row.names(pointsdata))
linregdata <- as.data.frame(predict(linreg, data.frame(x=x)))
linregdata$rownames <- as.numeric(row.names(linregdata))
polyregdata <- as.data.frame(predict(model_hyp,data.frame(x=x)))
polyregdata$rownames <- as.numeric(row.names(polyregdata))
modmaxdata <- as.data.frame(modmax)
modmaxdata$rownames <- as.numeric(row.names(modmaxdata))
nearneighdata <- testing
nearneighdata$preddata <- pred_nn$pred
nearneighdata <- nearneighdata[ , 4:5]
colnames(nearneighdata)[1] <- "rownames"

pointsdata <- merge(pointsdata, linregdata, by = "rownames", all =
TRUE, incomparables = NA)
pointsdata <- merge(pointsdata, polyregdata, by = "rownames", all =
TRUE, incomparables = NA)
pointsdata <- merge(pointsdata, modmaxdata, by = "rownames", all =
TRUE, incomparables = NA)
pointsdata <- merge(pointsdata, nearneighdata, by = "rownames", all =
TRUE, incomparables = NA)
colnames(pointsdata)[10:13] <- c("linregdata", "polyregdata",
"modmaxdata", "preddata")

#correlation tests
correlations <- cor(pointsdata, use = "complete.obs")
```

```
correlations

#anova
anova <- read.csv("anovadata.csv", header = T, na = ".")
anovamodel <- aov(anomaly ~ method, data = anova)
anovamodel
summary(anovamodel)

################analysis 2################
#read fossil site data with precipitation
#global climate model values were extracted using ArcMap
fossildata <- read.csv("fossil_gcm_estimates.csv")
#transform paleoprecipitation to match precipitation
fossildata$LogMR <- 2 * (log1p(fossildata$mrlgmbi12) -
min(log1p(fossildata$mrlgmbi12), na.rm = T)) + 1
fossildata$LogCC <- 2 * (log1p(fossildata$cclgmbi12) -
min(log1p(fossildata$cclgmbi12), na.rm = T)) + 1
fossildata$LogIG <- 2 * (log1p(fossildata$interglacial) -
min(log1p(fossildata$interglacial), na.rm = T)) + 1

#read fossil site data with hypsodonty
#fossil sites are already limited to a richness > 5
fossil <- read.csv("fossilcomm.csv", header = T)
fossilmean <- aggregate(fossil[ , 10], list(fossil$siteID), mean, na.rm
= TRUE)
fossilsd <- aggregate(fossil[ , 10], list(fossil$siteID), sd, na.rm =
TRUE)
fossildata <- merge(fossildata, fossilmean, by.x = "siteID", by.y =
"Group.1")
fossildata <- merge(fossildata, fossilsd, by.x = "siteID", by.y =
"Group.1")
colnames(fossildata)[15:16] <- c("hyp_mean", "hyp_sd")

#generate paleoprecipitation predictions from previous models
#predict - linear regression
fossildata$LinReg <- predict(linreg, data.frame(x =
fossildata$hyp_mean))

#predict - polynomial regression
fossildata$PolyReg <- predict(model_hyp, data.frame(x =
fossildata$hyp_mean))

#predict - maximum likelihood
fossilpoints <- points
fossilpoints$mbc <- mbc
fossilpoints$sdbc <- sdbc
fossilpoints$modmax <- modmax
fossilmbc <- .bincode(fossildata$hyp_mean, breaks = mbrks)
fossilsdbc <- .bincode(fossildata$hyp_sd, breaks = sdbrks)

#predictions for each community
fossilmod <- list()
for (i in 1:length(fossildata[ , 1])) {
  if(!(is.na(fossilmbc[i]) | is.na(fossilsdbc[i]))) {
```

```
    fossilmod[[i]] <- fossilpoints[which(mbc == fossilmbc[i] & sdbc ==
fossilsdbc[i]), 11][1]
    }
}
fossildata$MaxLike <- as.numeric(fossilmod)

#predict - nearest neighbor
fossil_nn <- knn.reg(train = data.frame(training$Hypsodonty), test =
data.frame(fossildata$hyp_mean), y = training$LogPrecip, k = 15)
#Fortelius etal used k = 15
fossildata$NearNeigh <- fossil_nn$pred

#sort by latitude
fossildataorder <- fossildata[order(-fossildata$lat),]
#split sites into glacial and interglacial
glacial <- fossildataorder[fossildataorder$G_IG == "G", ]
interglacial <- fossildataorder[fossildataorder$G_IG == "IG", ]

######################Figure 2.6######################
#interglacial sites - Fig 6A
par(bg = NA, mar = c(14, 4.1, 2, 2.1))
interglacial$siteID <- as.factor(interglacial$siteID)
plot(NULL, xlim = c(1, 12), ylim = c(0, 8), ylab = "Log Precip", xlab =
" ", xaxt = "n")
axis(1, at = c(1:12), labels = interglacial$sitename, las = 2, cex.axis
= 0.8)
mtext("Interglacial Sites", side = 1, line = 12)
points(interglacial$siteID, interglacial$LogIG, col = "black", pch =
16, cex = 2)
points(interglacial$siteID, interglacial$LinReg, pch = 22, cex = 2, bg
= "#969696", col = "black")
points(interglacial$siteID, interglacial$PolyReg, pch = 24, cex = 2, bg
= "#bdbdbd", col = "black")
points(interglacial$siteID, interglacial$NearNeigh, pch = 23, cex = 2,
bg = "#d9d9d9", col = "black")
points(interglacial$siteID, interglacial$MaxLike, pch = 25, cex = 2, bg
= "#f7f7f7", col = "black")
legend("bottomright", c("Global circulation - interglacial", "Linear
regression", "Polynomial regression", "Nearest neighbor", "Maximum
likelihood"), pch = c(16, 22, 24, 23, 25), bty = "n", col = "black",
pt.cex = 2, pt.bg = c("black", "#969696", "#bdbdbd", "#d9d9d9",
"#f7f7f7"))

#glacial sites - Fig 6C
par(bg = NA, mar = c(14, 4.1, 2, 2.1))
glacial$siteID <- as.factor(glacial$siteID)
plot(NULL, xlim = c(1, 31), ylim = c(0, 8), ylab = "Log Precip", xlab =
" ", xaxt = "n")
axis(1, at = c(1:31), labels = glacial$sitename, las = 2, cex.axis =
0.8)
mtext("Glacial Sites", side = 1, line = 12)
segments(as.numeric(glacial$siteID), glacial$LogMR,
as.numeric(glacial$siteID), glacial$LogCC, col = "black", lwd = 7)
```

```
points(glacial$siteID, glacial$LinReg, pch = 22, cex = 2, bg =
"#969696", col = "black")
points(glacial$siteID, glacial$PolyReg, pch = 24, cex = 2, bg =
"#bdbdbd", col = "black")
points(glacial$siteID, glacial$NearNeigh, pch = 23, cex = 2, bg =
"#d9d9d9", col = "black")
points(glacial$siteID, glacial$MaxLike, pch = 25, cex = 2, bg =
"#f7f7f7", col = "black")
legend("bottomright", c("Global circulation - glacial", "Linear
regression", "Polynomial regression", "Nearest neighbor", "Maximum
likelihood"), pch = c(16, 22, 24, 23, 25), bty = "n", col = "black",
pt.cex = 2, pt.bg = c("black", "#969696", "#bdbdbd", "#d9d9d9",
"#f7f7f7"))

dev.off()

#calculate differences between GCM and predictions for interglacial
sites
interglacial$GCMlin <- interglacial$LogIG - interglacial$LinReg
interglacial$GCMpoly <- interglacial$LogIG - interglacial$PolyReg
interglacial$GCMnear <- interglacial$LogIG - interglacial$NearNeigh
interglacial$GCMmax <- interglacial$LogIG - interglacial$MaxLike

#interglacial curves - Fig. 6B
e <- density(interglacial$GCMlin)
f <- density(interglacial$GCMpoly)
g <- density(interglacial$GCMnear)
h <- density(interglacial$GCMmax, na.rm = T)
par(bg = NA)
plot(e, col = "black", xlim = c(-5, 5), ylim = c(0, 0.6), yaxs = "i",
main = " ", xlab = "Anomaly")
abline(v = 0, lwd = 2)
polygon(e, border = "black", col = adjustcolor("#969696", alpha = 0.5),
lty = 1, lwd= 2)
polygon(f, border = "black", col = adjustcolor("#bdbdbd", alpha = 0.5),
lty = 2, lwd= 2)
polygon(g, border = "black", col = adjustcolor("#d9d9d9", alpha = 0.5),
lty = 3, lwd= 2)
polygon(h, border = "black", col = adjustcolor("#f7f7f7", alpha = 0.5),
lty = 6, lwd= 2)
legend("topright", c("Linear regression", "Polynomial regression",
"Nearest neighbor", "Maximum likelihood"), bty = "n", col = "black",
lty = c(1, 2, 3, 6), lwd = 2)

#calculate differences between GCM and predictions for glacial sites
glacial$glacGCM <- (glacial$LogMR + glacial$LogCC)/2
glacial$GCMlin <- glacial$glacGCM - glacial$LinReg
glacial$GCMpoly <- glacial$glacGCM - glacial$PolyReg
glacial$GCMnear <- glacial$glacGCM - glacial$NearNeigh
glacial$GCMmax <- glacial$glacGCM - glacial$MaxLike

#glacial curves - Fig. 6D
a <- density(glacial$GCMlin)
b <- density(glacial$GCMpoly)
```

```
c <- density(glacial$GCMnear)
d <- density(glacial$GCMmax, na.rm = T)
par(bg = NA)
plot(a, col = "black", xlim = c(-5, 5), ylim = c(0, 0.6), yaxs = "i",
main = " ", xlab = "Anomaly")
abline(v = 0, lwd = 2)
polygon(a, border = "black", col = adjustcolor("#969696", alpha = 0.5),
lty = 1, lwd= 2)
polygon(b, border = "black", col = adjustcolor("#bdbdbd", alpha = 0.5),
lty = 2, lwd= 2)
polygon(c, border = "black", col = adjustcolor("#d9d9d9", alpha = 0.5),
lty = 3, lwd= 2)
polygon(d, border = "black", col = adjustcolor("#f7f7f7", alpha = 0.5),
lty = 6, lwd= 2)
legend("topright", c("Linear regression", "Polynomial regression",
"Nearest neighbor", "Maximum likelihood"), bty = "n", col = "black",
lty = c(1, 2, 3, 6), lwd = 2)

######################Figure 2.7######################
#interglacial sites with glacial GCM - Fig 7A
par(bg = NA, mar = c(14, 4.1, 2, 2.1))
interglacial$siteID <- as.factor(interglacial$siteID)
plot(NULL, xlim = c(1, 12), ylim = c(0, 8), ylab = "Log Precip", xlab =
" ", xaxt = "n")
axis(1, at = c(1:12), labels = interglacial$sitename, las = 2, cex.axis
= 0.8)
mtext("Interglacial Sites", side = 1, line = 12)
segments(as.numeric(interglacial$siteID), interglacial$LogMR,
as.numeric(interglacial$siteID), interglacial$LogCC, col = "black", lwd
= 7)
points(interglacial$siteID, interglacial$LinReg, pch = 22, cex = 2, bg
= "#969696", col = "black")
points(interglacial$siteID, interglacial$PolyReg, pch = 24, cex = 2, bg
= "#bdbdbd", col = "black")
points(interglacial$siteID, interglacial$NearNeigh, pch = 23, cex = 2,
bg = "#d9d9d9", col = "black")
points(interglacial$siteID, interglacial$MaxLike, pch = 25, cex = 2, bg
= "#f7f7f7", col = "black")
legend("bottomright", c("Global circulation - interglacial", "Linear
regression", "Polynomial regression", "Nearest neighbor", "Maximum
likelihood"), pch = c(16, 22, 24, 23, 25), bty = "n", col = "black",
pt.cex = 2, pt.bg = c("black", "#969696", "#bdbdbd", "#d9d9d9",
"#f7f7f7"))

dev.off()

#calculate differences between glacial GCM and predictions for
interglacial sites - Fig. 7B
interglacial$glacGCM_glac <- (interglacial$LogMR +
interglacial$LogCC)/2
interglacial$GCMlin_glac <- interglacial$glacGCM_glac -
interglacial$LinReg
interglacial$GCMpoly_glac <- interglacial$glacGCM_glac -
interglacial$PolyReg
```

```
interglacial$GCMnear_glac <- interglacial$glacGCM_glac -
interglacial$NearNeigh
interglacial$GCMmax_glac <- interglacial$glacGCM_glac -
interglacial$MaxLike

#interglacial curves with glacial predictions
r <- density(interglacial$GCMlin_glac)
s <- density(interglacial$GCMpoly_glac)
t <- density(interglacial$GCMnear_glac)
u <- density(interglacial$GCMmax_glac, na.rm = T)
par(bg = NA)
plot(r, col = "black", xlim = c(-5, 5), ylim = c(0, 0.6), yaxs = "i",
main = " ", xlab = "Anomaly")
abline(v = 0, lwd = 2)
polygon(r, border = "black", col = adjustcolor("#969696", alpha = 0.5),
lty = 1, lwd= 2)
polygon(s, border = "black", col = adjustcolor("#bdbdbd", alpha = 0.5),
lty = 2, lwd= 2)
polygon(t, border = "black", col = adjustcolor("#d9d9d9", alpha = 0.5),
lty = 3, lwd= 2)
polygon(u, border = "black", col = adjustcolor("#f7f7f7", alpha = 0.5),
lty = 6, lwd= 2)
legend("topright", c("Linear regression", "Polynomial regression",
"Nearest neighbor", "Maximum likelihood"), bty = "n", col = "black",
lty = c(1, 2, 3, 6), lwd = 2)
```

APPENDIX B

SUPPLEMENTAL MATERIAL FOR CHAPTER 3

**Table B-1. Ecoregion predictions. Total points are the number of grid points in each domain or division. Predicted points are the number of the total points for which a prediction was produced. Correct points are the number of predicted points that correctly matched the observed ecoregion category. Correct percentage is the percentage of the predicted points that were correct.**

| Domain | Division | Total Points | Predicted Points | Correct Points | Correct Percentage |
|---|---|---|---|---|---|
| Dry | | 18552 | 3689 | 2593 | 70.3% |
| | Tropical/subtropical desert regime mountains | 1275 | 453 | 410 | 90.5% |
| | Temperate steppe | 1900 | 546 | 379 | 69.4% |
| | Temperate desert | 2193 | 295 | 173 | 58.6% |
| | Tropical/subtropical steppe | 3878 | 995 | 303 | 30.5% |
| | Temperate steppe regime mountains | 429 | 303 | 81 | 26.7% |
| | Tropical/subtropical desert | 6836 | 497 | 112 | 22.5% |
| | Tropical/subtropical steppe regime mountains | 1792 | 583 | 116 | 19.9% |
| | Temperate desert megime mountains | 249 | 17 | 0 | 0% |
| Humid temperate | | 8552 | 2320 | 1129 | 48.7% |
| | Subtropical regime mountains | 590 | 375 | 197 | 52.5% |
| | Subtropical | 1331 | 472 | 161 | 34.1% |
| | Marine | 465 | 91 | 26 | 28.6% |
| | Marine regime mountains | 823 | 227 | 37 | 16.3% |
| | Warm continental regime mountains | 417 | 367 | 43 | 11.7% |
| | Mediterranean | 383 | 28 | 0 | 0% |
| | Mediterranean regime mountains | 591 | 27 | 0 | 0% |
| | Prairie | 1759 | 238 | 0 | 0% |
| | Prairie regime mountains | 512 | 114 | 0 | 0% |
| | Hot continental | 641 | 164 | 0 | 0% |
| | Warm continental | 850 | 217 | 0 | 0% |
| | Hot continental regime mountains | 190 | 0 | 0 | -- |
| Humid tropical | | 15024 | 11992 | 11474 | 95.7% |
| | Savanna | 8062 | 6806 | 5583 | 82.0% |
| | Rainforest | 3962 | 3435 | 2791 | 81.3% |
| | Rainforest regime mountains | 1251 | 597 | 160 | 26.8% |
| | Savanna regime | 1749 | 1154 | 154 | 13.3% |
| Polar | | 9926 | 2378 | 1812 | 76.2% |
| | Subarctic regime mountains | 2301 | 1129 | 812 | 71.9% |
| | Subarctic | 4835 | 1165 | 784 | 67.3% |
| | Tundra | 1425 | 31 | 0 | 0% |
| | Tundra regime mountains | 560 | 53 | 0 | 0% |
| | Icecap | 805 | 0 | 0 | . |

**Table B-2. Vegetation cover predictions. Total points are the number of grid points in each vegetation category. Predicted points are the number of the total points for which a prediction was produced. Correct points are the number of predicted points that correctly matched the observed vegetation cover. Correct percentage is the percentage of the predicted points that were correct.**

| Vegetation | Vegetation Cover | Total Points | Predicted Points | Correct Points | Correct Percentage |
|---|---|---|---|---|---|
| Evergreen | | 13965 | 7139 | 5618 | 78.7% |
| | Tropical evergreen rainforest | 4802 | 4023 | 3637 | 90.4% |
| | Tropical/subtropical evergreen seasonal broad-leaved forest | 1551 | 1078 | 551 | 51.1% |
| | Temperate evergreen seasonal broadleaved forest, summer rain | 423 | 282 | 122 | 43.3% |
| | Tropical/subtropical evergreen needle-leaved forest | 204 | 176 | 64 | 36.4% |
| | Temperate/subpolar evergreen needle-leaved forest | 3755 | 1038 | 193 | 18.6% |
| | Evergreen needle-leaved woodland | 1078 | 376 | 50 | 13.3% |
| | Evergreen broadleaved sclerophyllous woodland | 889 | 80 | 0 | 0% |
| | Evergreen broadleaved shrubland/thick, evergreen dwarf-shrubland | 556 | 58 | 0 | 0% |
| | Evergreen needle-leaved or microphyllous shrubland/thicket | 258 | 26 | 0 | 0% |
| | Subtropical evergreen rainforest | 93 | 2 | 0 | 0% |
| | Evergreen broadleaved sclerophyllous forest, winter rain | 214 | 0 | 0 | -- |
| | Temperate/subpolar evergreen rainforest | 142 | 0 | 0 | -- |
| Deciduous | | 10155 | 5000 | 3219 | 64.4% |
| | Cold-deciduous forest, without evergreens | 2193 | 1027 | 1026 | 99.9% |
| | Tropical/subtropical drought-deciduous forest | 1493 | 1146 | 726 | 63.4% |
| | Tropical/subtropical drought-deciduous woodland | 1886 | 1750 | 1044 | 59.7% |
| | Cold-deciduous forest, with evergreens | 2978 | 721 | 146 | 20.2% |
| | Drought-deciduous shrubland/thicket | 385 | 133 | 7 | 5.3% |
| | Cold-deciduous subalpine/subpolar shrubland/dwarf shrub | 173 | 2 | 0 | 0% |
| | Cold-deciduous woodland | 1047 | 221 | 0 | 0% |
| Grassland | | 13508 | 5986 | 3780 | 63.1% |
| | Medium grassland, no woody cover | 569 | 291 | 154 | 52.9% |
| | Tall/medium/short grassland, shrub cover | 4292 | 1513 | 794 | 52.5% |
| | Tall/medium/short grassland, < 10% woody cover | 1644 | 1035 | 368 | 35.6% |
| | Tall/medium/short grassland, 10-40% woody cover | 3409 | 2076 | 420 | 20.2% |
| | Meadow, short grassland, no woody cover | 2902 | 753 | 73 | 9.7% |
| | Tall grassland, no woody cover | 583 | 268 | 5 | 1.9% |
| | Forb formations | 109 | 50 | 0 | 0% |
| Desert | | 11035 | 1892 | 825 | 43.6% |
| | Desert | 6231 | 641 | 439 | 68.5% |
| | Xeromorphic shrubland/dwarf shrubland | 3626 | 786 | 287 | 36.5% |

| | | | | | |
|---|---|---|---|---|---|
| | Xeromorphic forest/woodland | 1178 | 465 | 101 | 21.7% |
| Arctic | | 3643 | 374 | 0 | 0% |
| | Arctic/alpine tundra, mossy bog | 2714 | 360 | 62 | 17.2% |
| | Ice | 929 | 14 | 0 | 0% |

**Table B-3. Kenyan sites and ecometric data from Figure 6. Sites are from Tóth et al. (2014). Time intervals are historical (H) and modern (M). Mean and standard deviation are community calcaneal gear ratio measurements. Ecoregion division, vegetation cover, and precipitation are predictions using ecometric models.**

| Site ID | Site | Time | Mean | Standard Deviation | Ecoregion Division | Vegetation Cover | Precipitation (log mm) |
|---|---|---|---|---|---|---|---|
| 1 | Kakamega Forest Reserve | H | 1.509 | 0.033 | Savanna | tropical/subtropical drought-deciduous woodland | 7.002 |
| | | M | 1.517 | 0.036 | Savanna | tall/medium/short grassland, 10-40% woody cover | 7.013 |
| 2 | Maasai Mara National Reserve | H | 1.481 | 0.047 | Tropical/Subtropical Steppe | xeromorphic shrubland/dwarf shrubland | 5.801 |
| | | M | 1.496 | 0.048 | Savanna | tall/medium/short grassland, shrub cover | 6.636 |
| 3 | Nairobi National Park | H | 1.493 | 0.047 | Savanna | tall/medium/short grassland, shrub cover | 6.503 |
| | | M | 1.492 | 0.050 | Savanna | tall/medium/short grassland, shrub cover | 6.503 |
| 4 | Lake Naivasha National Park | H | 1.505 | 0.057 | Savanna | tropical/subtropical drought-deciduous forest | 6.809 |
| | | M | 1.493 | 0.052 | Savanna | xeromorphic forest/woodland | 6.509 |
| 5 | Samburu Game Reserve | H | 1.497 | 0.053 | Savanna | tall/medium/short grassland, 10-40% woody cover | 6.553 |
| | | M | 1.497 | 0.055 | Savanna | trop/subtropical evergreen seasonal broad-leaved forest | 6.272 |
| 6 | Tsavo East and West National Parks | H | 1.505 | 0.052 | Savanna | tropical/subtropical drought-deciduous forest | 7.086 |
| | | M | 1.493 | 0.048 | Savanna | tall/medium/short grassland, shrub cover | 6.503 |

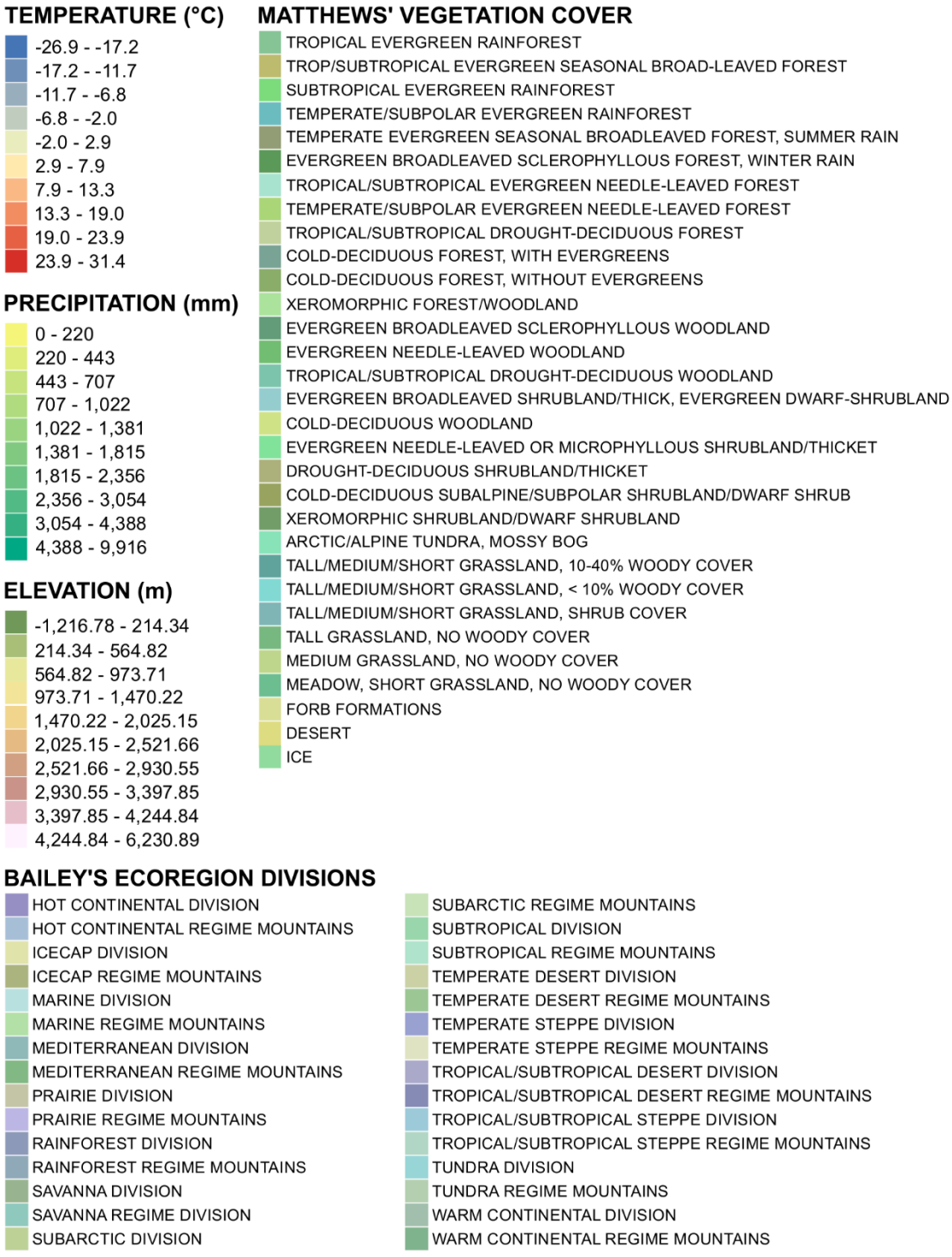


**Figure B-1. Legend values for Figure 3.2.**

**Data collected for ecometric analyses. 1, Length of calcaneum; 2, Length of calcaneal tuber. Gear ratio is measurement 1 divided by measurement 2.**

| Family | Genus | Species | Museum | Number | Sex | 1 | 2 | Gear ratio | Mean | Standard Deviation |
|---|---|---|---|---|---|---|---|---|---|---|
| Antilocapridae | Antilocapra | americana | | | | | | | 1.46 | 0.02 |
| | | | DMNS | 7035 | U | 88.31 | 60.27 | 1.47 | | |
| | | | USNM | 251131 | M | 77.34 | 51.84 | 1.49 | | |
| | | | USNM | 266393 | M | 79.00 | 54.66 | 1.45 | | |
| | | | USNM | 271663 | F | 82.49 | 57.89 | 1.43 | | |
| | | | USNM | A 22387 | M | 80.03 | 54.91 | 1.46 | | |
| Bovidae | Addax | nasomaculatus | | | | | | | 1.52 | 0.05 |
| | | | ZMB_Mam | 70824 | F | 89.89 | 60.66 | 1.48 | | |
| | | | ZMB_Mam | 78826 | F | 83.49 | 53.72 | 1.55 | | |
| Bovidae | Aepyceros | melampus | | | | | | | 1.45 | 0.03 |
| | | | USNM | 162001 | M | 81.82 | 56.36 | 1.45 | | |
| | | | USNM | 241588 | F | 75.53 | 53.32 | 1.42 | | |
| | | | USNM | 261111 | F | 79.42 | 53.76 | 1.48 | | |
| Bovidae | Alcelaphus | buselaphus | | | | | | | 1.46 | 0.04 |
| | | | USNM | 161950 | F | 81.13 | 57.38 | 1.41 | | |
| | | | USNM | 163147 | M | 116.20 | 79.49 | 1.46 | | |
| | | | USNM | 164705 | F | 100.39 | 67.92 | 1.48 | | |
| | | | ZMB_Mam | 77219 | F | 91.88 | 61.43 | 1.50 | | |
| Bovidae | Alcelaphus | lichtensteinii | | | | | | | 1.47 | -- |
| | | | NHM | 1940.82 | U | 109.32 | 74.42 | 1.47 | | |
| Bovidae | Ammodorcas | clarkei | | | | | | | 1.40 | 0.02 |
| | | | LaSpecola | 2164 | M | 73.66 | 53.18 | 1.39 | | |
| | | | LaSpecola | 2165 | F | 69.99 | 48.95 | 1.43 | | |
| | | | LaSpecola | 3309 | M | 71.43 | 51.28 | 1.39 | | |
| | | | LaSpecola | 3311 | F | 70.59 | 50.12 | 1.41 | | |
| | | | NHM | 1896.10.6.2. | F | 72.90 | 52.62 | 1.39 | | |
| | | | NHM | 1935.12.13.5. | M | 72.79 | 52.15 | 1.40 | | |
| | | | NHM | 1935.12.13.6. | M | 75.58 | 53.92 | 1.40 | | |
| Bovidae | Ammotragus | lervia | | | | | | | 1.49 | 0.06 |
| | | | LaSpecola | 9818 | M | 86.92 | 61.50 | 1.41 | | |
| | | | USNM | 13069 | M | 75.81 | 49.70 | 1.53 | | |
| | | | USNM | 287527 | M | 78.36 | 53.03 | 1.48 | | |

| | | | | | | | | | | |
|---|---|---|---|---|---|---|---|---|---|---|
| | | | USNM | A 49996 | F | 69.47 | 45.21 | 1.54 | | |
| Bovidae | Antidorcas | marsupialis | | | | | | | 1.44 | -- |
| | | | USNM | 173040 | M | 65.80 | 45.68 | 1.44 | | |
| Bovidae | Antilope | cervicapra | | | | | | | 1.44 | 0.02 |
| | | | USNM | 124653 | M | 67.95 | 46.31 | 1.47 | | |
| | | | USNM | 174628 | M | 62.14 | 42.42 | 1.46 | | |
| | | | USNM | 259836 | F | 65.87 | 45.68 | 1.44 | | |
| | | | USNM | 268196 | F | 61.77 | 43.92 | 1.41 | | |
| | | | ZMB_Mam | 78829 | F | 61.30 | 43.21 | 1.42 | | |
| | | | ZMB_Mam | 78830 | U | 64.10 | 44.66 | 1.44 | | |
| Bovidae | Beatragus | hunteri | | | | | | | 1.44 | 0.02 |
| | | | LaSpecola | 2835 | M | 95.51 | 67.18 | 1.42 | | |
| | | | NHM | 1936.3.28.12 | M | 94.22 | 65.91 | 1.43 | | |
| | | | NHM | 1936.3.28.13 | U | 92.04 | 64.65 | 1.42 | | |
| | | | NHM | 1938.7.11.1 | U | 99.59 | 69.15 | 1.44 | | |
| | | | OM | 1901 | U | 101.00 | 68.21 | 1.48 | | |
| Bovidae | Bison | bison | | | | | | | 1.52 | 0.02 |
| | | | DMNS | 8477 | U | 158.92 | 105.78 | 1.50 | | |
| | | | USNM | 172689 | M | 170.85 | 112.73 | 1.52 | | |
| | | | USNM | 249894 | M | 161.92 | 105.10 | 1.54 | | |
| | | | USNM | 251147 | M | 142.67 | 93.84 | 1.52 | | |
| | | | USNM | 286873 | U | 159.02 | 105.25 | 1.51 | | |
| | | | ZMB_Mam | 14800 | M | 147.30 | 95.77 | 1.54 | | |
| | | | ZMB_Mam | 38676 | U | 152.57 | 103.34 | 1.48 | | |
| | | | ZMB_Mam | 46559 | M | 171.96 | 113.39 | 1.52 | | |
| Bovidae | Bison | bonasus | | | | | | | 1.48 | 0.03 |
| | | | USNM | 546176 | M | 173.79 | 114.92 | 1.51 | | |
| | | | ZMB_Mam | 2229 | U | 161.20 | 110.78 | 1.46 | | |
| | | | ZMB_Mam | 14798 | F | 152.52 | 102.53 | 1.49 | | |
| | | | ZMB_Mam | 33834 | U | 167.89 | 115.11 | 1.46 | | |
| | | | ZMB_Mam | 33837 | U | 143.73 | 99.04 | 1.45 | | |
| | | | ZMB_Mam | 33838 | F | 141.06 | 95.57 | 1.48 | | |
| | | | ZMB_Mam | 33865 | F | 146.91 | 99.65 | 1.47 | | |
| | | | ZMB_Mam | 44213 | M | 172.16 | 120.13 | 1.43 | | |
| | | | ZMB_Mam | 46548 | M | 165.84 | 109.33 | 1.52 | | |
| | | | ZMB_Mam | 47193 | F | 151.30 | 102.81 | 1.47 | | |
| | | | ZMB_Mam | 77264 | F | 155.54 | 104.37 | 1.49 | | |

| | | | | | | | | | | |
|---|---|---|---|---|---|---|---|---|---|---|
| | | | ZMB_Mam | 77277 | F | 149.26 | 98.59 | 1.51 | | |
| | | | ZMB_Mam | 84981 | F | 156.29 | 107.15 | 1.46 | | |
| Bovidae | Bos | javanicus | | | | | | | 1.47 | -- |
| | | | NHM | 1910.11.29.4 | M | 115.91 | 78.71 | 1.47 | | |
| Bovidae | Bos | sauveli | | | | | | | 1.53 | 0.00 |
| | | | USNM | 361392 | F | 130.08 | 85.13 | 1.53 | | |
| | | | USNM | 399379 | F | 126.65 | 83.04 | 1.53 | | |
| Bovidae | Boselaphus | tragocamelus | | | | | | | 1.51 | 0.01 |
| | | | LaSpecola | 1461 | F | 112.35 | 74.85 | 1.50 | | |
| | | | NHM | 1937.5.1.1. | F | 121.53 | 80.63 | 1.51 | | |
| | | | NHM | 1949.12.30.1 | M | 121.39 | 80.31 | 1.51 | | |
| | | | NHM | 648.b. | U | 123.08 | 81.53 | 1.51 | | |
| | | | ZMB_Mam | 14737 | F | 111.77 | 73.46 | 1.52 | | |
| Bovidae | Bubalus | depressicornis | | | | | | | 1.56 | 0.01 |
| | | | NHM | 1983.2 | U | 84.47 | 54.29 | 1.56 | | |
| | | | ZMB_Mam | 14758 | M | 82.22 | 52.32 | 1.57 | | |
| Bovidae | Budorcas | taxicolor | | | | | | | 1.52 | 0.01 |
| | | | USNM | 258652 | M | 126.31 | 83.80 | 1.51 | | |
| | | | USNM | 258656 | F | 115.56 | 75.45 | 1.53 | | |
| | | | USNM | 259415 | M | 125.74 | 83.33 | 1.51 | | |
| Bovidae | Capra | caucasica | | | | | | | 1.51 | 0.00 |
| | | | NHM | 1892.31.6.1 (689.3) | M | 83.13 | 54.90 | 1.51 | | |
| | | | ZMB_Mam | 53012 | F | 70.15 | 46.49 | 1.51 | | |
| Bovidae | Capra | falconeri | | | | | | | 1.44 | -- |
| | | | ZMB_Mam | 43651 | M | 65.89 | 45.73 | 1.44 | | |
| Bovidae | Capra | ibex | | | | | | | 1.45 | -- |
| | | | ZMB_Mam | 6530 | F | 51.67 | 35.71 | 1.45 | | |
| Bovidae | Capra | nubiana | | | | | | | 1.48 | 0.01 |
| | | | ZMB_Mam | 2196 | M | 60.88 | 41.16 | 1.48 | | |
| | | | ZMB_Mam | 2197 | U | 63.69 | 42.84 | 1.49 | | |
| Bovidae | Capricornis | crispus | | | | | | | 1.53 | -- |
| | | | USNM | 13829 | M | 68.20 | 44.68 | 1.53 | | |
| Bovidae | Capricornis | milneedwardsii | | | | | | | 1.48 | 0.03 |
| | | | NHM | 1965.3.25.1 | U | 81.93 | 57.04 | 1.44 | | |
| | | | USNM | 152165 | F | 87.49 | 58.84 | 1.49 | | |
| | | | USNM | 258653 | F | 99.45 | 66.03 | 1.51 | | |
| | | | USNM | 258670 | M | 95.00 | 64.22 | 1.48 | | |

| | | | | | | | | | | |
|---|---|---|---|---|---|---|---|---|---|---|
| | | | USNM | 259025 | F | 95.59 | 64.69 | 1.48 | | |
| Bovidae | Capricornis | sumatraensis | | | | | | | 1.49 | 0.01 |
| | | | NHM | 1970.187 | U | 97.26 | 65.09 | 1.49 | | |
| | | | NHM | 1937.2.10.1 | U | 79.99 | 53.28 | 1.50 | | |
| | | | NHM | 1965.3.25.2 | U | 79.54 | 53.88 | 1.48 | | |
| Bovidae | Capricornis | swinhoei | | | | | | | 1.52 | 0.04 |
| | | | USNM | 308872 | M | 56.84 | 36.77 | 1.55 | | |
| | | | USNM | 311229 | F | 62.56 | 41.85 | 1.49 | | |
| Bovidae | Cephalophus | adersi | | | | | | | 1.55 | -- |
| | | | OM | 5338 | M | 36.17 | 23.37 | 1.55 | | |
| Bovidae | Cephalophus | dorsalis | | | | | | | 1.50 | 0.02 |
| | | | NHM | 1863.12.29.1 (1439.A.) | U | 46.50 | 30.54 | 1.52 | | |
| | | | NHM | 1936.10.28.34. | M | 48.45 | 32.00 | 1.51 | | |
| | | | NHM | 1936.10.28.35. | M | 52.91 | 35.80 | 1.48 | | |
| Bovidae | Cephalophus | leucogaster | | | | | | | 1.51 | -- |
| | | | NHM | 1950.9.23.1 | M | 49.65 | 32.90 | 1.51 | | |
| Bovidae | Cephalophus | natalensis | | | | | | | 1.56 | 0.01 |
| | | | NHM | 1936.3.30.3 | M | 44.55 | 28.44 | 1.57 | | |
| | | | NHM | 1936.3.30.5 | F | 46.36 | 30.08 | 1.54 | | |
| | | | NHM | 1948.7.19.10 | U | 46.97 | 30.02 | 1.56 | | |
| Bovidae | Cephalophus | nigrifrons | | | | | | | 1.53 | 0.01 |
| | | | NHM | 1936.10.28.32. | M | 48.67 | 31.37 | 1.55 | | |
| | | | NHM | 1936.10.28.33. | M | 48.09 | 31.23 | 1.54 | | |
| | | | NHM | 1936.12.1.61 | U | 54.95 | 35.91 | 1.53 | | |
| | | | NHM | 1950.9.23.2. | U | 47.74 | 31.39 | 1.52 | | |
| | | | NHM | 31.11.1.79 | M | 47.97 | 31.33 | 1.53 | | |
| Bovidae | Cephalophus | rufilatus | | | | | | | 1.51 | 0.03 |
| | | | NHM | 1865.5.9.9 | F | 42.01 | 27.83 | 1.51 | | |
| | | | NHM | 1928.8.2.12. | U | 46.68 | 31.63 | 1.48 | | |
| | | | ZMB_Mam | 71443 | U | 38.65 | 25.12 | 1.54 | | |
| Bovidae | Cephalophus | silvicultor | | | | | | | 1.50 | 0.01 |
| | | | NHM | 1691.8.9.80 | F | 77.38 | 52.12 | 1.48 | | |
| | | | USNM | 537289 | M | 86.09 | 57.09 | 1.51 | | |
| | | | USNM | 542447 | M | 80.42 | 53.86 | 1.49 | | |
| Bovidae | Cephalophus | zebra | | | | | | | 1.55 | 0.00 |
| | | | DMNS | 6047 | U | 45.45 | 29.30 | 1.55 | | |
| | | | NHM | 1887.9.15.2 | U | 43.86 | 28.36 | 1.55 | | |

| | | | | | | | | | | |
|---|---|---|---|---|---|---|---|---|---|---|
| Bovidae | Connochaetes | gnou | | | | | | | 1.54 | 0.03 |
| | | | NHM | 1981.802. | U | 100.19 | 63.96 | 1.57 | | |
| | | | NHM | 645.d. | F | 94.65 | 62.21 | 1.52 | | |
| Bovidae | Connochaetes | taurinus | | | | | | | 1.49 | 0.02 |
| | | | DMNS | 8106 | U | 114.21 | 76.46 | 1.49 | | |
| | | | USNM | 161974 | M | 112.93 | 76.82 | 1.47 | | |
| | | | USNM | 161976 | M | 116.54 | 78.05 | 1.49 | | |
| | | | USNM | 578576 | F | 109.00 | 72.16 | 1.51 | | |
| Bovidae | Damaliscus | korrigum | | | | | | | 1.42 | 0.01 |
| | | | USNM | 163008 | M | 98.40 | 69.50 | 1.42 | | |
| | | | USNM | 163170 | F | 99.42 | 69.44 | 1.43 | | |
| Bovidae | Damaliscus | lunatus | | | | | | | 1.45 | 0.02 |
| | | | LaSpecola | 3998 | M | 105.23 | 71.74 | 1.47 | | |
| | | | OM | 123 | U | 107.23 | 74.97 | 1.43 | | |
| | | | OM | 3564 | M | 103.21 | 71.10 | 1.45 | | |
| Bovidae | Damaliscus | pygargus | | | | | | | 1.46 | 0.01 |
| | | | OM | 129 | U | 88.11 | 60.91 | 1.45 | | |
| | | | USNM | 218725 | F | 85.15 | 58.42 | 1.46 | | |
| | | | USNM | 537290 | M | 86.46 | 58.57 | 1.48 | | |
| | | | USNM | 537649 | F | 85.51 | 58.14 | 1.47 | | |
| Bovidae | Dorcatragus | megalotis | | | | | | | 1.41 | -- |
| | | | NHM | 1895.5.2.1 | U | 47.83 | 33.88 | 1.41 | | |
| Bovidae | Eudorcas | rufifrons | | | | | | | 1.42 | 0.02 |
| | | | NHM | 39.2544 | M | 64.96 | 45.31 | 1.43 | | |
| | | | NHM | 28.8.2.7. | U | 64.84 | 45.53 | 1.42 | | |
| | | | NHM | 73.8.29.9 | U | 59.33 | 42.63 | 1.39 | | |
| | | | USNM | 252685 | M | 62.28 | 44.32 | 1.41 | | |
| | | | USNM | 252686 | M | 63.68 | 44.52 | 1.43 | | |
| | | | ZMB_Mam | 13578 | M | 61.63 | 42.97 | 1.43 | | |
| Bovidae | Eudorcas | thomsonii | | | | | | | 1.42 | 0.02 |
| | | | OM | 774 | M | 55.59 | 38.50 | 1.44 | | |
| | | | OM | 840 | F | 53.99 | 37.84 | 1.43 | | |
| | | | USNM | 162007 | M | 58.85 | 41.00 | 1.44 | | |
| | | | USNM | 163067 | F | 54.79 | 39.73 | 1.38 | | |
| | | | USNM | 164850 | U | 58.58 | 41.46 | 1.41 | | |
| | | | ZMB_Mam | 44157 | M | 61.20 | 42.49 | 1.44 | | |
| Bovidae | Gazella | bennettii | | | | | | | 1.45 | 0.03 |

| | | | | | | | | | | |
|---|---|---|---|---|---|---|---|---|---|---|
| | | | USNM | 328578 | F | 50.67 | 34.56 | 1.47 | | |
| | | | USNM | 329354 | M | 55.96 | 38.36 | 1.46 | | |
| | | | USNM | 329355 | M | 55.89 | 39.53 | 1.41 | | |
| Bovidae | Gazella | cuvieri | | | | | | | 1.46 | -- |
| | | | NHM | 1866.12.30.24 (1675.a) | U | 63.07 | 43.27 | 1.46 | | |
| Bovidae | Gazella | dorcas | | | | | | | 1.44 | 0.01 |
| | | | USNM | 241500 | M | 50.45 | 34.91 | 1.45 | | |
| | | | USNM | 325878 | M | 50.75 | 34.91 | 1.45 | | |
| | | | USNM | 395622 | M | 50.53 | 35.52 | 1.42 | | |
| | | | USNM | 395623 | F | 51.25 | 35.56 | 1.44 | | |
| | | | USNM | 575152 | F | 48.24 | 33.32 | 1.45 | | |
| Bovidae | Gazella | leptoceros | | | | | | | 1.46 | 0.01 |
| | | | DMNS | 7381 | U | 54.18 | 36.87 | 1.47 | | |
| | | | NHM | 1936.3.26.1 | M | 56.08 | 38.63 | 1.45 | | |
| Bovidae | Gazella | spekei | | | | | | | 1.43 | 0.02 |
| | | | NHM | 1935.12.13.2 | F | 57.83 | 39.46 | 1.47 | | |
| | | | NHM | 1935.12.13.4 | F | 58.20 | 41.02 | 1.42 | | |
| | | | NHM | 96.10.6.1. | U | 54.70 | 38.43 | 1.42 | | |
| | | | USNM | 581995 | F | 47.69 | 33.62 | 1.42 | | |
| | | | USNM | 582089 | F | 49.59 | 34.20 | 1.45 | | |
| | | | USNM | 588207 | F | 47.06 | 33.61 | 1.40 | | |
| Bovidae | Gazella | subgutturosa | | | | | | | 1.42 | 0.01 |
| | | | NHM | 1890.4.20.1 (1702.g.) | F | 62.52 | 44.19 | 1.41 | | |
| | | | NHM | 1897.1.14.6 | M | 51.30 | 36.09 | 1.42 | | |
| | | | NHM | 1897.1.14.7 | F | 52.37 | 36.36 | 1.44 | | |
| | | | NHM | 97.1.14.9 | F | 51.44 | 36.48 | 1.41 | | |
| | | | USNM | 240691 | M | 62.80 | 43.71 | 1.44 | | |
| | | | USNM | 240693 | M | 63.41 | 44.81 | 1.42 | | |
| Bovidae | Hemitragus | hylocrius | | | | | | | 1.46 | -- |
| | | | NHM | 1936.3.2.1 | M | 70.18 | 48.19 | 1.46 | | |
| Bovidae | Hemitragus | jemlahicus | | | | | | | 1.44 | 0.01 |
| | | | DMNS | 6818 | U | 69.04 | 47.52 | 1.45 | | |
| | | | NHM | 886.p | M | 75.39 | 52.56 | 1.43 | | |
| | | | USNM | 143864 | M | 83.60 | 58.67 | 1.42 | | |
| | | | USNM | 251850 | M | 72.28 | 49.98 | 1.45 | | |
| Bovidae | Hippotragus | equinus | | | | | | | 1.51 | 0.05 |
| | | | LaSpecola | 829 | M | 133.70 | 90.00 | 1.49 | | |

| | | | | | | | | | | |
|---|---|---|---|---|---|---|---|---|---|---|
| | | | OM | 1528 | F | 120.89 | 76.79 | 1.57 | | |
| | | | ZMB_Mam | 67967 | M | 137.58 | 90.84 | 1.51 | | |
| | | | ZMB_Mam | 68009 | U | 137.69 | 94.11 | 1.46 | | |
| | Bovidae | Hippotragus | niger | | | | | | 1.51 | 0.02 |
| | | | NHM | 1964.7.8.1 | F | 112.22 | 73.85 | 1.52 | | |
| | | | OM | 7330 | U | 119.12 | 79.08 | 1.51 | | |
| | | | USNM | 21638 | M | 126.53 | 84.18 | 1.50 | | |
| | | | USNM | 252518 | M | 119.85 | 80.22 | 1.49 | | |
| | | | USNM | 396597 | F | 101.14 | 65.93 | 1.53 | | |
| | Bovidae | Kobus | ellipsiprymnus | | | | | | 1.48 | 0.02 |
| | | | OM | 876 | F | 109.36 | 73.12 | 1.50 | | |
| | | | OM | 909 | F | 120.92 | 81.74 | 1.48 | | |
| | | | OM | 910 | M | 118.36 | 79.86 | 1.48 | | |
| | | | OM | 2266 | U | 119.21 | 82.87 | 1.44 | | |
| | | | OM | 7768 | U | 112.72 | 76.67 | 1.47 | | |
| | | | ZMB_Mam | 68128 | U | 120.25 | 80.22 | 1.50 | | |
| | | | ZMB_Mam | 77169 | F | 85.55 | 58.10 | 1.47 | | |
| | Bovidae | Kobus | kob | | | | | | 1.50 | 0.03 |
| | | | NHM | 1934.5.1.12 | M | 92.26 | 61.94 | 1.49 | | |
| | | | NHM | 28.8.2.6 | M | 88.38 | 59.21 | 1.49 | | |
| | | | NHM | 79.6.23.4 | M | 81.48 | 55.80 | 1.46 | | |
| | | | OM | 915 | U | 92.91 | 61.99 | 1.50 | | |
| | | | ZMB_Mam | 16577 | M | 82.55 | 53.65 | 1.54 | | |
| | Bovidae | Kobus | leche | | | | | | 1.50 | 0.01 |
| | | | NHM | 69.1147 | U | 99.86 | 66.17 | 1.51 | | |
| | | | NHM | 70.103 | U | 95.09 | 63.65 | 1.49 | | |
| | | | OM | 913 | M | 90.94 | 61.01 | 1.49 | | |
| | Bovidae | Kobus | megaceros | | | | | | 1.48 | -- |
| | | | NHM | 1934.5.1.9. | M | 91.95 | 62.31 | 1.48 | | |
| | Bovidae | Kobus | vardonii | | | | | | 1.52 | 0.01 |
| | | | NHM | 62.799 | F | 83.66 | 55.03 | 1.52 | | |
| | | | NHM | 62.801 | M | 84.22 | 55.16 | 1.53 | | |
| | | | NHM | 62.803 | M | 84.52 | 56.01 | 1.51 | | |
| | Bovidae | Litocranius | walleri | | | | | | 1.41 | 0.01 |
| | | | DMNS | 14514 | U | 73.07 | 51.80 | 1.41 | | |
| | | | DMNS | 15682 | U | 69.46 | 48.90 | 1.42 | | |
| | | | USNM | 164033 | F | 72.04 | 51.19 | 1.41 | | |

| | | | | | | | | | | |
|---|---|---|---|---|---|---|---|---|---|---|
| | | | USNM | 164034 | M | 75.41 | 53.52 | 1.41 | | |
| | | | USNM | 164035 | F | 71.39 | 50.42 | 1.42 | | |
| Bovidae | Madoqua | guentheri | | | | | | | 1.48 | 0.03 |
| | | | OM | 5341 | M | 33.10 | 22.11 | 1.50 | | |
| | | | OM | 5343 | F | 35.21 | 24.31 | 1.45 | | |
| | | | USNM | 589450 | M | 34.36 | 22.86 | 1.50 | | |
| Bovidae | Madoqua | kirkii | | | | | | | 1.54 | 0.02 |
| | | | NHM | 1932.6.6.46. | F | 38.44 | 24.93 | 1.54 | | |
| | | | NHM | 1932.6.6.49. | F | 38.09 | 25.06 | 1.52 | | |
| | | | NHM | 1932.6.6.51. | M | 37.41 | 23.76 | 1.57 | | |
| | | | NHM | 1936.5.28.1. | F | 37.17 | 24.58 | 1.51 | | |
| | | | USNM | 163039 | M | 38.42 | 24.64 | 1.56 | | |
| | | | USNM | 396306 | F | 37.78 | 24.54 | 1.54 | | |
| | | | USNM | 538104 | F | 36.45 | 23.76 | 1.53 | | |
| Bovidae | Madoqua | piacentinii | | | | | | | 1.47 | 0.04 |
| | | | LaSpecola | 6389 | F | 29.49 | 20.40 | 1.45 | | |
| | | | LaSpecola | 9822 | M | 27.68 | 18.42 | 1.50 | | |
| Bovidae | Madoqua | saltiana | | | | | | | 1.50 | 0.03 |
| | | | LaSpecola | 1903 | U | 29.41 | 19.53 | 1.51 | | |
| | | | LaSpecola | 3534 | F | 29.93 | 19.87 | 1.51 | | |
| | | | LaSpecola | 4138 | F | 27.93 | 18.72 | 1.49 | | |
| | | | LaSpecola | 5541 | F | 31.73 | 20.83 | 1.52 | | |
| | | | LaSpecola | 5543 | M | 30.06 | 20.63 | 1.46 | | |
| | | | LaSpecola | 5545 | M | 30.13 | 20.06 | 1.50 | | |
| | | | LaSpecola | 18850 | F | 29.94 | 20.39 | 1.47 | | |
| | | | OM | 7338 | M | 32.75 | 21.29 | 1.54 | | |
| Bovidae | Naemorhedus | goral | | | | | | | 1.47 | 0.02 |
| | | | ZMB_Mam | 14451 | U | 61.35 | 42.13 | 1.46 | | |
| | | | ZMB_Mam | 70035 | F | 62.80 | 43.50 | 1.44 | | |
| | | | ZMB_Mam | 70721 | F | 65.36 | 44.03 | 1.48 | | |
| | | | ZMB_Mam | 83318 | F | 61.86 | 41.47 | 1.49 | | |
| Bovidae | Naemorhedus | griseus | | | | | | | 1.50 | 0.04 |
| | | | USNM | 258674 | F | 67.63 | 46.22 | 1.46 | | |
| | | | USNM | 259023 | F | 68.21 | 44.37 | 1.54 | | |
| | | | USNM | 259398 | M | 64.21 | 42.81 | 1.50 | | |
| Bovidae | Nanger | dama | | | | | | | 1.43 | 0.02 |
| | | | LaSpecola | 22316 | U | 78.38 | 55.46 | 1.41 | | |

| | | | | | | | | | | |
|---|---|---|---|---|---|---|---|---|---|---|
| | | | USNM | 543093 | M | 86.22 | 60.17 | 1.43 | | |
| | | | USNM | 578578 | F | 85.83 | 60.58 | 1.42 | | |
| | | | USNM | 599686 | M | 84.42 | 58.37 | 1.45 | | |
| Bovidae | Nanger | granti | | | | | | | 1.42 | 0.02 |
| | | | OM | 810 | U | 83.75 | 59.31 | 1.41 | | |
| | | | OM | 814 | F | 78.66 | 55.12 | 1.43 | | |
| | | | OM | 6272 | U | 83.19 | 60.17 | 1.38 | | |
| | | | USNM | 162013 | M | 87.80 | 60.27 | 1.46 | | |
| | | | USNM | 163083 | M | 79.45 | 55.83 | 1.42 | | |
| | | | USNM | 164655 | F | 77.79 | 54.29 | 1.43 | | |
| Bovidae | Nanger | soemmerringii | | | | | | | 1.43 | 0.02 |
| | | | NHM | 1935.12.12.9. | U | 72.72 | 51.14 | 1.42 | | |
| | | | NHM | 1935.12.13.1. | M | 78.05 | 55.60 | 1.40 | | |
| | | | USNM | 582229 | M | 73.83 | 51.15 | 1.44 | | |
| | | | ZMB_Mam | 77205 | F | 70.74 | 48.90 | 1.45 | | |
| | | | ZMB_Mam | 77223 | M | 79.94 | 55.50 | 1.44 | | |
| Bovidae | Neotragus | batesi | | | | | | | 1.51 | 0.01 |
| | | | NHM | 1981.796 | M | 28.58 | 18.79 | 1.52 | | |
| | | | NHM | 1936.10.28.36 | M | 28.83 | 19.15 | 1.51 | | |
| | | | NHM | 1937.8.4.26. | U | 29.87 | 19.92 | 1.50 | | |
| | | | NHM | 1937.8.4.27 | U | 25.79 | 17.17 | 1.50 | | |
| Bovidae | Neotragus | moschatus | | | | | | | 1.50 | 0.04 |
| | | | NHM | 1936.3.30.3 | F | 33.38 | 22.68 | 1.47 | | |
| | | | NHM | 1962.12.14.5 | M | 31.72 | 20.59 | 1.54 | | |
| | | | OM | 2570 | F | 28.93 | 19.24 | 1.50 | | |
| | | | OM | 5457 | F | 32.49 | 21.13 | 1.54 | | |
| | | | OM | 7597 | M | 32.09 | 22.21 | 1.44 | | |
| Bovidae | Neotragus | pygmaeus | | | | | | | 1.54 | -- |
| | | | USNM | 429835 | M | 25.10 | 16.34 | 1.54 | | |
| Bovidae | Oreamnos | americanus | | | | | | | 1.52 | 0.04 |
| | | | DMNS | 7738 | U | 83.16 | 52.86 | 1.57 | | |
| | | | USNM | 319790 | F | 77.05 | 51.76 | 1.49 | | |
| | | | ZMB_Mam | 67805 | U | 79.43 | 53.76 | 1.48 | | |
| | | | ZMB_Mam | 83324 | M | 77.64 | 51.00 | 1.52 | | |
| Bovidae | Oreotragus | oreotragus | | | | | | | 1.50 | 0.05 |
| | | | OM | 2220 | M | 47.08 | 30.69 | 1.53 | | |
| | | | USNM | 163024 | M | 48.25 | 33.77 | 1.43 | | |

| | | | | | | | | | | |
|---|---|---|---|---|---|---|---|---|---|---|
| | | | USNM | 314958 | M | 48.94 | 33.09 | 1.48 | | |
| | | | USNM | 589129 | U | 49.54 | 31.99 | 1.55 | | |
| Bovidae | Oryx | beisa | | | | | | | 1.51 | 0.02 |
| | | | OM | 1529 | M | 115.10 | 77.62 | 1.48 | | |
| | | | OM | 1531 | M | 102.37 | 67.03 | 1.53 | | |
| | | | OM | 2493 | U | 114.26 | 76.30 | 1.50 | | |
| | | | USNM | 163215 | M | 108.07 | 71.92 | 1.50 | | |
| | | | USNM | 267605 | M | 105.96 | 68.71 | 1.54 | | |
| Bovidae | Oryx | dammah | | | | | | | 1.47 | 0.02 |
| | | | USNM | 575162 | F | 98.78 | 66.53 | 1.48 | | |
| | | | USNM | A 35256 | U | 94.60 | 63.65 | 1.49 | | |
| | | | ZMB_Mam | 70822 | F | 98.96 | 68.36 | 1.45 | | |
| Bovidae | Oryx | gazella | | | | | | | 1.44 | 0.03 |
| | | | ZMB_Mam | 16029 | F | 90.34 | 63.46 | 1.42 | | |
| | | | ZMB_Mam | 77257 | M | 91.51 | 62.48 | 1.46 | | |
| Bovidae | Oryx | leucoryx | | | | | | | 1.49 | 0.02 |
| | | | USNM | 282796 | M | 77.99 | 51.23 | 1.52 | | |
| | | | USNM | 580353 | M | 88.25 | 59.40 | 1.49 | | |
| | | | USNM | 581996 | F | 88.85 | 59.79 | 1.49 | | |
| | | | ZMB_Mam | 14730 | U | 96.06 | 64.82 | 1.48 | | |
| Bovidae | Ourebia | ourebi | | | | | | | 1.47 | 0.01 |
| | | | OM | 2232 | F | 54.29 | 37.13 | 1.46 | | |
| | | | OM | 2234 | U | 54.97 | 37.70 | 1.46 | | |
| | | | USNM | 163243 | M | 53.39 | 35.73 | 1.49 | | |
| | | | USNM | 163244 | M | 60.22 | 41.06 | 1.47 | | |
| | | | USNM | 164711 | M | 54.50 | 36.80 | 1.48 | | |
| Bovidae | Ovibos | moschatus | | | | | | | 1.48 | 0.04 |
| | | | NHM | 16.3.28.3 | U | 104.69 | 72.03 | 1.45 | | |
| | | | ZMB_Mam | 8048 | F | 98.17 | 63.87 | 1.54 | | |
| | | | ZMB_Mam | 14789 | M | 118.15 | 81.59 | 1.45 | | |
| | | | ZMB_Mam | 67804 | U | 113.62 | 77.04 | 1.47 | | |
| Bovidae | Ovis | ammon | | | | | | | 1.46 | 0.05 |
| | | | NHM | 1898.2.6.9 | U | 99.62 | 69.66 | 1.43 | | |
| | | | ZMB_Mam | 83438 | F | 64.24 | 42.99 | 1.49 | | |
| Bovidae | Ovis | canadensis | | | | | | | 1.48 | 0.01 |
| | | | DMNS | 6898 | U | 85.06 | 57.19 | 1.49 | | |
| | | | DMNS | 10977 | U | 82.93 | 56.73 | 1.46 | | |

| | | | | | | | | | | |
|---|---|---|---|---|---|---|---|---|---|---|
| | | | DMNS | 12667 | U | 78.47 | 52.84 | 1.49 | | |
| Bovidae | Ovis | dalli | | | | | | | 1.46 | 0.01 |
| | | | DMNS | 187 | U | 82.82 | 57.04 | 1.45 | | |
| | | | DMNS | 17530 | U | 68.88 | 46.87 | 1.47 | | |
| Bovidae | Pantholops | hodgsonii | | | | | | | 1.46 | 0.02 |
| | | | NHM | 1970.191 | U | 65.14 | 45.30 | 1.44 | | |
| | | | NHM | 614.c | U | 67.39 | 45.98 | 1.47 | | |
| | | | USNM | 62086 | F | 59.24 | 40.07 | 1.48 | | |
| Bovidae | Philantomba | monticola | | | | | | | 1.55 | 0.02 |
| | | | DMNS | 14752 | U | 27.72 | 17.92 | 1.55 | | |
| | | | NHM | 1901.8.9.132. | F | 30.70 | 20.19 | 1.52 | | |
| | | | NHM | 1936.10.28.28. | M | 34.33 | 22.39 | 1.53 | | |
| | | | NHM | 1936.10.28.29. | M | 32.89 | 20.84 | 1.58 | | |
| | | | NHM | 1936.10.28.30. | F | 35.25 | 22.46 | 1.57 | | |
| | | | NHM | 1936.10.28.31. | F | 33.88 | 21.83 | 1.55 | | |
| | | | OM | 5339 | U | 35.91 | 23.46 | 1.53 | | |
| Bovidae | Pseudois | nayaur | | | | | | | 1.44 | 0.00 |
| | | | NHM | 70.19 | U | 69.56 | 48.28 | 1.44 | | |
| | | | NHM | 66.8.c | U | 73.23 | 50.65 | 1.45 | | |
| | | | ZMB_Mam | 68734 | U | 70.08 | 48.50 | 1.44 | | |
| Bovidae | Raphicerus | campestris | | | | | | | 1.44 | 0.10 |
| | | | OM | 2250 | F | 45.04 | 30.49 | 1.48 | | |
| | | | OM | 2251 | M | 46.15 | 30.89 | 1.49 | | |
| | | | USNM | 161981 | M | 41.89 | 33.07 | 1.27 | | |
| | | | USNM | 161983 | M | 49.11 | 33.44 | 1.47 | | |
| | | | USNM | 586524 | U | 50.45 | 34.09 | 1.48 | | |
| Bovidae | Raphicerus | melanotis | | | | | | | 1.50 | -- |
| | | | NHM | 1862.3.19.13. (994.B.) | F | 48.30 | 32.17 | 1.50 | | |
| Bovidae | Raphicerus | sharpei | | | | | | | 1.52 | 0.02 |
| | | | OM | 2254 | M | 41.03 | 27.35 | 1.50 | | |
| | | | USNM | 367434 | M | 41.31 | 27.22 | 1.52 | | |
| | | | USNM | 367445 | M | 38.43 | 24.90 | 1.54 | | |
| Bovidae | Redunca | arundinum | | | | | | | 1.53 | -- |
| | | | NHM | 1966.7.19.1 | U | 93.89 | 61.34 | 1.53 | | |
| Bovidae | Redunca | fulvorufula | | | | | | | 1.44 | 0.02 |
| | | | NHM | 1936.3.30.9. | M | 62.68 | 43.04 | 1.46 | | |
| | | | ZMB_Mam | 70097 | M | 67.33 | 47.21 | 1.43 | | |

| | | | | | | | | | | |
|---|---|---|---|---|---|---|---|---|---|---|
| | | | ZMB_Mam | 70511 | F? | 70.75 | 48.81 | 1.45 | | |
| Bovidae | Redunca | redunca | | | | | | | 1.47 | 0.03 |
| | | | NHM | 1934.5.1.7. | M | 77.19 | 52.74 | 1.46 | | |
| | | | NHM | 1960.11.10.1. | F | 73.88 | 50.56 | 1.46 | | |
| | | | NHM | 1962.12.14.7. | F | 77.68 | 52.40 | 1.48 | | |
| | | | NHM | 28.8.2.5. | U | 80.36 | 54.12 | 1.48 | | |
| | | | OM | 901 | U | 78.44 | 52.26 | 1.50 | | |
| | | | OM | 902 | M | 78.64 | 54.51 | 1.44 | | |
| | | | OM | 7117 | M | 77.69 | 54.48 | 1.43 | | |
| Bovidae | Rupicapra | rupicapra | | | | | | | 1.46 | 0.01 |
| | | | LaSpecola | 3927 | M | 66.99 | 45.86 | 1.46 | | |
| | | | NHM | 1886.12.27.1 (631.q.) | U | 74.36 | 50.12 | 1.48 | | |
| | | | NHM | 1892.3.16.8 (631.u.) | M | 71.69 | 49.47 | 1.45 | | |
| | | | ZMB_Mam | 70531 | U | 60.63 | 41.37 | 1.47 | | |
| Bovidae | Saiga | tatarica | | | | | | | 1.48 | 0.03 |
| | | | USNM | 304688 | F | 56.10 | 38.59 | 1.45 | | |
| | | | ZMB_Mam | 14741 | M | 65.76 | 44.31 | 1.48 | | |
| | | | ZMB_Mam | 46558 | M | 58.01 | 39.67 | 1.46 | | |
| | | | ZMB_Mam | 55370 | M | 60.96 | 39.91 | 1.53 | | |
| | | | ZMB_Mam | 61578 | F | 59.01 | 39.47 | 1.50 | | |
| Bovidae | Sylvicapra | grimmia | | | | | | | 1.48 | 0.01 |
| | | | OM | 261 | M | 49.60 | 33.59 | 1.48 | | |
| | | | OM | 778 | U | 51.29 | 34.33 | 1.49 | | |
| | | | OM | 792 | M | 49.07 | 33.36 | 1.47 | | |
| | | | USNM | 161979 | F | 50.42 | 33.93 | 1.49 | | |
| | | | USNM | 367409 | F | 55.53 | 38.12 | 1.46 | | |
| | | | USNM | 586526 | U | 55.05 | 36.95 | 1.49 | | |
| Bovidae | Syncerus | caffer | | | | | | | 1.58 | 0.02 |
| | | | DMNS | 9977 | U | 151.92 | 97.40 | 1.56 | | |
| | | | OM | 498 | F | 155.92 | 98.69 | 1.58 | | |
| | | | OM | 500 | M | 155.19 | 99.33 | 1.56 | | |
| | | | OM | 540 | U | 144.91 | 91.74 | 1.58 | | |
| | | | OM | 5542 | F | 134.34 | 82.85 | 1.62 | | |
| Bovidae | Taurotragus | derbianus | | | | | | | 1.48 | 0.02 |
| | | | NHM | 1934.5.16 | M | 168.84 | 115.55 | 1.46 | | |
| | | | OM | 2265 | U | 161.35 | 109.86 | 1.47 | | |
| | | | OM | 6331 | U | 158.79 | 105.60 | 1.50 | | |

| | | | | | | | | | | | |
|---|---|---|---|---|---|---|---|---|---|---|---|
| Bovidae | Taurotragus | oryx | | | | | | | 1.52 | 0.03 |
| | | | DMNS | 16381 | U | 159.08 | 108.35 | 1.47 | | |
| | | | OM | 942 | F | 139.54 | 90.19 | 1.55 | | |
| | | | OM | 945 | U | 145.09 | 94.15 | 1.54 | | |
| | | | OM | 946 | F | 134.46 | 87.72 | 1.53 | | |
| | | | OM | 4299 | F | 145.31 | 94.97 | 1.53 | | |
| Bovidae | Tetracerus | quadricornis | | | | | | | 1.43 | -- |
| | | | NHM | 1858.5.4.41. (628.h.) | U | 60.67 | 42.29 | 1.43 | | |
| Bovidae | Tragelaphus | angasii | | | | | | | 1.45 | 0.04 |
| | | | DMNS | 6817 | U | 100.78 | 69.69 | 1.45 | | |
| | | | NHM | 1936.3.30.1. | M | 102.94 | 72.81 | 1.41 | | |
| | | | NHM | 1936.3.30.2 | F | 84.72 | 59.20 | 1.43 | | |
| | | | USNM | 258851 | F | 83.04 | 55.05 | 1.51 | | |
| Bovidae | Tragelaphus | eurycerus | | | | | | | 1.53 | 0.02 |
| | | | DMNS | 7821 | U | 138.51 | 91.68 | 1.51 | | |
| | | | USNM | 163226 | F | 119.32 | 78.32 | 1.52 | | |
| | | | USNM | 396015 | M | 131.23 | 84.48 | 1.55 | | |
| | | | USNM | 542466 | F | 132.64 | 86.83 | 1.53 | | |
| Bovidae | Tragelaphus | imberbis | | | | | | | 1.49 | 0.00 |
| | | | LaSpecola | 3994 | M | 91.61 | 61.64 | 1.49 | | |
| | | | NHM | 1935.12.13.7 | U | 102.16 | 68.50 | 1.49 | | |
| | | | NHM | 35.7.24.4 | M | 98.83 | 66.13 | 1.49 | | |
| Bovidae | Tragelaphus | scriptus | | | | | | | 1.47 | 0.05 |
| | | | OM | 935 | M | 85.95 | 58.49 | 1.47 | | |
| | | | OM | 6606 | M | 76.76 | 50.01 | 1.53 | | |
| | | | OM | 7149 | F | 71.23 | 48.44 | 1.47 | | |
| | | | USNM | 164500 | F | 72.84 | 48.67 | 1.50 | | |
| | | | USNM | 164560 | M | 86.48 | 61.78 | 1.40 | | |
| Bovidae | Tragelaphus | spekii | | | | | | | 1.49 | 0.03 |
| | | | NHM | 73.11 | U | 90.97 | 62.16 | 1.46 | | |
| | | | NHM | 1.8.9.82 | M | 103.84 | 70.75 | 1.47 | | |
| | | | NHM | 1882.7.24.11. (1989.c.) | U | 100.60 | 67.07 | 1.50 | | |
| | | | NHM | 1929.1.1.28 | U | 87.40 | 58.34 | 1.50 | | |
| | | | NHM | 1929.1.1.31. | F | 73.57 | 47.78 | 1.54 | | |
| | | | NHM | 1967.8.18.1. | U | 98.47 | 66.08 | 1.49 | | |
| | | | OM | 1895 | U | 82.32 | 56.67 | 1.45 | | |
| | | | USNM | 164558 | M | 91.34 | 60.59 | 1.51 | | |

| | | | | | | | | | | |
|---|---|---|---|---|---|---|---|---|---|---|
| Bovidae | Tragelaphus | strepsiceros | | | | | | | 1.47 | 0.02 |
| | | | OM | 7764 | M | 133.91 | 90.19 | 1.48 | | |
| | | | USNM | 21652 | F | 127.41 | 85.18 | 1.50 | | |
| | | | USNM | 21655 | F | 116.13 | 80.27 | 1.45 | | |
| | | | USNM | 163320 | M | 131.97 | 89.94 | 1.47 | | |
| Camelidae | Camelus | dromedarius | | | | | | | 1.65 | 0.02 |
| | | | DMNS | 15684 | U | 156.93 | 95.76 | 1.64 | | |
| | | | DMNS | 17550 | U | 147.01 | 88.04 | 1.67 | | |
| Camelidae | Vicugna | vicugna | | | | | | | 1.54 | 0.05 |
| | | | LaSpecola | 1443 | M | 86.36 | 55.98 | 1.54 | | |
| | | | NHM | 1861.1.18.3 (675.c) | M | 60.37 | 38.09 | 1.58 | | |
| | | | ZMB_Mam | 56204 | M | 70.54 | 47.52 | 1.48 | | |
| Cervidae | Alces | alces | | | | | | | 1.48 | 0.03 |
| | | | NHM | 1850.11.22.72 (703.h.) | M | 152.01 | 101.76 | 1.49 | | |
| | | | NHM | 1851.11.10.3 (703.i.) | F | 143.42 | 95.65 | 1.50 | | |
| | | | NHM | 1951.6.4.1 | M | 162.14 | 107.97 | 1.50 | | |
| | | | ZMB_Mam | 7155 | U | 153.53 | 107.66 | 1.43 | | |
| | | | ZMB_Mam | 62663 | M | 168.51 | 114.56 | 1.47 | | |
| Cervidae | Alces | americanus | | | | | | | 1.49 | 0.02 |
| | | | USNM | 275127 | M | 163.98 | 109.11 | 1.50 | | |
| | | | USNM | A 12758 | M | 160.12 | 108.46 | 1.48 | | |
| Cervidae | Axis | axis | | | | | | | 1.47 | 0.03 |
| | | | DMNS | 6800 | U | 80.90 | 55.49 | 1.46 | | |
| | | | ZMB_Mam | 2050 | F | 61.01 | 42.16 | 1.45 | | |
| | | | ZMB_Mam | 77166 | F | 74.10 | 49.18 | 1.51 | | |
| Cervidae | Axis | porcinus | | | | | | | 1.50 | 0.01 |
| | | | NHM | 1858.12.16.2 (698s) | U | 64.91 | 43.64 | 1.49 | | |
| | | | ZMB_Mam | 6667 | F | 66.23 | 44.17 | 1.50 | | |
| | | | ZMB_Mam | 14817 | F | 62.03 | 41.01 | 1.51 | | |
| Cervidae | Blastocerus | dichotomus | | | | | | | 1.46 | 0.02 |
| | | | DMNS | 2579 | U | 67.63 | 46.89 | 1.44 | | |
| | | | USNM | 261017 | M | 106.22 | 72.57 | 1.46 | | |
| | | | USNM | 261018 | F | 97.32 | 66.03 | 1.47 | | |
| Cervidae | Capreolus | capreolus | | | | | | | 1.48 | 0.03 |
| | | | LaSpecola | 9731 | M | 68.57 | 46.78 | 1.47 | | |
| | | | LaSpecola | 9817 | M | 61.11 | 41.77 | 1.46 | | |
| | | | LaSpecola | 9876 | M | 65.83 | 44.81 | 1.47 | | |

| | | | | | | | | | | |
|---|---|---|---|---|---|---|---|---|---|---|
| | | | ZMB_Mam | 43119 | U | 56.99 | 37.39 | 1.52 | | |
| Cervidae | Capreolus | pygargus | | | | | | | 1.46 | 0.01 |
| | | | ZMB_Mam | 97904 | M | 71.73 | 49.07 | 1.46 | | |
| | | | ZMB_Mam | 97907 | F | 66.56 | 45.81 | 1.45 | | |
| Cervidae | Cervus | elaphus | | | | | | | 1.50 | 0.02 |
| | | | USNM | 251054 | M | 136.94 | 90.27 | 1.52 | | |
| | | | USNM | A 13973 | M | 151.12 | 99.39 | 1.52 | | |
| | | | USNM | A 49424 | M | 143.15 | 95.39 | 1.50 | | |
| | | | ZMB_Mam | 17910 | F | 99.01 | 65.37 | 1.51 | | |
| | | | ZMB_Mam | 31246a | M | 130.06 | 88.68 | 1.47 | | |
| Cervidae | Dama | dama | | | | | | | 1.44 | 0.05 |
| | | | DMNS | 9311 | U | 84.73 | 57.10 | 1.48 | | |
| | | | USNM | 197040 | M | 77.73 | 56.50 | 1.38 | | |
| | | | ZMB_Mam | 34544 | M | 84.96 | 58.56 | 1.45 | | |
| | | | ZMB_Mam | 94751 | F | 88.06 | 60.23 | 1.46 | | |
| Cervidae | Elaphodus | cephalophus | | | | | | | 1.48 | 0.01 |
| | | | NHM | 1970.186 | U | 56.69 | 37.86 | 1.50 | | |
| | | | NHM | 1878.11.14.4 (1699.b.) | U | 56.11 | 37.98 | 1.48 | | |
| | | | ZMB_Mam | 70004 | F | 60.50 | 41.18 | 1.47 | | |
| | | | ZMB_Mam | 86277 | F | 57.11 | 38.88 | 1.47 | | |
| Cervidae | Elaphurus | davidianus | | | | | | | 1.51 | 0.02 |
| | | | NHM | 1929.7.3.1 | M | 122.51 | 82.49 | 1.49 | | |
| | | | USNM | 307612 | F | 108.15 | 71.84 | 1.51 | | |
| | | | USNM | 396592 | M | 116.99 | 77.69 | 1.51 | | |
| | | | ZMB_Mam | 67527 | M | 123.75 | 81.62 | 1.52 | | |
| | | | ZMB_Mam | 77243 | M | 122.32 | 79.37 | 1.54 | | |
| Cervidae | Hippocamelus | antisensis | | | | | | | 1.50 | -- |
| | | | NHM | 1934.9.2.189 | F | 75.61 | 50.37 | 1.50 | | |
| Cervidae | Hippocamelus | bisulcus | | | | | | | 1.42 | -- |
| | | | USNM | 92167 | F | 87.13 | 61.24 | 1.42 | | |
| Cervidae | Hydropotes | inermis | | | | | | | 1.53 | 0.01 |
| | | | USNM | 290513 | U | 48.47 | 31.56 | 1.54 | | |
| | | | USNM | 304664 | U | 46.45 | 30.24 | 1.54 | | |
| | | | ZMB_Mam | 65432 | F | 48.83 | 32.10 | 1.52 | | |
| Cervidae | Mazama | americana | | | | | | | 1.46 | 0.04 |
| | | | NHM | 1878.8.31.13 (1700.a.) | F | 65.98 | 44.27 | 1.49 | | |
| | | | USNM | 269164 | F | 52.90 | 36.81 | 1.44 | | |

| | | | | | | | | | | |
|---|---|---|---|---|---|---|---|---|---|---|
| Cervidae | Mazama | gouazoubira | | | | | | | 1.48 | 0.04 |
| | | | DMNS | 2586 | U | 62.88 | 41.37 | 1.52 | | |
| | | | USNM | 236649 | M | 52.91 | 36.62 | 1.44 | | |
| | | | USNM | 251747 | M | 49.56 | 33.65 | 1.47 | | |
| Cervidae | Mazama | temama | | | | | | | 1.49 | -- |
| | | | DMNS | 6474 | U | 54.72 | 36.85 | 1.49 | | |
| Cervidae | Muntiacus | muntjak | | | | | | | 1.50 | 0.03 |
| | | | NHM | 1894.6.12.11 | M | 54.07 | 35.64 | 1.52 | | |
| | | | NHM | 1895.5.7.6 | U | 52.19 | 35.16 | 1.48 | | |
| | | | NHM | 701.y. | M | 45.38 | 29.55 | 1.54 | | |
| | | | ZMB_Mam | 46530 | F | 57.08 | 39.11 | 1.46 | | |
| Cervidae | Muntiacus | reevesi | | | | | | | 1.49 | 0.09 |
| | | | NHM | 84.1247 | U | 46.69 | 31.52 | 1.48 | | |
| | | | NHM | 1985.747 | U | 47.43 | 31.31 | 1.51 | | |
| | | | NHM | 1997.269 | M | 48.88 | 32.06 | 1.52 | | |
| | | | NHM | 2006.685 | F | 38.43 | 29.21 | 1.32 | | |
| | | | NHM | 1862.12.23.2 (1524.a.) | M | 37.20 | 24.07 | 1.55 | | |
| | | | NHM | 1872.9.3.8 (1524.b.) | U | 49.70 | 32.35 | 1.54 | | |
| Cervidae | Odocoileus | hemionus | | | | | | | 1.44 | 0.00 |
| | | | DMNS | 7752 | U | 90.46 | 62.75 | 1.44 | | |
| | | | DMNS | 11018 | U | 101.95 | 71.02 | 1.44 | | |
| Cervidae | Odocoileus | virginianus | | | | | | | 1.44 | 0.03 |
| | | | DMNS | 2604 | U | 82.29 | 57.56 | 1.43 | | |
| | | | DMNS | 7438 | U | 85.22 | 58.96 | 1.45 | | |
| | | | NHM | 1850.11.22.25 (681.j) | U | 79.29 | 56.01 | 1.42 | | |
| | | | NHM | 1851.11.10.6 (681.r.) | U | 84.27 | 56.80 | 1.48 | | |
| | | | ZMB_Mam | 8553 | U | 68.20 | 47.70 | 1.43 | | |
| Cervidae | Ozotoceros | bezoarticus | | | | | | | 1.45 | 0.04 |
| | | | NHM | 54.8.16.1 (686.c.) | U | 70.72 | 49.53 | 1.43 | | |
| | | | NHM | 61.11.15.2 (686.j.) | F | 71.56 | 49.24 | 1.45 | | |
| | | | NHM | 686.k | F | 55.51 | 37.98 | 1.46 | | |
| | | | USNM | 270379 | F | 66.78 | 46.85 | 1.43 | | |
| | | | USNM | 270380 | M | 66.41 | 47.29 | 1.40 | | |
| | | | ZMB_Mam | 2055 | M | 69.26 | 46.00 | 1.51 | | |
| Cervidae | Pudu | mephistophiles | | | | | | | 1.51 | 0.01 |
| | | | USNM | 282141 | M | 35.63 | 23.73 | 1.50 | | |
| | | | USNM | 309045 | F | 36.70 | 24.17 | 1.52 | | |

| | | | | | | | | | | |
|---|---|---|---|---|---|---|---|---|---|---|
| | | | ZMB_Mam | 54389 | F | 37.15 | 24.71 | 1.50 | | |
| | | | ZMB_Mam | 61582 | F | 36.74 | 24.13 | 1.52 | | |
| Cervidae | Pudu | puda | | | | | | | 1.48 | 0.02 |
| | | | USNM | 580352 | F | 41.27 | 27.29 | 1.51 | | |
| | | | USNM | 582443 | F | 41.91 | 28.37 | 1.48 | | |
| | | | USNM | 582917 | F | 40.64 | 27.63 | 1.47 | | |
| | | | ZMB_Mam | 9152 | M | 42.76 | 29.00 | 1.47 | | |
| Cervidae | Rangifer | tarandus | | | | | | | 1.47 | 0.03 |
| | | | NHM | 1855.5.14.2 (702.w.) | U | 101.26 | 69.58 | 1.46 | | |
| | | | NHM | 1881.9.28.2 (702.j.) | U | 91.21 | 61.72 | 1.48 | | |
| | | | NHM | 1956.4.13.1 (702.g.) | U | 92.18 | 63.02 | 1.46 | | |
| | | | USNM | 241581 | M | 98.82 | 64.59 | 1.53 | | |
| | | | USNM | 282815 | M | 90.96 | 63.05 | 1.44 | | |
| Cervidae | Rucervus | duvaucelii | | | | | | | 1.46 | 0.01 |
| | | | NHM | 1884.4.14.2 | F | 106.16 | 72.13 | 1.47 | | |
| | | | NHM | 694.h. | U | 110.84 | 76.98 | 1.44 | | |
| | | | USNM | 151606 | M | 121.82 | 83.11 | 1.47 | | |
| | | | USNM | 258616 | M | 110.72 | 76.34 | 1.45 | | |
| Cervidae | Rucervus | eldii | | | | | | | 1.47 | 0.03 |
| | | | USNM | 260832 | M | 87.82 | 58.95 | 1.49 | | |
| | | | USNM | 545015 | M | 105.02 | 72.92 | 1.44 | | |
| | | | USNM | 588355 | F | 86.25 | 58.60 | 1.47 | | |
| Cervidae | Rucervus | schomburgki | | | | | | | 1.54 | -- |
| | | | ZMB_Mam | 16032 | M | 108.78 | 70.85 | 1.54 | | |
| Cervidae | Rusa | alfredi | | | | | | | 1.54 | 0.00 |
| | | | ZMB_Mam | 32014 | F | 68.17 | 44.40 | 1.54 | | |
| | | | ZMB_Mam | 73526 | U | 72.52 | 47.22 | 1.54 | | |
| Cervidae | Rusa | marianna | | | | | | | 1.48 | -- |
| | | | ZMB_Mam | 8993 | M | 70.01 | 47.23 | 1.48 | | |
| Cervidae | Rusa | timorensis | | | | | | | 1.48 | 0.01 |
| | | | USNM | 199847 | F | 89.05 | 60.22 | 1.48 | | |
| | | | USNM | 256784 | F | 81.94 | 55.05 | 1.49 | | |
| | | | USNM | 538456 | F | 84.76 | 57.38 | 1.48 | | |
| Cervidae | Rusa | unicolor | | | | | | | 1.52 | 0.03 |
| | | | NHM | 1868.12.29.8. (699y2) | U | 125.68 | 81.56 | 1.54 | | |
| | | | USNM | 151859 | F | 119.67 | 80.42 | 1.49 | | |
| | | | USNM | 240479 | M | 126.72 | 82.91 | 1.53 | | |

| | | | | | | | | | | |
|---|---|---|---|---|---|---|---|---|---|---|
| | | | ZMB_Mam | 14696 | M | 119.52 | 80.11 | 1.49 | | |
| | | | ZMB_Mam | 83436 | U | 119.50 | 77.63 | 1.54 | | |
| | Giraffidae | Giraffa | camelopardalis | | | | | | 1.56 | 0.03 |
| | | | OM | 2275 | M | 201.02 | 127.45 | 1.58 | | |
| | | | OM | 2277 | U | 190.05 | 123.04 | 1.54 | | |
| | | | OM | 2278 | F | 207.50 | 136.71 | 1.52 | | |
| | | | OM | 2736 | U | 215.00 | 136.71 | 1.57 | | |
| | | | OM | 6103 | U | 190.94 | 119.92 | 1.59 | | |
| | | | OM | 7008 | U | 206.33 | 133.62 | 1.54 | | |
| | | | ZMB_Mam | 11853 | M | 181.00 | 114.18 | 1.59 | | |
| | | | ZMB_Mam | 48440 | U | 181.50 | 116.13 | 1.56 | | |
| | | | ZMB_Mam | 66393 | M | 216.00 | 143.47 | 1.51 | | |
| | Giraffidae | Okapia | johnstoni | | | | | | 1.61 | 0.02 |
| | | | DMNS | 6441 | U | 124.80 | 77.20 | 1.62 | | |
| | | | DMNS | 6839 | U | 118.70 | 72.09 | 1.65 | | |
| | | | DMNS | 16380 | U | 125.47 | 79.10 | 1.59 | | |
| | | | DMNS | 17874 | U | 121.71 | 76.52 | 1.59 | | |
| | | | OM | 2282 | F | 118.18 | 73.10 | 1.62 | | |
| | | | ZMB_Mam | 62086 | M | 120.93 | 74.52 | 1.62 | | |
| | | | ZMB_Mam | 70325 | M | 118.18 | 73.42 | 1.61 | | |
| | Hippopotamidae | Hexaprotodon | liberiensis | | | | | | 1.74 | 0.03 |
| | | | NHM | 1914.6.21._.1 | U | 101.72 | 59.30 | 1.72 | | |
| | | | NHM | 1937.11.20.1 | U | 96.16 | 55.83 | 1.72 | | |
| | | | NHM | 1967.3.20.1 | U | 96.69 | 55.22 | 1.75 | | |
| | | | ZMB_Mam | 77240 | M | 90.95 | 50.92 | 1.79 | | |
| | | | ZMB_Mam | 77270 | F | 92.34 | 53.88 | 1.71 | | |
| | Hippopotamidae | Hippopotamus | amphibius | | | | | | 1.57 | 0.03 |
| | | | DMNS | 14995 | U | 187.50 | 118.38 | 1.58 | | |
| | | | OM | 2197 | F | 185.07 | 116.38 | 1.59 | | |
| | | | OM | 2198 | F | 183.71 | 120.20 | 1.53 | | |
| | | | ZMB_Mam | 44221 | F | 176.20 | 110.74 | 1.59 | | |
| | Moschidae | Moschus | berezovskii | | | | | | 1.53 | 0.01 |
| | | | USNM | 259381 | M | 46.51 | 30.20 | 1.54 | | |
| | | | USNM | 259384 | F | 46.43 | 30.27 | 1.53 | | |
| | | | USNM | 268878 | M | 44.84 | 29.43 | 1.52 | | |
| | Moschidae | Moschus | moschiferus | | | | | | 1.50 | 0.04 |
| | | | NHM | 45.1.12.449 (676.c.) | U | 48.79 | 31.71 | 1.54 | | |

| | | | | | | | | | | | |
|---|---|---|---|---|---|---|---|---|---|---|---|
| | | | | ZMB_Mam | 51830 | M | 52.57 | 35.77 | 1.47 | | |
| | | | | ZMB_Mam | 62079 | F | 53.04 | 35.75 | 1.48 | | |
| | Suidae | Babyrousa | babyrussa | | | | | | | 1.57 | 0.05 |
| | | | | DMNS | 7871 | U | 80.34 | 52.74 | 1.52 | | |
| | | | | NHM | 718 | U | 67.77 | 43.45 | 1.56 | | |
| | | | | ZMB_Mam | 1969 | M | 70.07 | 42.74 | 1.64 | | |
| | | | | ZMB_Mam | 38829 | U | 79.79 | 51.73 | 1.54 | | |
| | Suidae | Hylochoerus | meinertzhageni | | | | | | | 1.53 | 0.03 |
| | | | | OM | 2143 | M | 110.76 | 73.36 | 1.51 | | |
| | | | | OM | 3557 | U | 98.47 | 62.63 | 1.57 | | |
| | | | | OM | 6274 | M | 102.80 | 68.56 | 1.50 | | |
| | | | | ZMB_Mam | 83342 | F | 104.87 | 68.86 | 1.52 | | |
| | Suidae | Phacochoerus | aethiopicus | | | | | | | 1.58 | 0.02 |
| | | | | OM | 3313 | U | 79.73 | 51.37 | 1.55 | | |
| | | | | OM | 3324 | M | 75.55 | 47.08 | 1.60 | | |
| | | | | OM | 3546 | F | 70.71 | 44.94 | 1.57 | | |
| | | | | OM | 7605 | M | 77.66 | 49.81 | 1.56 | | |
| | | | | OM | 7712 | U | 71.66 | 45.01 | 1.59 | | |
| | Suidae | Phacochoerus | africanus | | | | | | | 1.57 | 0.04 |
| | | | | DMNS | 11994 | U | 80.69 | 52.93 | 1.52 | | |
| | | | | USNM | 21632 | M | 80.92 | 50.33 | 1.61 | | |
| | | | | USNM | 161939 | F | 73.90 | 46.44 | 1.59 | | |
| | | | | USNM | 162966 | M | 81.05 | 52.29 | 1.55 | | |
| | Suidae | Potamochoerus | porcus | | | | | | | 1.60 | 0.06 |
| | | | | OM | 2107 | U | 77.37 | 48.21 | 1.60 | | |
| | | | | OM | 3338 | M | 79.69 | 47.96 | 1.66 | | |
| | | | | OM | 8417 | U | 73.08 | 45.57 | 1.60 | | |
| | | | | USNM | 164542 | M | 76.44 | 46.11 | 1.66 | | |
| | | | | USNM | 259174 | F | 70.73 | 44.56 | 1.59 | | |
| | | | | ZMB_Mam | 1966 | U | 65.18 | 43.25 | 1.51 | | |
| | Suidae | Sus | barbatus | | | | | | | 1.49 | 0.04 |
| | | | | USNM | 151849 | M | 96.59 | 66.76 | 1.45 | | |
| | | | | ZMB_Mam | 69566 | U | 73.24 | 48.56 | 1.51 | | |
| | | | | ZMB_Mam | 69899 | M | 96.44 | 64.01 | 1.51 | | |
| | Suidae | Sus | salvanius | | | | | | | 1.60 | 0.03 |
| | | | | NHM | 805.01 | M | 35.50 | 22.29 | 1.59 | | |
| | | | | NHM | 805.02 | F | 34.69 | 22.28 | 1.56 | | |

| | | | | | | | | | | |
|---|---|---|---|---|---|---|---|---|---|---|
| | | | NHM | 1981.97 | U | 35.56 | 21.87 | 1.63 | | |
| | | | NHM | 1936.6-11.1 | M | 36.49 | 22.73 | 1.61 | | |
| Suidae | Sus | verrucosus | | | | | | | 1.51 | -- |
| | | | ZMB_Mam | 7975 | U | 79.66 | 52.62 | 1.51 | | |
| Tayassuidae | Pecari | tajacu | | | | | | | 1.59 | 0.03 |
| | | | DMNS | 2554 | U | 47.95 | 30.58 | 1.57 | | |
| | | | USNM | A 1076 | U | 49.70 | 30.84 | 1.61 | | |
| Tayassuidae | Tayassu | pecari | | | | | | | 1.56 | 0.04 |
| | | | USNM | 105081 | M | 60.51 | 38.07 | 1.59 | | |
| | | | USNM | 257318 | U | 59.86 | 39.19 | 1.53 | | |
| Tragulidae | Hyemoschus | aquaticus | | | | | | | 1.60 | 0.05 |
| | | | NHM | 1846.11.19.10 (680.c) | U | 45.43 | 27.55 | 1.65 | | |
| | | | NHM | 1965.8.26.2 | F | 50.26 | 32.28 | 1.56 | | |
| | | | ZMB_Mam | 103235 | M | 44.39 | 27.85 | 1.59 | | |
| Tragulidae | Moschiola | meminna | | | | | | | 1.59 | 0.00 |
| | | | NHM | 76.216 | F | 27.28 | 17.20 | 1.59 | | |
| | | | NHM | 76.217 | M | 27.91 | 17.53 | 1.59 | | |
| Tragulidae | Tragulus | javanicus | | | | | | | 1.57 | 0.05 |
| | | | NHM | 1361.a. | F | 24.90 | 16.41 | 1.52 | | |
| | | | NHM | 1860.3.18.29 (853.h) | F | 24.97 | 15.56 | 1.60 | | |
| | | | NHM | 1879.5.23.8 (1361.c.) | F | 25.55 | 16.04 | 1.59 | | |
| Tragulidae | Tragulus | kanchil | | | | | | | 1.54 | 0.02 |
| | | | NHM | 67.165 | F | 25.58 | 16.69 | 1.53 | | |
| | | | USNM | A 49461 | M | 24.42 | 16.03 | 1.52 | | |
| | | | USNM | A 49462 | F | 25.70 | 16.44 | 1.56 | | |
| Tragulidae | Tragulus | napu | | | | | | | 1.59 | 0.04 |
| | | | NHM | 1961.4.26.1 | U | 33.95 | 20.71 | 1.64 | | |
| | | | USNM | 317286 | M | 29.83 | 19.23 | 1.55 | | |
| | | | USNM | A 49605 | F | 30.56 | 18.95 | 1.61 | | |
| | | | USNM | A 49871 | M | 34.18 | 21.74 | 1.57 | | |

## Code

```
#all maps were made in ArcMap
#links to data sources are provided
#data available on request

#set working directory and install required packages
install.packages(c("sp", "raster", "rgdal", "pracma", "DescTools",
"ggplot2", "qdap", "plyr"))
library(sp)
library(raster)
library(rgdal)
library(pracma)
library(DescTools)
library(ggplot2)
library(qdap)
library(plyr)

#for categorical variables, mode is used to predict maximum likelihood
value
getmode <- function(v) {
  uniqv <- unique(v)
  uniqv[which.max(tabulate(match(v, uniqv)))]
}

################prepare data################
#traits
data <- read.csv("DATA_CALC_ARTIO.csv", header = T, na = ".")
data$C_1 <- as.numeric(data$C_1)
data$C_Jarch <- as.numeric(data$C_Jarch)
data$C_GR <- (data$C_1)/(data$C_Jarch)

binomial <- data.frame(genus = data$genus, species = data$species)
data$binomial <- paste(binomial$genus, binomial$species, sep = " ")
traits <- aggregate(data[ , 10], list(data$family, data$binomial),
mean, na.rm = TRUE)
traits_n <- aggregate(data[ , 10], list(data$binomial), sd, na.rm =
TRUE)
traits <- merge(traits, traits_n, by.x = "Group.2", by.y = "Group.1")
traits_n <- aggregate(data[ , 11], list(data$binomial), length)
traits <- merge(traits, traits_n, by.x = "Group.2", by.y = "Group.1" )
colnames(traits)[colnames(traits)==c("Group.2", "Group.1", "x.x",
"x.y", "x")] <- c("MSWbinom", "family","C_GR", "stdev", "n")
rownames(traits) <- traits$MSWbinom

#points
#points are from https://pollylab.indiana.edu/data/index.html
#environmental variables extract in ArcMap to points
#mean annual temperature and annual precipitation from
https://climatedataguide.ucar.edu/climate-data/global-land-
precipitation-and-temperature-willmott-matsuura-university-delaware
#elevation from www.ngdc.noaa.gov/mgg/topo/globe.html
#Matthews' vegetation cover from http://daac.ornl.gov
```

```
#Bailey's ecoregions from www.unep-wcmc.org/resources-and-data/baileys-
ecoregions-of-the-world

points <- read.csv("allpointsdata_noANT.csv")
points$BIO1 <- as.numeric(points$BIO1)
points$BIO12 <- as.numeric(points$BIO12)
points$Elevation <- as.numeric(points$Elevation)

#species ranges
#range maps available from IUCN (www.iucnredlist.org)
#ranges are limited to Order = Artiodactyla; Presence = 1, Extant;
Origin = 1, Native or 2, Reintroduced
mammals <- shapefile("terrmamm_ung.shp")
geography <- subset(mammals, presence == "1")
geography <- subset(geography, origin == "1" | origin == "2")

#convert sampling points to spatial points
sp <- SpatialPoints(points[ , 2:3], proj4string =
CRS(proj4string(geography)))

#sample species at each sampling locality
o <- over(sp, geography, returnList = T)

#calculate sample size at each point
richness <- unlist(lapply(o, function(x) length(traits[x$MSWbinom,
"C_GR"])))

#calculate sample size at each point with traits
count <- unlist(lapply(o, function(x) sum(!is.na(traits[x$binomial,
"C_GR"]))))

#summarize traits for community level distributions using mean and
standard deviation
ecometric_gearratio <- unlist(lapply(o, function(x)
mean(traits[x$MSWbinom, "C_GR"], na.rm = T)))
sd_ecometric_gearratio <- unlist(lapply(o, function(x)
sd(traits[x$MSWbinom, "C_GR"], na.rm = T)))

#add values to points data
points$richness <- richness
points$count <- count
points$ecometric_mean <- ecometric_gearratio
points$ecometric_sd <- sd_ecometric_gearratio

#group the trait distributions into 25 x 25 trait bins
#take the range
mhyp <- range(ecometric_gearratio, na.rm = T)
sdhyp <- range(sd_ecometric_gearratio, na.rm = T)
#get the break points for sd and mean
mbrks <- seq(mhyp[1]-0.001, mhyp[2]+0.001, diff(mhyp)/25)
sdbrks <- seq(sdhyp[1]-0.001, sdhyp[2]+0.001, diff(sdhyp)/25)
#assign bin codes
mbc <- .bincode(ecometric_gearratio, breaks = mbrks)
sdbc <- .bincode(sd_ecometric_gearratio, breaks = sdbrks)
```

```
##limit communities to those with 3 or more species
mbc[count < 3] <- NA
sdbc[count < 3] <- NA
cutoff <- 3

################normalize data################
points$richness3 <- points$richness ^ (1/3)
points$LogPrecip <- log(points$BIO12 + 1)
points$TempCube <- (points$BIO1/10) ^ 3
points$elev3 <- points$Elevation ^ (1/3)

################correlations################
#family and gear ratio
anova_phylo <- aov(C_GR ~ family, data = traits)
anova_phylo
summary(anova_phylo)
#calculate R2
0.1900/(0.1900 + 0.2116)

#richness and gear ratio
reg_rich <- lm(ecometric_mean ~ richness3, data = points)
reg_rich
summary(reg_rich)
cor_rich <- cor.test(points$richness3, points$ecometric_mean, method =
"pearson")
cor_rich

#precipitation and gear ratio
reg_precip <- lm(ecometric_mean ~ LogPrecip, data = points)
reg_precip
summary(reg_precip)
cor_precip <- cor.test(points$LogPrecip, points$ecometric_mean, method
= "pearson")
cor_precip

#temperature and gear ratio
reg_temp <- lm(ecometric_mean ~ TempCube, data = points)
reg_temp
summary(reg_temp)
cor_temp <- cor.test(points$TempCube, points$ecometric_mean, method =
"pearson")
cor_temp

#elevation and gear ratio
reg_elev <- lm(ecometric_mean ~ elev3, data = points)
reg_elev
summary(reg_elev)
cor_elev <- cor.test(points$elev3, points$ecometric_mean, method =
"pearson", use = "complete.obs")
cor_elev

#ecoregion division and gear ratio
anova_eco <- aov(ecometric_mean ~ DIV_DESC, data = points)
```

```
anova_eco
summary(anova_eco)
#calculate R2
24.76/(24.76 + 15.97)

#vegetation cover and gear ratio
anova_veg <- aov(ecometric_mean ~ VegName, data = points)
anova_veg
summary(anova_veg)
#calculate R2
23.52/(23.52 + 17.29)

################Figure 3.3################
#Figure 3.3A
traits$MSWbinom <- factor(traits$MSWbinom, levels =
traits$MSWbinom[order(traits$C_GR)])
rankorderspecies <- ggplot(traits, aes(x = MSWbinom, y = C_GR)) +
  geom_hline(yintercept = mean(traits$C_GR, na.rm = T), linetype =
"dashed", color = "black") +
  geom_hline(yintercept = mean(traits$C_GR, na.rm = T) -
sd(traits$C_GR), linetype = "solid", color = "black") +
  geom_hline(yintercept = mean(traits$C_GR, na.rm = T) +
sd(traits$C_GR), linetype = "solid", color = "black") +
  geom_segment(aes(xend = MSWbinom, yend = 1.3)) +
  geom_point(aes(x = MSWbinom, y = C_GR), color = "black", pch = 16,
cex = 2) +
  labs(x = "Species", y = "Calcaneal Gear Ratio") +
  scale_y_continuous(expand = c(0, 0), limits = c(1.3, 1.9), breaks =
c(1.3, 1.4, 1.5, 1.6, 1.7, 1.8, 1.9)) +
  theme(axis.line = element_line(color = "black"),
        panel.background = element_rect(color = "black", fill = NA),
        panel.grid = element_blank(),
        axis.text.y = element_text(color = "black", size = 10),
        axis.text.x = element_text(color = "black", angle = 90, size =
8, hjust = 1, vjust = 0.25), axis.title = element_text(color = "black",
size = 14))
rankorderspecies

#Figure 3.3B
familymean <- aggregate(data[ , 10], list(data$family), mean, na.rm =
TRUE)
familymean <- familymean[order(familymean$x), ]
traits$family <- factor(traits$family, levels = c("Antilocapridae",
"Bovidae", "Cervidae", "Moschidae", "Suidae", "Tayassuidae",
"Tragulidae", "Giraffidae", "Camelidae", "Hippopotamidae"))
plot(traits$family, traits$C_GR, ylim = c(1.3, 1.8), range = 0, las =
2, cex.axis = 0.7, col = "gray", ylab = "Gear Ratio", xlab = "Family")

################precipitation################
#calculate the data for the precipitation raster
obj <- array(NA, dim = c(25, 25))
for (i in 1:25) {
  for (j in 1:25) {
    dat <- points$LogPrecip[which(mbc == i & sdbc == j)]
```

```
    obj[26 - j, i] <- mean(dat, na.rm = T)
  }
}

#make raster for gear ratio and precipitation
r <- raster(extent(0, 25, 0, 25), resolution = 1)
#set the values to the obj
r <- setValues(r, obj)

#plot raster as ecometric space
par(bg = NA)
plot(0:25, 0:25, type = "n", xlim = c(0, 25), ylim = c(0, 25), xaxs =
"i", yaxs = "i", asp = 1, axes = F, xlab = " ", ylab = " ", cex.lab =
1.5)
rect(0, 0, 25, 25, lwd = 3)
lines(x = c(8.3, 8.3), y = c(0, 25))
lines(x = c(16.6, 16.6), y = c(0, 25))
lines(x = c(0, 25), y = c(8.3, 8.3))
lines(x = c(0, 25), y = c(16.6, 16.6))
plot(r, col = colorRampPalette(c("brown", "tan", "yellow", "green",
"darkgreen"))(round((maxValue(r) - minValue(r)) * 5)), add = T)
title(ylab = "Standard Deviation", line = -6, cex.lab = 1.5)
axis(side = 2, at = c(0.0, 8.3, 16.6, 25), labels = c(0, 0.035, 0.070,
0.105), line = -9)
title(xlab = "Mean", line = 2, cex.lab = 1.5)
axis(side = 1, at = c(0, 8.3, 16.6, 25), labels = c(1.42, 1.48, 1.53,
1.59))
mtext("Precipitation", side = 4, line = -4, cex = 1.5)

###example: to calculate the value in a trait bin, use the edge values
of a rectangle
#train bin formula is (left, bottom, right, top)
#example is modern Kakamega Forest Reserve
#use density estimate for value of precipitation
rect(14, 8, 15, 9, lwd = 4, border = "black")
dat <- points$LogPrecip[which(mbc == 15 & sdbc == 9)]
mod <- density(dat, bw = 1)
modmax <- mod$x[which.max(mod$y)]
modmax

#calculate maximum likelihood for all bins
modmax <- array(NA, dim = length(points[ , 1]))
mod <- list()
for (i in 1:length(points[ , 1])) {
  if(!(is.na(mbc[i]) | is.na(sdbc[i]))) {
    dat <- round(points$LogPrecip[which(mbc == mbc[i] & sdbc ==
sdbc[i])])
    mod[[i]] <- density(dat[!is.na(dat)], bw = 1)
    modmax[i] <- mod[[i]]$x[which.max(mod[[i]]$y)]
  }
}

#calculate precipitation anomaly
#observed precipitation - predicted precipitation
```

```
anom_precip <- points$LogPrecip - modmax
points$precipanom <- anom_precip
min(anom_precip, na.rm = T)
max(anom_precip, na.rm = T)
mean(anom_precip, na.rm = T)

################ecoregion division################
points$ECO <- as.numeric(points$DIV_DESC)
points$ECOdom <- as.numeric(points$DOM_DESC)

#code colors associated with each domain and division
#range subtracts 1 to remove NA
#dom1 = dry, dom2 = humid temperate, dom3 = humid tropical, dom4 =
polar
ecoregion_range <- length(unique(points$ECO)) - 1
dom1 <- points[which(points$ECOdom == 1), ]
dom1_range <- length(unique(dom1$ECO))
color1 <- colorRampPalette(c("brown",
"tan"))(dom1_range)[as.factor(dom1$ECO)]
dom2 <- points[which(points$ECOdom == 2), ]
dom2_range <- length(unique(dom2$ECO))
color2 <- colorRampPalette(c("darkblue",
"lightblue"))(dom2_range)[as.factor(dom2$ECO)]
dom3 <- points[which(points$ECOdom == 3), ]
dom3_range <- length(unique(dom3$ECO))
color3 <- colorRampPalette(c("darkgreen",
"lightgreen"))(dom3_range)[as.factor(dom3$ECO)]
dom4 <- points[which(points$ECOdom == 4), ]
dom4_range <- length(unique(dom4$ECO))
color4 <- colorRampPalette(c("purple",
"lavender"))(dom4_range)[as.factor(dom4$ECO)]

a <- c(unique(dom1$ECO), unique(dom2$ECO), unique(dom3$ECO),
unique(dom4$ECO))
b <- c(unique(color1), unique(color2), unique(color3), unique(color4))
d <- as.data.frame(cbind(a, b))
d$b <- as.character(d$b)
points$color <- "NA"
points$color <- lookup(as.factor(points$ECO), d$a, d$b)
points$color <- as.character(points$color)

#sort colors
#25:27 = ECO, ECOdom, color
e <- points[ , c(25:27)]
e <- unique(e[ , 1:3])
e <- na.omit(e)
e <- e[order(e$ECO), ]

#calculate the data for the ecoregion division raster
obj <- array(NA, dim = c(25, 25))
for (i in 1:25) {
  for (j in 1:25) {
    dat <- points$ECO[which(mbc == i & sdbc == j)]
    obj[26 - j, i] <- getmode(dat)
```

```
  }
}

#make raster for gear ratio and ecoregion division
r <- raster(extent(0, 25, 0, 25), resolution = 1)
#set the values to the obj
r <- setValues(r, obj)

#plot raster as ecometric space
par(bg = NA)
plot(0:25, 0:25, type = "n", xlim = c(0, 25), ylim = c(0, 25), xaxs =
"i", yaxs = "i", asp = 1, axes = F, xlab = " ", ylab = " ", cex.lab =
1.5)
rect(0, 0, 25, 25, lwd = 3)
lines(x = c(8.3, 8.3), y = c(0, 25))
lines(x = c(16.6, 16.6), y = c(0, 25))
lines(x = c(0, 25), y = c(8.3, 8.3))
lines(x = c(0, 25), y = c(16.6, 16.6))
plot(r, col = e$color[obj = e$ECO], add = T)
title(ylab = "Standard Deviation", line = -6, cex.lab = 1.5)
axis(side = 2, at = c(0.0, 8.3, 16.6, 25), labels = c(0.0, 0.035,
0.070, 0.105), line = -9)
title(xlab = "Mean", line = 2, cex.lab = 1.5)
axis(side = 1, at = c(0, 8.3, 16.6, 25), labels = c(1.42, 1.48, 1.53,
1.59))
mtext("Ecoregion", side = 4, line = -4, cex = 1.5)

###example: to calculate the value in a trait bin, use the edge values
of a rectangle
#train bin formula is (left, bottom, right, top)
#example is modern Kakamega Forest Reserve
#use density estimate for value of ecoregion division
rect(14, 8, 15, 9, lwd = 4, border = "black")
dat <- points$ECO[which(mbc == 15 & sdbc == 9)]
mod <- getmode(dat[!is.na(dat)])
unique(points$DIV_DESC[which(points$ECO == mod)])

#calculate most likely ecoregion division for all bins using mode
modmax <- array(NA, dim = length(points[ , 1]))
mod <- list()
for (i in 1:length(points[ , 1])) {
  if(!(is.na(mbc[i]) | is.na(sdbc[i]))) {
    dat <- points$ECO[which(mbc == mbc[i] & sdbc == sdbc[i])]
    mod[[i]] <- getmode(dat[!is.na(dat)])
    modmax[i] <- mod[[i]]
  }
}

#calculate ecoregion division anomaly
#observed ecoregion division - predicted ecoregion division
#with categorical variable, 0 = correct prediction, !0 = incorrect
prediction
anom_ecodiv <- points$ECO - modmax
points$ecoanomaly <- anom_ecodiv
```

```
m <- points[count > 2, ]
n <- points[which(points$ecoanomaly != "NA"), ]
k <- n[which(n$ecoanomaly == 0), ]
correct <- ((dim(k)[1])/(dim(n)[1])) * 100
correct
incorrect <- 100 - correct
incorrect

################ecoregion domain################
#code is for predictions only
#calculate most likely ecoregion domain for all bins using mode
modmax <- array(NA, dim = length(points[ , 1]))
mod <- list()
for (i in 1:length(points[ , 1])) {
  if(!(is.na(mbc[i]) | is.na(sdbc[i]))) {
    dat <- points$ECOdom[which(mbc == mbc[i] & sdbc == sdbc[i])]
    mod[[i]] <- getmode(dat[!is.na(dat)])
    modmax[i] <- mod[[i]]
  }
}

#calculate ecoregion domain anomaly
#observed ecoregion domain - predicted ecoregion domain
#with categorical variable, 0 = correct prediction, !0 = incorrect
prediction
anom_ecodom <- points$ECOdom - modmax ##observed - predicted
points$ecoanomalydom <- anom_ecodom
m <- points[count > 2, ] #limit to comm. with data 3+ species
n <- points[which(points$ecoanomalydom != "NA"), ]
k <- n[which(n$ecoanomalydom == 0), ]
correct <- ((dim(k)[1])/(dim(n)[1])) * 100
correct
incorrect <- 100 - correct
incorrect

################vegetation cover################
points$veg <- as.numeric(points$VegName, na.rm = T)

#code colors associated with vegetation classes
#range subtracts 1 to remove NA
#veg1 = evergreen, veg2 = deciduous, veg3 = desert, veg4 = arctic, veg5
= grassland
veg_range <- length(unique(points$veg)) - 1 #remove NA
veg1 <- points[which(points$VegSimple == 1), ]
veg1_range <- length(unique(veg1$veg))
color1 <- colorRampPalette(c("darkblue",
"lightblue"))(veg1_range)[as.factor(veg1$veg)]
veg2 <- points[which(points$VegSimple == 2), ]
veg2_range <- length(unique(veg2$veg))
color2 <- colorRampPalette(c("red",
"pink"))(veg2_range)[as.factor(veg2$veg)]
veg3 <- points[which(points$VegSimple == 3), ]
veg3_range <- length(unique(veg3$veg))
```

```
color3 <- colorRampPalette(c("sienna4",
"tan"))(veg3_range)[as.factor(veg3$veg)]
veg4 <- points[which(points$VegSimple == 4), ]
veg4_range <- length(unique(veg4$veg))
color4 <- colorRampPalette(c("purple",
"lavender"))(veg4_range)[as.factor(veg4$veg)]
veg5 <- points[which(points$VegSimple == 5), ]
veg5_range <- length(unique(veg5$veg))
color5 <- colorRampPalette(c("darkgreen",
"lightgreen"))(veg5_range)[as.factor(veg5$veg)]

a <- c(unique(veg1$veg), unique(veg2$veg), unique(veg3$veg),
unique(veg4$veg), unique(veg5$veg))
b <- c(unique(color1), unique(color2), unique(color3), unique(color4),
unique(color5))
d <- as.data.frame(cbind(a, b))
d$b <- as.character(d$b)
points$color2 <- "NA"
points$color2 <- lookup(as.factor(points$veg), d$a, d$b)
points$color2 <- as.character(points$color2)

#sort colors
#30:31 = veg, color2
e <- points[ , c(30:31)]
e <- unique(e[ , 1:2])
e <- na.omit(e)
e <- e[order(e$veg), ]

#calculate the data for the vegetation cover raster
obj <- array(NA, dim = c(25, 25))
for (i in 1:25) {
  for (j in 1:25) {
    dat <- points$veg[which(mbc == i & sdbc == j)]
    obj[26 - j, i] <- getmode(dat)
  }
}

#make raster for gear ratio and vegetation cover
r <- raster(extent(0, 25, 0, 25), resolution = 1)
#set the values to the obj
r <- setValues(r, obj)

#plot raster and highlight bin
par(bg = NA)
plot(0:25, 0:25, type = "n", xlim = c(0, 25), ylim = c(0, 25), xaxs =
"i", yaxs = "i", asp = 1, axes = F, xlab = " ", ylab = " ", cex.lab =
1.5)
rect(0, 0, 25, 25, lwd = 3)
lines(x = c(8.3, 8.3), y = c(0, 25))
lines(x = c(16.6, 16.6), y = c(0, 25))
lines(x = c(0, 25), y = c(8.3, 8.3))
lines(x = c(0, 25), y = c(16.6, 16.6))
plot(r, col = e$color[obj = e$veg], add = T)
title(ylab = "Standard Deviation", line = -6, cex.lab = 1.5)
```

```
axis(side = 2, at = c(0.0, 8.3, 16.6, 25), labels = c(0.0, 0.035,
0.070, 0.105), line = -9)
title(xlab = "Mean", line = 2, cex.lab = 1.5)
axis(side = 1, at = c(0, 8.3, 16.6, 25), labels = c(1.42, 1.48, 1.53,
1.59))
mtext("Vegetation Cover", side = 4, line = -4, cex = 1.5)

###example: to calculate the value in a trait bin, use the edge values
of a rectangle
#train bin formula is (left, bottom, right, top)
#example is modern Kakamega Forest Reserve
#use density estimate for value of vegetation cover
rect(14, 8, 15, 9, lwd = 4, border = "black")
dat <- points$veg[which(mbc == 15 & sdbc == 9)]
mod <- getmode(dat[!is.na(dat)])
unique(points$VegName[which(points$veg == mod)])

#calculate most likely vegetation cover for all bins using mode
modmax <- array(NA, dim = length(points[ , 1]))
mod <- list()
for (i in 1:length(points[ , 1])) {
  if (!(is.na(mbc[i]) | is.na(sdbc[i]))) {
    dat <- points$veg[which(mbc == mbc[i] & sdbc == sdbc[i])]
    mod[[i]] <- getmode(dat[!is.na(dat)])
    modmax[i] <- mod[[i]]
  }
}

#calculate ecoregion division anomaly
#observed ecoregion division - predicted ecoregion division
#with categorical variable, 0 = correct prediction, !0 = incorrect
prediction
anom_veg <- points$veg - modmax
points$veganom <- anom_veg
m <- points[which(points$count > 2), ]
n <- m[which(m$veganom != "NA"), ]
k <- n[which(n$veganom == 0), ]
correct <- ((dim(k)[1])/(dim(n)[1])) * 100
correct
incorrect <- 100 - correct
incorrect

################vegetation cover - 5 classes################
#code is for predictions only
points$VegSimple <- as.numeric(points$VegSimple, na.rm = T)

#calculate most likely ecoregion domain for all bins using mode
modmax <- array(NA, dim = length(points[ , 1]))
mod <- list()
for (i in 1:length(points[ , 1])) {
  if(!(is.na(mbc[i]) | is.na(sdbc[i]))) {
    dat <- points$VegSimple[which(mbc == mbc[i] & sdbc == sdbc[i])]
    mod[[i]] <- getmode(dat[!is.na(dat)])
    modmax[i] <- mod[[i]]
```

```
  }
}

#calculate vegetation cover - 5 classes anomaly
#observed vegetation class - predicted vegetation class
#with categorical variable, 0 = correct prediction, !0 = incorrect
prediction
anom_veg5 <- points$VegSimple - modmax ##observed - predicted
points$veg5anom <- anom_veg5
m <- points[which(points$count > 2), ]
n <- m[which(m$veg5anom != "NA"), ]
k <- n[which(n$veg5anom == 0), ]
correct <- ((dim(k)[1])/(dim(n)[1])) * 100
correct
incorrect <- 100 - correct
incorrect

#write.csv(points, file = "output_points.csv")
```

# APPENDIX C

## SUPPLEMENTAL MATERIAL FOR CHAPTER 4

**Table C-1. *Canis dirus* measurements of TERA 450. Log-ratios are relative to *Eucyon davisi* following Tedford et al. (2009).**

| Measurement | Definition | Térapa (mm) | Log-ratio |
|---|---|---|---|
| Left maxilla | | | |
| JD | jugal depth | 20.05 | 0.3479 |
| LP4 | length of P4 | 30.59 | 0.2900 |
| WP4 | width of P4 | 14.70 | 0.3899 |
| LM1 | length of M1 | 18.19 | 0.2212 |
| WM1 | width of M1 | 24.25 | 0.2731 |
| Left mandible | | | |
| Lp3 | length of p3 | 16.88 | 0.2261 |
| Lp4 | length of p4 | 20.86 | 0.2697 |
| Wp4 | width of p4 | 11.39 | 0.4004 |
| Lm1 | length of m1 | 37.88 | 0.3462 |
| Wm1tr | width of m1 trigonid | 15.33 | 0.3828 |
| Wm1tl | width of m1 talonid | 13.71 | 0.3425 |

**Table C-2. Previous taxonomic assignments with sources and revised identifications presented here.**

| Order | Family | Previous identifications | Revised identifications |
|---|---|---|---|
| Perissodactyla | Equidae | *Equus*[1] | *Equus scotti* |
| | | *Equus excelsus*[2] | *Equus* cf. *E. scotti* |
| | | *Equus conversidens*[2] | *Equus* sp. |
| | Tapiridae | *Tapirus*[1] | Not present |
| Artiodactyla | Tayassuidae | cf. *Platygonus*[1] | *Platygonus compressus* |
| | Camelidae | *Camelops*-sized[1] | *Camelops hesternus* |
| | | *Hemiauchenia*-sized[1] | *Palaeolama mirifica* |
| Carnivora | Canidae | *Canis dirus*[1, 3] | *Canis dirus* |
| | Procyonidae | *Procyon*[1] | *Procyon lotor* |
| | Felidae | *Lynx rufus*[1] | *Lynx rufus* |
| | | | *Smilodon* cf. *S. fatalis* |

Note: [1] Mead et al. (2006), [2] Carranza-Castañeda and Roldán-Quintana (2007), [3] Hodnett et al. (2009).

**Figure C-1. Statistical analyses of equid specimens. A, Principal component analysis of *Equus* second phalanx (TERA 319), which is identified as *E. scotti* with 87.5% confidence. B, Quadratic discriminant analysis of *Equus* second phalanx (TERA 319), which is identified as *E. scotti* with 87.5% confidence. C, Principal component analysis of *Equus* metacarpal (TERA 313), which is identified as *E. scotti* with 100% confidence. D, Quadratic discriminant analysis of *Equus* metacarpal (TERA 313), which is identified as *E. scotti* with 100% confidence.**

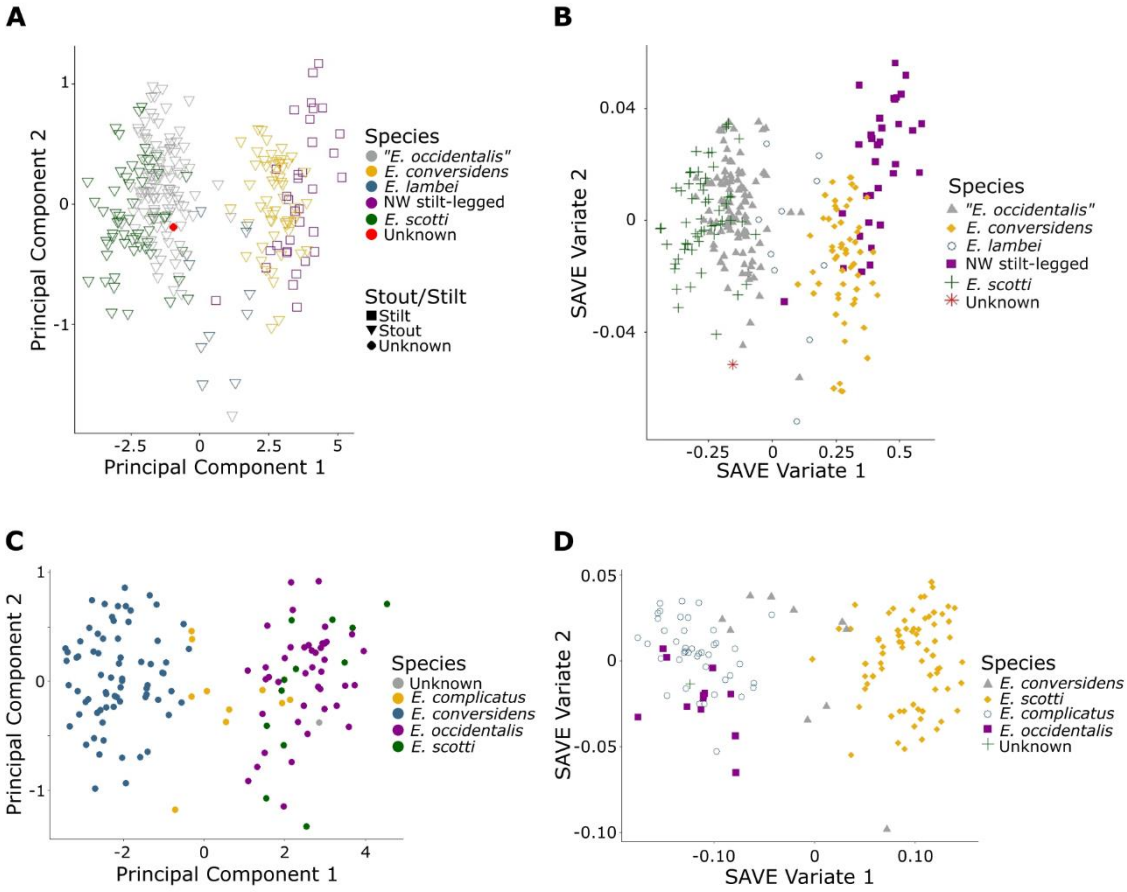

APPENDIX D

SUPPLEMENTAL MATERIAL FOR CHAPTER 5

**Table D-1. Rural-Urban Continuum Codes with population totals from the ACS 2017 5-year estimate dataset (USDA ERS 2013b, USCB 2018).**

| RUCC | Metro designation | County population | Metro adjacent | Number of counties | Total population |
|---|---|---|---|---|---|
| 1 | Metro | Metro area of 1 million or more | -- | 432 | 177,601,619 |
| 2 | Metro | Metro area of 250,000 to 1 million | -- | 379 | 68,242,203 |
| 3 | Metro | Metro area of fewer than 250,000 | -- | 356 | 29,067,253 |
| 4 | Non-metro | Urban area of 20,000 or more | Yes | 214 | 13,549,273 |
| 5 | Non-metro | Urban area of 20,000 or more | No | 92 | 5,028,805 |
| 6 | Non-metro | Urban area of 2,500 to 19,999 | Yes | 593 | 14,642,448 |
| 7 | Non-metro | Urban area of 2,500 to 19,999 | No | 433 | 8,176,439 |
| 8 | Non-metro | Completely rural or urban area with less than 2,500 | Yes | 220 | 2,122,539 |
| 9 | Non-metro | Completely rural or urban area with less than 2,500 | No | 424 | 2,573,828 |

**Table D-2. Poverty categories using by Jenks' Natural Breaks of percentage of poverty. Maximum value is 56.7%. Poverty data and population values are from the US Census Bureau (USCB 2017).**

| Poverty category | Percentage of poverty | Total population |
|---|---|---|
| 1 | 0 – 10.1 | 82,305,003 |
| 2 | 10.2 – 14.1 | 95,747,420 |
| 3 | 14.2 – 18.4 | 100,696,255 |
| 4 | 18.5 – 23.5 | 28,811,267 |
| 5 | 23.6 – 31.4 | 1,229,241 |
| 6 | > 31.5 | 1,172,384 |

**Table D-3. Quantile breaks for maps in Figure 5.1A and Figures 5.1C-H. Break values are the maximum ILI value per 1000 km$^2$ of each quantile.**

| Quantile | All | NPS | FSML | ZOO | MUS | LIB | BOT |
|---|---|---|---|---|---|---|---|
| 1 | 0.363 | 0.004 | 0.005 | 0.0061 | 0.012 | 0.102 | 0.013 |
| 2 | 0.726 | 0.006 | 0.012 | 0.017 | 0.049 | 0.410 | 0.033 |
| 3 | 1.57 | 0.009 | 0.021 | 0.029 | 0.089 | 1.02 | 0.062 |
| 4 | 2.54 | 0.014 | 0.033 | 0.045 | 0.142 | 1.95 | 0.108 |
| 5 | 3.99 | 0.022 | 0.061 | 0.064 | 0.240 | 3.17 | 0.187 |
| 6 | 30.9 | 0.748 | 0.137 | 0.257 | 1.04 | 26.1 | 0.838 |

**Table D-4. Mean, standard deviation, and standard error of ILI density for each type. Mean per 1000 km$^2$ is displayed in Figure 5.1B.**

| Type | Mean | Standard deviation | Standard error |
|---|---|---|---|
| ALL | 6.48 | 6.54 | 0.046 |
| NPS | 2.70 | 5.53 | 0.428 |
| FSML | 4.51 | 4.59 | 0.220 |
| ZOO | 6.16 | 6.51 | 0.303 |
| MUS | 6.52 | 6.39 | 0.166 |
| LIB | 6.53 | 6.56 | 0.051 |
| BOT | 7.24 | 6.89 | 0.217 |

**Table D-5. Standard deviation values for residuals for Figure 5.2A. Residuals are between log ILI density and the interaction of log population density and poverty percentage.**

| Standard deviation | Residuals |
|---|---|
| < -2.5 | -2.81 – -1.59 |
| -2.5 | -1.59 – -0.922 |
| -1.5 | -0.922 – -0.259 |
| -0.5 | -0.259 – 0.404 |
| 0.5 | 0.404 – 1.07 |
| > 1.5 | 1.07 – 2.20 |

**Table D-6. Racial and ethnic groups in underserved counties for Figure 5.3D. Column names correspond to the three underserved groups of counties in Figure 5.3: A, Counties that do not have ILIs; B, Counties with ILI residuals in the lowest 0.5%; and C, Non-metro, not adjacent counties with urban populations over 20,000 (RUCC 5). Population values are from the US Census Bureau (USCB 2018).**

| Group | Population | Population % Figure 5.3A | Population % Figure 5.3B | Population % Figure 5.3C |
|---|---|---|---|---|
| US population | 321,004,407 | 0.10 | 0.43 | 1.57 |
| American Indian and Alaska Native | 2,098,763 | 0.95 | 1.00 | 5.26 |
| Asian | 16,989,540 | 0.03 | 0.11 | 0.72 |
| Black or African American | 39,445,495 | 0.08 | 0.39 | 0.92 |
| Hispanic or Latino | 56,510,571 | 0.09 | 0.42 | 1.14 |
| Native Hawaiian and Other Pacific Islander | 515,522 | 0.05 | 0.79 | 6.50 |
| White | 197,277,789 | 0.11 | 0.46 | 1.82 |
| Two or more races | 7,451,295 | 0.05 | 0.25 | 0.62 |
| Other | 715,432 | 0.09 | 0.56 | 2.17 |

## Code

```
#all maps were made in ArcMap using point data from R code
#links to data sources are provided
#data available on request

#set working directory and install required packages
install.packages(c("ggplot2", "plyr", "gridExtra", "BAMMtools", "ape",
"spdep", "nlme", "MuMIn", "rcompanion"))
library(ggplot2)
library(plyr)
library(gridExtra)
library(BAMMtools)
library(ape)
library(spdep)
library(nlme)
library(MuMIn)
library(rcompanion)

################prepare ILI data################
#ILI data from the Museum Universe Data File
(https://www.imls.gov/research-evaluation/data-collection/museum-data-
files),
#the Public Library Survey's Outlet Data File
(https://www.imls.gov/research-evaluation/data-collection/public-
libraries-survey),
#the National Park Service
(https://data.doi.gov/dataset/administrative-boundaries-centroids-of-
national-park-system-units-9-30-2017),
#the Organization of Biological Field Stations
(https://www.obfs.org/directories#/), and
#the National Association of Marine Laboratories
(http://www.naml.org/members/directory.php)

#kernel densities produced in ArcMap and extracted to points
ILI <- read.csv("ili_points_data.csv", header = TRUE, stringsAsFactors
= F)
ILI$KernelD_bo[ILI$ILI_TYPE != "BOT"] <- NA
ILI$KernelD_mu[ILI$ILI_TYPE != "MUS"] <- NA
ILI$KernelD_li[ILI$ILI_TYPE != "LIB"] <- NA
ILI$KernelD_za[ILI$ILI_TYPE != "ZAW"] <- NA
ILI$KernelD_fs[ILI$ILI_TYPE != "FSML"] <- NA
ILI$KernelD_np[ILI$ILI_TYPE != "NPS"] <- NA

#transform kernel density by 1000
ILI[ , 6:12] <- ILI[ , 6:12] * 1000

#aggregate kernel density values for Figure 5.1B
ilidens <- aggregate(ILI[ , 6], list(ILI$ILI_TYPE), mean, na.rm = TRUE)
ilidens2 <- aggregate(ILI[ , 6], list(ILI$ILI_TYPE), sd, na.rm = TRUE)
st.err <- function(x) {sd(x)/sqrt(length(x))}
ilidens3 <- aggregate(ILI[ , 6], list(ILI$ILI_TYPE), st.err)
ilidens <- merge(ilidens, ilidens2, by.x = "Group.1", by.y = "Group.1")
```

```
ilidens <- merge(ilidens, ilidens3, by.x = "Group.1", by.y = "Group.1")
colnames(ilidens) <- c("type", "mean", "sd", "stderror")
ilidens <- rbind(ilidens, "6th" = c("ALL", mean(ILI$KernelD_il),
sd(ILI$KernelD_il), st.err(ILI$KernelD_il)))
ilidens$mean <- as.numeric(ilidens$mean)
ilidens$sd <- as.numeric(ilidens$sd)
ilidens$stderror <- as.numeric(ilidens$stderror)

######################Figure 5.1B######################
fill <- c('#CCCCFF', '#F0ECAA', '#E5D5F2', '#D7F0AF', '#FFE0E0',
'#DCF5E9', '#FAE9D4')
bars_ili <- ggplot(ilidens, aes(x = type, y = mean)) +
  geom_bar(stat = "identity", fill = fill, color = "black", width =
0.5) +
  geom_errorbar(stat = "identity", ymin = ilidens$mean, ymax =
ilidens$mean + ilidens$stderror,  color = "black", width = 0.5) +
  labs(x = "ILI Types", y = "Mean ILI per 1000km2") +
  scale_x_discrete(limits = c("ALL", "NPS", "FSML", "ZAW", "MUS",
"LIB", "BOT")) +
  scale_y_continuous(limits = c(0, 10), breaks = c(0, 2, 4, 6, 8, 10))
+
  theme(axis.line = element_line(color = "black"),
        panel.background = element_rect(color = "black", fill = "NA"),
        panel.grid = element_blank(),
        axis.text = element_text(color = "black", size = 15),
        axis.title = element_text(color = "black", size = 20))
bars_ili

#anova of bar plot
baranova <- aov(KernelD_il ~ ILI_TYPE, data = ILI)
summary(baranova)

################prepare county data################
#county data from the American Community Survey (ACS) 2017 5-year
estimate dataset
(https://data.census.gov/cedsci/table?q=population&hidePreview=false&ta
ble=DP05&tid=ACSDP5Y2017.DP05&lastDisplayedRow=33)
#ILI count extracted to county in ArcMap
county <- read.csv("county.csv", header = T)
county <- county[order(county3$GEOID), ]
county$SimpDens <- county$ILIcount/county$ALAND_km2
county$Logsimpdens <- log(county$SimpDens)
county$LogPopDens <- log(county$PopDenskm2)
county <- county[-which(county$ILIcount == 0), ]

################account for spatial autocorrelation################
#calculate a distance matrix for testing for spatial autocorrelation
#to account for spatial autocorrelation between ILI density and
population variables, use GLS models with correlation structure
#five models are options - exponential, gaussian, spherical, linear,
and rational quadratic

#relationship between Log(ILI density) and Log(population density)
modelsimppop <- gls(Logsimpdens ~ LogPopDens, data = county)
```

```
expo.autosimppop <- gls(Logsimpdens ~ LogPopDens, correlation =
corExp(form = ~centroid_long + centroid_lat, nugget = T), data =
county)
gauss.autosimppop <- gls(Logsimpdens ~ LogPopDens, correlation =
corGaus(form = ~centroid_long + centroid_lat, nugget = T), data =
county)
spher.autosimppop <- gls(Logsimpdens ~LogPopDens, correlation =
corSpher(form = ~centroid_long + centroid_lat, nugget = T), data =
county)
lin.autosimppop <- gls(Logsimpdens ~ LogPopDens, correlation =
corLin(form = ~centroid_long + centroid_lat, nugget = T), data =
county)
ratio.autosimppop <- gls(Logsimpdens ~ LogPopDens, correlation =
corRatio(form = ~centroid_long + centroid_lat, nugget = T), data =
county)

#AIC model selection
model.sel(modelsimppop, expo.autosimppop, gauss.autosimppop,
spher.autosimppop, lin.autosimppop, ratio.autosimppop)

#here, rational quadratic correlation structure is the best fit
#residuals can be used for further analyses
plot(fitted(ratio.autosimppop), residuals(ratio.autosimppop))
abline(h = 0, lty = 3)
summary(ratio.autosimppop)

#relationship between Log(ILI density) and poverty percentage
#test the same correlation structures
#rational quadratic is the best fit again
#residuals can be used for further analyses
modelsimppov <- gls(Logsimpdens ~ POVERTY_PERC, data = county)
expo.autosimppov <- gls(Logsimpdens ~ POVERTY_PERC, correlation =
corExp(form = ~centroid_long + centroid_lat, nugget = T), data =
county)
gauss.autosimppov <- gls(Logsimpdens ~ POVERTY_PERC, correlation =
corGaus(form = ~centroid_long + centroid_lat, nugget = T), data =
county)
spher.autosimppov <- gls(Logsimpdens ~POVERTY_PERC, correlation =
corSpher(form = ~centroid_long + centroid_lat, nugget = T), data =
county)
lin.autosimppov <- gls(Logsimpdens ~ POVERTY_PERC, correlation =
corLin(form = ~centroid_long + centroid_lat, nugget = T), data =
county)
ratio.autosimppov <- gls(Logsimpdens ~ POVERTY_PERC, correlation =
corRatio(form = ~centroid_long + centroid_lat, nugget = T), data =
county)

model.sel(modelsimppov, expo.autosimppov, gauss.autosimppov,
spher.autosimppov, lin.autosimppov, ratio.autosimppov)

plot(fitted(ratio.autosimppov), residuals(ratio.autosimppov))
abline(h = 0, lty = 3)
summary(ratio.autosimppov)
```

```
#relationship between Log(ILI density) and Log(population density) *
poverty percentage
#test the same correlation structures
#rational quadratic is the best fit again
#residuals can be used for further analyses
modelsimpboth <- gls(Logsimpdens ~ LogPopDens * POVERTY_PERC, data =
county3)
expo.autosimpboth <- gls(Logsimpdens ~ LogPopDens * POVERTY_PERC,
correlation = corExp(form = ~centroid_long + centroid_lat, nugget = T),
data = county)
gauss.autosimpboth <- gls(Logsimpdens ~ LogPopDens * POVERTY_PERC,
correlation = corGaus(form = ~centroid_long + centroid_lat, nugget =
T), data = county)
spher.autosimpboth <- gls(Logsimpdens ~ LogPopDens * POVERTY_PERC,
correlation = corSpher(form = ~centroid_long + centroid_lat, nugget =
T), data = county)
lin.autosimpboth <- gls(Logsimpdens ~ LogPopDens * POVERTY_PERC,
correlation = corLin(form = ~centroid_long + centroid_lat, nugget = T),
data = county)
ratio.autosimpboth <- gls(Logsimpdens ~ LogPopDens * POVERTY_PERC,
correlation = corRatio(form = ~centroid_long + centroid_lat, nugget =
T), data = county)

model.sel(modelsimpboth, expo.autosimpboth, gauss.autosimpboth,
spher.autosimpboth, lin.autosimpboth, ratio.autosimpboth)

plot(fitted(ratio.autosimpboth), residuals(ratio.autosimpboth))
abline(h = 0, lty = 3)
summary(ratio.autosimpboth)

#calculate pseudo-R2 values
nagelkerke(ratio.autosimppop)
nagelkerke(ratio.autosimppov)
nagelkerke(ratio.autosimpboth)

#add residuals to data table
ratioresid <- county
ratioresid$popresid <- ratio.autosimppop$residuals
ratioresid$povresid <- ratio.autosimppov$residuals
ratioresid$bothresid <- ratio.autosimpboth$residuals

######################Figure 5.2B-C######################
#use interaction residuals (ratioresid$bothresid)

#Figure 5.2B - bar plot of interaction residuals by RUCC
#calculate mean, standard deviation, and standard error of residuals
for each RUCC grouping
mean_pop <- aggregate(ratioresid$bothresid, by = list(ratioresid$RUCC),
mean, na.rm = TRUE)
sd_pop <- aggregate(ratioresid$bothresid, by = list(ratioresid$RUCC),
sd, na.rm = TRUE)
sterr_pop <- aggregate(ratioresid$bothresid, by =
list(ratioresid$RUCC), st.err)
pop <- merge(mean_pop, sd_pop, by.x = "Group.1", by.y = "Group.1")
```

```
pop <- merge(pop, sterr_pop, by.x = "Group.1", by.y = "Group.1")
names(pop) <- c("RUCode", "mean", "sd", "stderror")

bars_pop <- ggplot(pop, aes(x = factor(RUCode), y = mean)) +
  geom_bar(stat = "identity", fill = "gray", color = "black", width =
0.7) +
  labs(x = "Rural-Urban Codes", y = "ILI residuals") +
  scale_y_continuous(limits = c(-0.5, 0.5)) +
  geom_errorbar(stat = "identity", ymin = pop$mean - (pop$mean <
0)*pop$stderror, ymax = pop$mean + (pop$mean > 0) * pop$stderror,
color = "black", width = 0.7) +
  geom_hline(yintercept = 0.0, linetype = "solid", color = "black") +
  theme(axis.line = element_line(color = "black"),
        panel.background = element_rect(color = "black", fill = NA),
        panel.grid = element_blank(),
        axis.text = element_text(color = "black", size = 15),
        axis.title = element_text(color = "black", size = 20))
bars_pop

#Figure 5.2C - bar plot of interaction residuals by poverty category
#calculate mean, standard deviation, and standard error of residuals
for each poverty category
mean_pov <- aggregate(ratioresid$bothresid, by =
list(ratioresid$povcat), mean, na.rm = TRUE)
sd_pov <- aggregate(ratioresid$bothresid, by = list(ratioresid$povcat),
sd, na.rm = TRUE)
sterr_pov <- aggregate(ratioresid$bothresid, by =
list(ratioresid$povcat), st.err)
pov <- merge(mean_pov, sd_pov, by.x = "Group.1", by.y = "Group.1")
pov <- merge(pov, sterr_pov, by.x = "Group.1", by.y = "Group.1")
names(pov) <- c("PovCat", "mean", "sd", "stderror")

bars_pov <- ggplot(pov, aes(x = factor(PovCat), y = mean)) +
  geom_bar(stat = "identity", fill = "gray", color = "black", width =
0.7) +
  labs(x = "Poverty Category", y = "ILI residuals") +
  scale_x_discrete(limits = c(1, 2, 3, 4, 5, 6)) +
  scale_y_continuous(limits = c(-0.5, 0.5)) +
  geom_errorbar(stat = "identity", ymin = pov$mean - (pov$mean <
0)*pov$stderror, ymax = pov$mean + (pov$mean > 0) * pov$stderror,
color = "black", width = 0.7) +
  geom_hline(yintercept = 0.0, linetype = "solid", color = "black") +
  theme(axis.line = element_line(color = "black"),
        panel.background = element_rect(color = "black", fill = NA),
        panel.grid = element_blank(),
        axis.text = element_text(color = "black",size = 15),
        axis.title = element_text(color = "black",size = 20))
bars_pov
```